Nuclear Power Plant Building Wake Effects on Atmospheric Diffusion: Simulation in Wind Tunnel

EPRI

EPRI NP-1891
Project 1073-2
Final Report
June 1981

Keywords:
Plume Diffusion
Atmospheric Releases
Wind Tunnel
Meteorological Dispersion
Radioactive Releases

Prepared by
Colorado State University
Fort Collins, Colorado

ELECTRIC POWER RESEARCH INSTITUTE

Nuclear Power Plant Building Wake Effects on Atmospheric Diffusion: Simulation in Wind Tunnel

---

NP-1891
Research Project 1073-2

Final Report, June 1981

Prepared by

COLORADO STATE UNIVERSITY
Fluid Dynamics and Diffusion Laboratory
Department of Civil Engineering
Fort Collins, Colorado 80523

Principal Investigators
K. M. Kothari
R. N. Meroney
J. A. Peterka

Prepared for

Electric Power Research Institute
3412 Hillview Avenue
Palo Alto, California 94304

EPRI Project Manager
H. Till

Chemistry, Radiation, and Monitoring Program
Nuclear Power Division

ORDERING INFORMATION

Requests for copies of this report should be directed to Research Reports Center (RRC), Box 50490, Palo Alto, CA 94303, (415) 965-4081. There is no charge for reports requested by EPRI member utilities and affiliates, contributing nonmembers, U.S. utility associations, U.S. government agencies (federal, state, and local), media, and foreign organizations with which EPRI has an information exchange agreement. On request, RRC will send a catalog of EPRI reports.

NOTICE

Prepared by
Colorado State University
Fort Collins, Colorado

EPRI PERSPECTIVE

PROJECT DESCRIPTION

This final report for RP1073-2 describes work conducted to determine the aerodynamic effects of large structures on the dispersion of atmospheric plumes. Characterization of atmospheric dispersion in the vicinity of nuclear power plants is needed to accurately evaluate the radiological impact of routine and postulated accidental releases of radioactive effluents. From a previous field study (EPRI Final Report NP-1380), it was determined that buildings have a significant effect on plumes. The study described in this report is a wind tunnel mock-up of the field study to demonstrate the application of the wind tunnel for application to meteorological simulations. Other wind tunnel simulations were conducted to determine methods for maximizing the plume dispersion from vent releases.

PROJECT OBJECTIVES

This study was conducted to evaluate the use of wind tunnels to characterize plume dispersion from nuclear power plants. Wind tunnel measurements were compared to the measured field data for similar meteorological conditions. The simulation was performed to determine if wind tunnels can possibly be used as a convenient tool in atmospheric plume analysis for licensing. Simulations were also conducted to determine the minimum building vent height to eliminate, or reduce significantly, plume downwash. Typical structures and several vent release locations were applied.

PROJECT RESULTS

The wind tunnel results simulated the field measurements within 87% at 300 meters and a factor of 2 at 1000 meters. Other tests showed that building shapes, release locations, and vent height can significantly alter plume dispersion out to approximately one kilometer. The study demonstrated that wind tunnels can be effective instruments for effluent vent design and near-field plume concentration predictions.

This report contains information of interest to those reponsible for determining the radiological environmental impact of operating nuclear power plants.

Henry Till, Project Manager
Nuclear Power Division

ABSTRACT

A 1:400 scale model of the nuclear power plant and the surrounding complex located in the midwest was placed into the Meteorological Wind Tunnel at Colorado State University to study the building wake effects on atmospheric diffusion.

The mean concentration measurements were made at five arcs downwind of the complex. Results show that the buildings significantly alter the dispersion patterns downwind of the complex. The maximum ground level concentration for each of the sample arcs occurred during the moderately stable stratification for the turbine building release. Similar maximum ground level concentration results were obtained for the other two release locations except for the 73.7 m downwind arc. The maximum ground level concentration at each arc occurred for a wind direction of 135° except at 147.3 m arc. At the arc distance of 147.3 m this maximum was obtained for a 157.5° wind direction.

The modified Gaussian predictive equation underpredicted the measured concentration. The wind tunnel measurements were modified using weighted algorithm method to account for the variations in the wind direction and stratification observed in the field data. The method was realistic in both predicting centerline concentration values as well as the horizontal spread of the plume.

The additional concentration measurements were performed in the wake of cylindrical, cubical and hemispherical buildings with various vent heights and neutral stability. The maximum ground level concentrations were in the wake of cylindrical buildings. The experimental results show that for the vent heights of 1.5 times the building height, the building wake effects were minimum on the ground level concentration.

ACKNOWLEDGMENTS

This study was performed under Contracts Nos. RP-1073-2 and RP-1073-2-1 with the Nuclear Power, Safety and Analysis Department of the Electric Power Research Institute whose financial assistance is gratefully acknowledged. The guidance of Mr. Henry Till, EPRI, in coordinating this effort with the field measurements was essential to the completion of this program. A special thanks goes to Research Associate, Mr. David Neff, for his help during the experimental measurements.

TABLE OF CONTENTS

LIST OF FIGURES

LIST OF TABLES

LIST OF SYMBOLS

Symbol	Definition	Dimensions
A	area	$[L^2]$
c	constant = 0.5	--
C_f	one-hour average concentration coefficient, $\frac{\chi U}{Q}$	$[L^{-2}]$
dy	differential length in the horizontal perpendicular to plume axis	[L]
g	acceleration due to gravity	$[L/T^2]$
H	reference height (50 m prototype), 12.5 cm (model))	[L]
h_b	height of building	[L]
h_s	height of release	[L]
k	von Karman's constant, k = 0.4	--
K_c or K	nondimensional concentration coefficient	--
K_{c_1}	concentration coefficient, K_c/H^2	$[L^{-2}]$
L	Monin-Obukhov length	[L]
p	power-law exponent	--
P-G	Pasquill-Gifford stability category	--
q	pollutant mass per unit of plume area	$[M/L^2]$
Q_{source}	source flow rate	$[M^3/T]$
Re	Reynolds number	--
Ri_b	bulk Richardson number, $Ri_b = g(\Delta T)(\Delta z)/[T(\Delta U)^2]$	--
t	time	[T]
T	temperature	$[\theta]$

Symbol	Definition	Dimensions
ΔT	temperature difference across reference layer	$[\theta]$
U	reference velocity at release point and used in deriving K_c	[L/T]
U_r	reference velocity	[L/T]
U_∞	freestream velocity	[L/T]
U_*	friction velocity	[L/T]
x	distance downwind from source	[L]
y	horizontal perpendicular distance from plume center	[L]
$\bar{y}$	center of pollutant mass	[L]
z	vertical distance above ground	[L]
z_o	surface roughness	[L]
z_r	reference height	[L]

Greek Symbols

χ	local concentration	--
χ_{source}	source strength	--
σ_y	horizontal dispersion coefficient	[L]
σ_z	vertical dispersion coefficient	[L]
	kinematic viscosity	$[L^2/T]$

Release Points

A	ground level release	--
B	turbine building release	--
C	reactor vent (stack height) release	--

Building, Release Height and Source Location Identification

1	source release location 1 (see Figures 31-32)
2	sourse release location 2 (see Figures 31-32)
3	source release location 3 (see Figures 31-32)
4	source release location 4 (see Figures 31-32)

Symbol	Definition	Dimensions
H	idealized building height	
CULA	cubical building, height 13.6 cm, roof top source release	
CULB	cubical building, height 13.6 cm, source release height of 0.25 H above building	
CULC	cubical building, height 13.6 cm, source release height of 0.50 H above building	
CULD	cubical building, height 13.6 cm, source release height of 1.0 H above building	
CUSA	cubical building, height 7.6 cm, roof top source release	
CUSB	cubical building, height 7.6 cm, source release height of 0.25 H above building	
CUSC	cubical building, height 7.6 cm, source release height of 0.50 H above building	
CUSD	cubical building, height 7.6 cm, source release height of 1.0 H above building	
CYLA	cylindrical building, height 13.6 cm, roof top source release	
CYLB	cylindrical building, height 13.6 cm, source release height of 0.25 H above building	
CYSA	cylindrical building, height 7.6 cm, roof top source release	
CYSB	cylindrical building, height 7.6 cm, sourse release height of 0.25 H above building	
SPLA	hemispherical building, radius 13.6 cm, roof top source release	
SPLB	hemispherical building, radius 13.6 cm, source release height of 0.25 H above building	
SPSA	hemispherical building, radius 7.6 cm, roof top source release	
SPSB	hemispherical building, radius 7.6 cm, source release height of 0.25 H above building	

SUMMARY

A series of dispersion tests were performed downwind of a 1:400 scale model of a nuclear power plant and the surrounding complex in the Meteorological Wind Tunnel at Colorado State University. The wind-tunnel study was conducted for the Electric Power Research Institute (EPRI).

Mean concentration measurements and a flow visualization study were performed over the model. The test program consisted of systematic tracer gas releases from ground, turbine building vent (23 m above grade) and reactor vent (stack height, 46 m above grade) heights. The gases were released at such a rate that no appreciable plume rise was observed. The tracer gases were methane, ethane and propane appropriately mixed with carbon dioxide and nitrogen to obtain a molecular weight approximately equal to that of air. Samples were collected downwind of the release locations and then analyzed using a HewlettPackard 5700A gas chromatograph with a flame ionization detector. The samples were taken at five arc distances at ground level. Elevated profiles of concentration were also observed on the centerline of the complex at two arc distances. Tests were also repeated under neutral condition to emphasize near wake plume behavior. The test program included 48 sets of concentration measurements for various wind directions with neutral, moderately stable and slightly unstable stratification conditions.

Flow visualization was performed for 11 wind directions with neutral stability and releases from the three same locations using titanium tetrachloride as a visible tracer. Color slides, black and white stills and 16 mm motion pictures were taken to define the plume boundary and submitted to EPRI under a separate cover.

Results show that the buildings significantly alter the dispersion patterns downwind of the nuclear power plant complex. The maximum ground level concentration for each of the sample arcs occurred during the moderately stable stratification for the turbine building release. Similar maximum ground level

concentration results were obtained for the other two release locations except for the 73.7 m downwind arc. The maximum ground level concentration at each arc occurred for a wind direction of 135° except for the 147.3 m arc. At the arc distance of 147.3 m this maximum was obtained for a 157.5° wind direction. For three wind directions (135°, 180° and 225°) selected for additional data reduction, the maximum concentrations were about the same at each arc indicating the wake of the building complex is nearly independent of these wind directions.

The ground level concentration is generally overpredicted by the Pasquill-Gifford formulae, for all three releases, up to about 300 m downwind. This suggests increased mixing exists due to excessive turbulence created by the building complex. On an average the modified gaussian diffusion formulae underpredicts the experimental measurements of ground level concentration. For the three selected wind directions, for each stability and at each downwind distance, the σ_y values were approximately constant. This again emphasizes that slight changes in the wind direction do not alter the concentration pattern. For the neutral and stable conditions, the σ_y observed were much larger than those predicted by the Pasquill-Gifford formulae, which also demonstrates the enhanced dispersion due to building wake effects.

The wind-tunnel ground level concentration results were modified using a weighted algorithm developed by Kothari et al. (1980) to account for the changes in the wind direction and stability during the field tests. The weighted algorithm on an average slightly underpredicts at 300 m arc and overpredicts by two times at 1000 m arc the observed maximum ground level concentrations.

The additional concentration measurements and a flow visualization study were performed in the wakes of cylindrical, cubical and hemispherical buildings with neutral stability and smooth floor conditions. The experimental measurements were performed with free stream velocity of 3 m/sec. The total of four vent heights viz. z/H = 1.0, 1.25, 1.50 and 2.0 were investigated. For two lower vent heights, the four vent locations on the buildings were investigated. For the vent heights of z/H = 1.50 and 2.0 the concentration measurements were performed with only center release location on the building. It was also determined that for the two higher stack heights and cubical building, the plume was not affected by the building wake. Hence, no concentration measurements were performed with these two stack heights for cylindrical and hemispherical objects. The maximum ground level concentrations were in the wake of cylindrical obstacles. This is the result of smaller cavity and hence less initial plume dilution, and the strong horseshoe vortices bringing the plume downward towards the ground along the centerline of the cylindrical building wake. The effect of building wakes on plumes were reduced as the vent heights were increased, as expected.

Chapter 1

INTRODUCTION

Wind-tunnel diffusion tests were conducted on a 1:400 scale model of the nuclear power plant located in the midwest. The experiments were carried out in the low speed meteorological wind tunnel (Figure 1) located in the Fluid Dynamics and Diffusion Laboratory (FDDL) at Colorado State University.

This wind-tunnel study is part of a research program developed by Electric Power Research Institute (EPRI) to empirically determine the effect of containment buildings on the atmospheric flow field and gaseous diffusion during different atmospheric stabilities. The program consisted of field measurement and physical modeling in the laboratory. The field program was conducted by Stanford Research Institute of California and the field evaluation report has been prepared by them (SRI Project 6888, 1979). The aim of the project was to compare the field data with laboratory data. Similar field studies have been performed at the EOCR complex in Idaho and the Rancho Seco in California by Start et al. (1977). The corresponding wind-tunnel studies were performed by Hatcher et al. (1977) and Allwine et al. (1978) at Colorado State University.

Three atmospheric stabilities characteristic of the 1978 field study at the nuclear power plant located in the midwest were simulated in the wind tunnel. These stabilities were neutral, slightly unstable, and moderately stable. Wind speed and temperature data collected from a 50 meter meteorological tower was used to specify the atmospheric stabilities and the approach flows. Data was collected on the tower at the 10 and 50.0 meter levels. The velocity data were interpolated at 23.5 m height also. From this data a bulk Richardson number (Ri_b) was calculated over the layer 10 to 50 meters for each of the 44 field tests.

Representative bulk Richardson numbers were chosen from these field results and simulated over the corresponding layer in the wind-tunnel experiments. Other approach flow modeling parameters such as surface roughness (z_0), friction velocity (U_*), and velocity profile power-law exponent (p) were also determined from the field tower data.

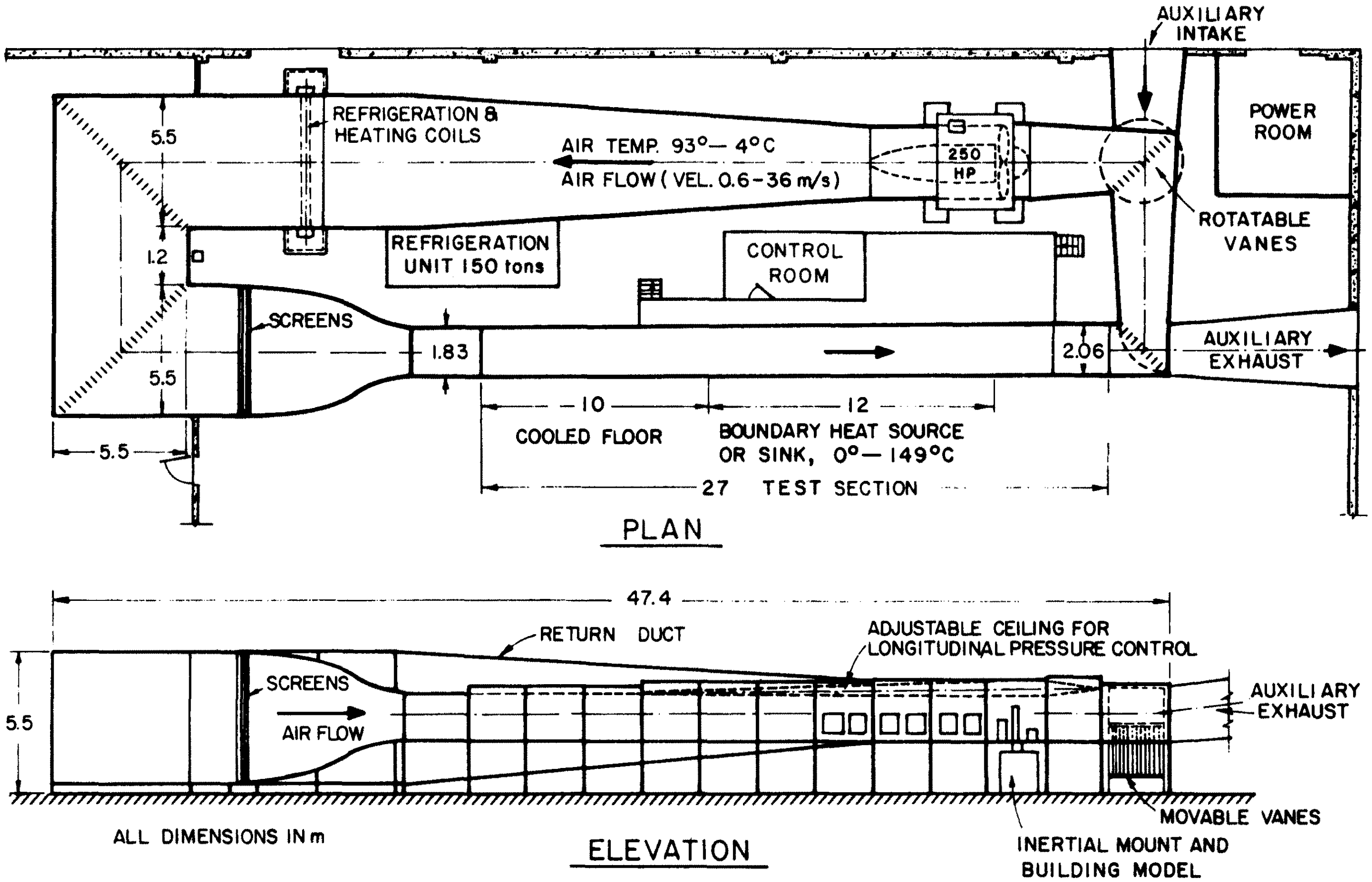

Figure 1. Meteorological Wind Tunnel

The wind-tunnel test program consisted of the simultaneous release of three different tracer gases from three points on the containment vessel and the subsequent measurement of ground level concentrations up to 1031 meters (prototype) downwind. These tests were conducted under three different stabilities for eight different wind directions, giving a total of 24 runs. The eight wind directions were at 22.5° increments starting at 90 degrees. Additional tests were also conducted under neutral condition for six wind directions starting with wind directions of 135° and increments of 22.5°. These tests were conducted to obtain the near wake plume behavior in greater detail. Measurements were made at a distance of 60, 80, 120 and 160 m (prototype). This resulted in an additional 24 tests. Measurements of concentration distribution were also made for a no building case for three release heights (equivalent to the release heights with the nuclear power plant present) under three stability conditions up to a distance of 1000 m (prototype). It should be noted that wind direction of 0°, 90°, 180° and 270° refers to wind approaching the power plant from North, East, South and West respectively. This study was conducted to validate the windtunnel for simulating plume dispersion from nuclear power plants as an aid in obtaining the licensing of nuclear power plants under low wind speed conditions.

The concentration measurements were also performed in the wakes of cylindrical cubical and hemispherical buildings with neutral stability and smooth floor conditions in the Industrial Aerodynamics Wind Tunnel (Figure 2). The wind-tunnel test program consisted of the simultaneous release of four different tracer gases from four points on the idealized buildings. These release points were at the center, on the leeward, on the windward and on the crosswind sides of building. The experimental measurements were performed with four vent heights. These vent heights were at the buildig height and 1.25, 1.5 and 2.0 times the building height. The vertical and groundlevel concentration profiles were measured from 1 to 30 heights downstream of the buildings. A flow visualization study was performed for all six buildings and four vent heights with center release to determine the plume downwash by the building shape and size, and to determine at what minimum vent height the plume downwash can be reduced or eliminated.

The report presents the experimental program and a detailed presentation of the concentration results for three of the eight wind directions, three release points and three stability conditions. The idealized wake concentration measurements are discussed in subsequent sections.

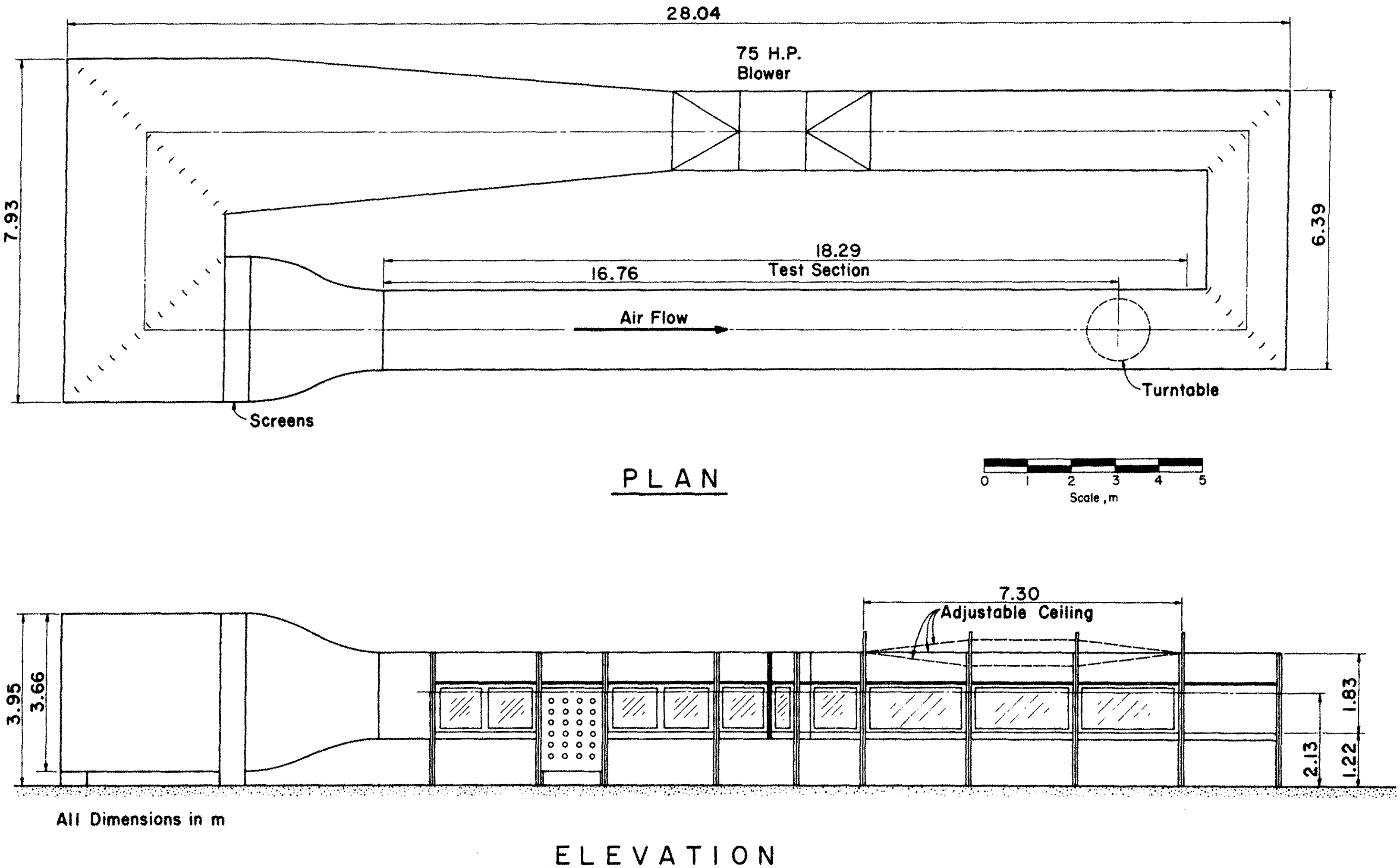

Figure 2. Industrial Aerodynamics Wind Tunnel, Fluid Dynamics and Diffusion Laboratory, Colorado State University.

Chapter 2

RESULTS AND DISCUSSIONS

CONCENTRATION MEASUREMENTS

The nuclear power plant field samples were collected over a one-hour period. Hatcher et al. (1977) and Allwine et al. (1978) suggest that one can reasonably assign an effective full-scale averaging time of 10 minutes to mean laboratory data.

It is known that average maximum concentrations of gaseous dispersion in the atmosphere tend to decrease with increasing sampling time. Since the motion of airflow in the lower atmosphere is limited in the vertical direction by the presence of the ground, the magnitude of eddy size in the transverse direction may be much greater than that in the vertical direction. Thus, the meandering behavior or gustiness effect produced by the large lateral scale of the eddy in the atmosphere causes a greater transverse dispersion. Since the larger eddy motion cannot be produced in the wind tunnel, some adjustments must be made for field application.

This phenomenon, often known as the gustiness effect, was first considered by Hino (1968). He reported that a smoke cloud width increases at a rate proportional to the 1/2 power of the observation time. Ogura (1959) developed a mathematical model which suggested a -1/2 power variation of the maximum concentration with time. Hino (1967) performed a large-scale study for a time range from 10 minutes to 5 hours. The study which involved releasing tracer materials from high stacks of thermal electric power stations also gives support to the -1/2 power law. Hino found that atmospheric instability has only a small effect on the exponent of the power law, i.e., $\chi \sim \tau^{-1/2}$. The applicable range of the -1/2 law is greater for unstable than for neutral stratification.

An alternative -1/5 power law was proposed by Nonhebel. Hino (1968) suggested, however, that the applicable time range for this law is less than 10 minutes. Other exponents for the peak to mean concentration ratio which range from -0.65

to -0.35 depending on meteorological condition, have been recommended by the ASME Committee on Air Pollution Control. Hinds (1967) measured the peak to mean concentration ratios in a building wake region. Data indicated the -1/2 law can also be used satisfactorily to predict the dispersion in the wake flow.

More recently, Brun et al. (1973) reviewed all prior experiments for peak to mean variations with averaging time. Although they report values of the power-law coefficient which vary from -0.12 to -0.86, depending upon stratification and averaging time, they conclude a value of -0.5 is most appropriate when tranposing from 0.25 to one-hour averaging times.

Applying Hino's (1968) minus one-half power law,

$$\chi_p = \chi_m \left(\frac{t_p}{t_m}\right)^{-1/2} \tag{2-1}$$

where χ_p is prototype concentration, χ_m is model concentration, t_p is prototype sampling time, and t_m is model equivalent field sampling time, we have for this study,

$$\chi_p = \chi_m \left(\frac{60}{10}\right)^{-1/2} = 0.4\ \chi_m \quad . \tag{2-2}$$

This means that the wind-tunnel measurements overpredict prototype concentrations by a factor of two and one-half for typical near neutral flow conditions.

Of course site specific climatology may result in further dilution of the subject plumes. The field results suggest large lateral meandering occurred during some runs. A separate algorithm has been prepared to approximately estimate one-hour concentrations from windtunnel measurements by Bouwmeester, Kothari and Meroney (1979). The results of such an analysis are presented in a subsequent chapter. The modeling requirements and experimental methods with the symbols used are described in Appendices A and B, respectively.

MAXIMUM GROUND LEVEL CONCENTRATIONS AND COMPARISONS WITH GAUSSIAN DIFFUSION EQUATION

Table 1 provides a list of the maximum ground level concentration, K_{c_1}, for each of the five sampling arcs for far wake wind-tunnel runs for all three stabilities investigated. The maximum ground level concentration for each of the sampling arcs occurred during the moderately stable stratification for the turbine building release. The stack height release (reactor vent) and ground level release also show a similar trend, except for the 73.7 m arc. The maximum ground level concentrations were observed for wind directions 135°, 157.5°, 135°, 135°, and 135° (157.4° also) for each of the arc lengths 73.7, 147.3, 304.8, 609.6, and 1031.2 m, respectively.

The maximum observed ground level concentration coefficient, K_{c_1}, versus distance downwind has been plotted against the Gaussian diffusion equation prediction using Pasquill-Gifford values for the horizontal and vertical dispersion coefficients. The results of wind directions 135°, 180° and 225° are presented in Figures 3 through 11. It should be noted that release locations A, B and C correspond to ground release, turbine building release and reactor vent release (or stack height release) respectively. The results of field data are also presented on these figures. The Gaussian diffusion equation which has been evaluated at the centerline with $h_s = 0$ and $z = 0$ is

$$\frac{\chi U}{Q} = \frac{1}{\pi \sigma_y \sigma_z} , \qquad (2\text{-}3)$$

where σ_y and σ_z are the dispersion coefficients derived from Gifford (1965).

For the elevated release, it is apparent that the plume is brought to the ground downwind of the complex for all wind directions. The building wake interaction has increased mechanical mixing and this effect is most pronounced for turbine building releases. The concentration distributions were about the same at each arc for three wind directions. This also indicates that mechanical turbulence created by building wake is nearly independent of the wind direction. The figures also indicate that the ground level Pasquill-Gifford formula produces overprediction, for all three releases, up to about 300 m downwind. This suggests increased mixing due to excessive turbulence created by building complex. Calculated concentration from perturbation theory developed by Kothari

Table 1

MAXIMUM GROUND LEVEL CONCENTRATION COEFFICIENT, $K_{c_1} \times 10^4 m^{-2}$,

FOR FAR WAKE WIND-TUNNEL RUNS

Arc Distance Meters	Stability°	Release Point*	Wind Direction 90°	112.5°	135°	157.5°	180°	202.5°	225°	247.5°
73.7	x	A	9.78	6.37	5.15	15.06	33.69	24.76	19.77	6.06
		B	1.27	11.79	28.51	26.89	22.89	6.23	9.93	22.11
		C	0.41	1.37	1.43	1.08	2.85	4.00	8.08	6.44
	y	A	8.80	2.60	1.43	10.65	33.95	29.61	25.52	10.03
		B	20.79	15.79	36.07	31.71	12.84	6.42	11.13	11.04
		C	0.46	1.60	24.98	0.21	3.03	4.12	9.21	6.17
	z	A	8.96	11.07	4.00	9.00	21.50	27.89	1.98	4.49
		B	14.63	14.04	36.90	20.09	9.84	6.02	10.56	13.04
		C	0.97	14.72	1.77	1.98	3.92	6.42	10.54	7.85
147.3	x	A	5.50	6.06	8.06	15.06	11.20	9.05	17.03	18.94
		B	4.83	8.97	8.94	13.58	7.44	5.81	7.13	8.65
		C	0.60	2.04	2.33	1.49	2.27	6.66	10.07	6.83
	y	A	6.23	8.65	7.12	15.06	14.13	9.61	15.04	18.46
		B	9.75	11.25	12.84	16,86	8.87	6.56	7.80	9.28
		C	0.33	2.33	1.99	0.29	3.01	6.18	11.67	7.56
	z	A	5.35	7.58	5.29	19.16	16.76	9.51	4.62	14.14
		B	6.91	9.49	10.26	11.22	6.99	5.98	7.40	8.52
		C	0.12	2.46	2.25	2.76	4.07	6.91	10.66	8.19
304.8	x	A	3.01	4.22	6.20	5.16	4.73	3.56	5.66	3.81
		B	3.69	3.86	3.06	4.15	3.69	3.21	3.91	4.32
		C	2.08	2.51	2.81	2.12	2.38	3.80	3.36	3.13
	y	A	3.68	8.20	9.92	5.34	6.28	4.39	6.93	5.49
		B	6.60	4.94	4.62	5.36	5.35	4.06	4.82	5.26
		C	1.01	3.24	4.04	0.35	2.80	5.18	3.44	3.59
	z	A	3.23	3.84	5.82	9.04	6.41	4.03	1.32	3.14
		B	3.82	4.11	3.34	4.34	3.37	3.20	3.56	3.92
		C	2.28	3.07	3.20	3.42	3.30	3.76	3.35	2.60
609.6	x	A	2.34	2.36	2.70	3.14	3.34	2.10	2.44	2.74
		B	2.02	2.13	1.88	2.32	2.22	2.27	2.16	2.42
		C	1.65	1.98	1.97	1.82	1.63	2.22	1.94	1.86
	y	A	2.42	5.12	6.54	5.25	4.54	3.11	4.06	2.80
		B	3.56	3.48	2.92	3.71	3.38	3.06	2.04	3.14
		C	2.17	2.66	3.24	0.22	2.17	3.36	2.39	2.12
	z	A	2.05	2.21	2.76	3.59	3.90	2.72	2.50	2.73
		B	2.18	2.16	1.88	2.26	2.38	2.32	2.14	2.00
		C	1.75	2.26	2.08	1.13	2.18	2.02	1.63	1.50
1031.2	x	A	1.58	2.04	0.89	2.00	1.98	1.38	1.30	1.90
		B	1.19	1.10	1.10	1.24	1.42	1.44	1.30	1.46
		C	1.14	1.29	1.24	1.19	1.16	1.38	1.03	1.12
	y	A	2.00	3.60	4.29	4.29	3.47	1.97	2.14	2.72
		B	2.63	1.93	2.08	2.15	2.27	1.96	2.39	2.43
		C	2.37	1.98	2.44	0.19	1.58	2.28	1.96	1.54
	z	A	1.23	1.47	1.94	1.85	2.38	1.61	1.91	1.84
		B	1.17	1.38	1.18	1.26	1.39	1.29	1.18	1.15
		C	0.90	1.46	1.27	1.28	1.38	1.08	0.92	0.88

°x neutral
y moderately stable
z slightly unstable

*A ground level release
B turbine building release
C reactor vent (stack height) release

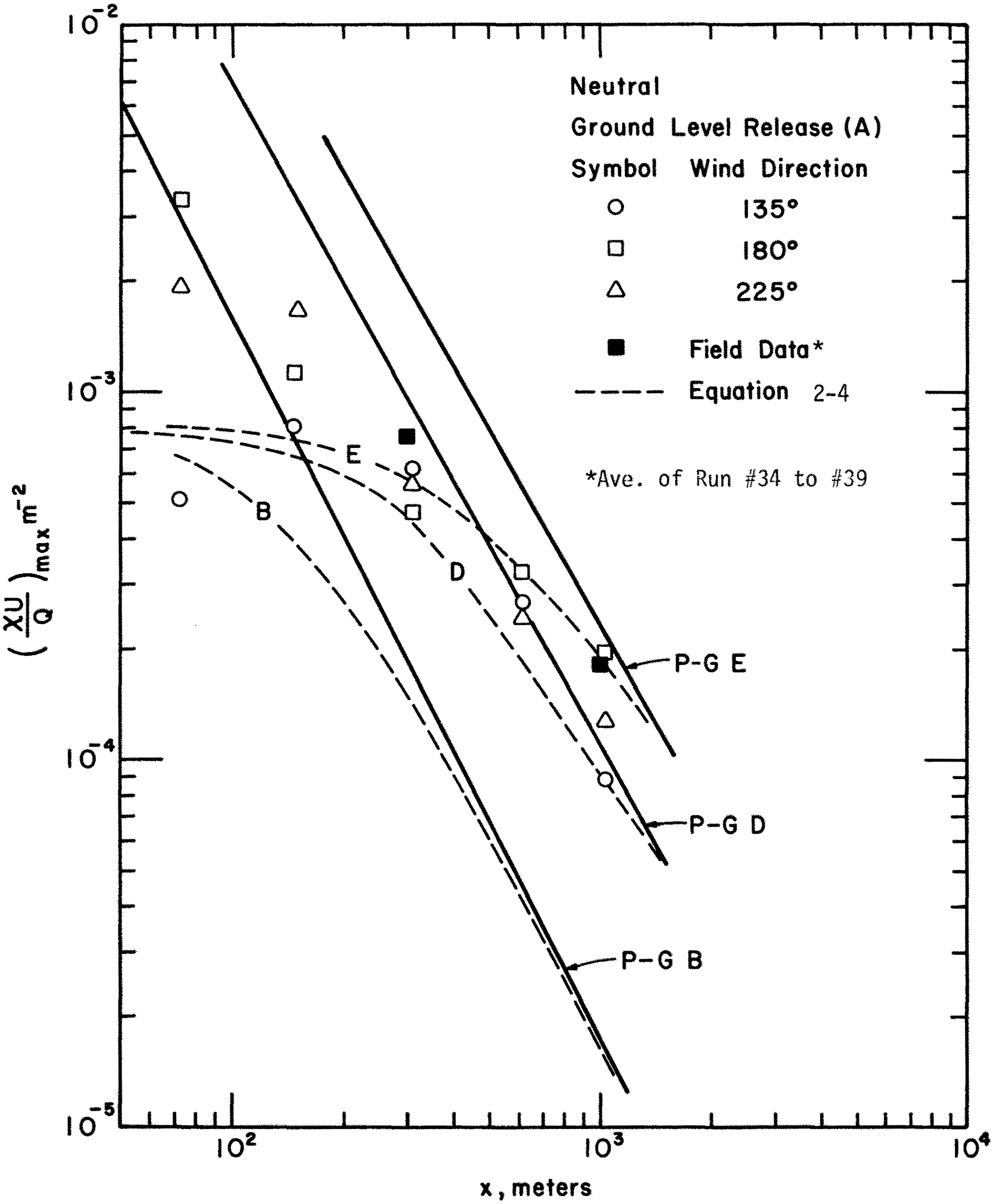

Figure 3. Plot of maximum ground level concentration coefficient, K_{c_1}, versus x.

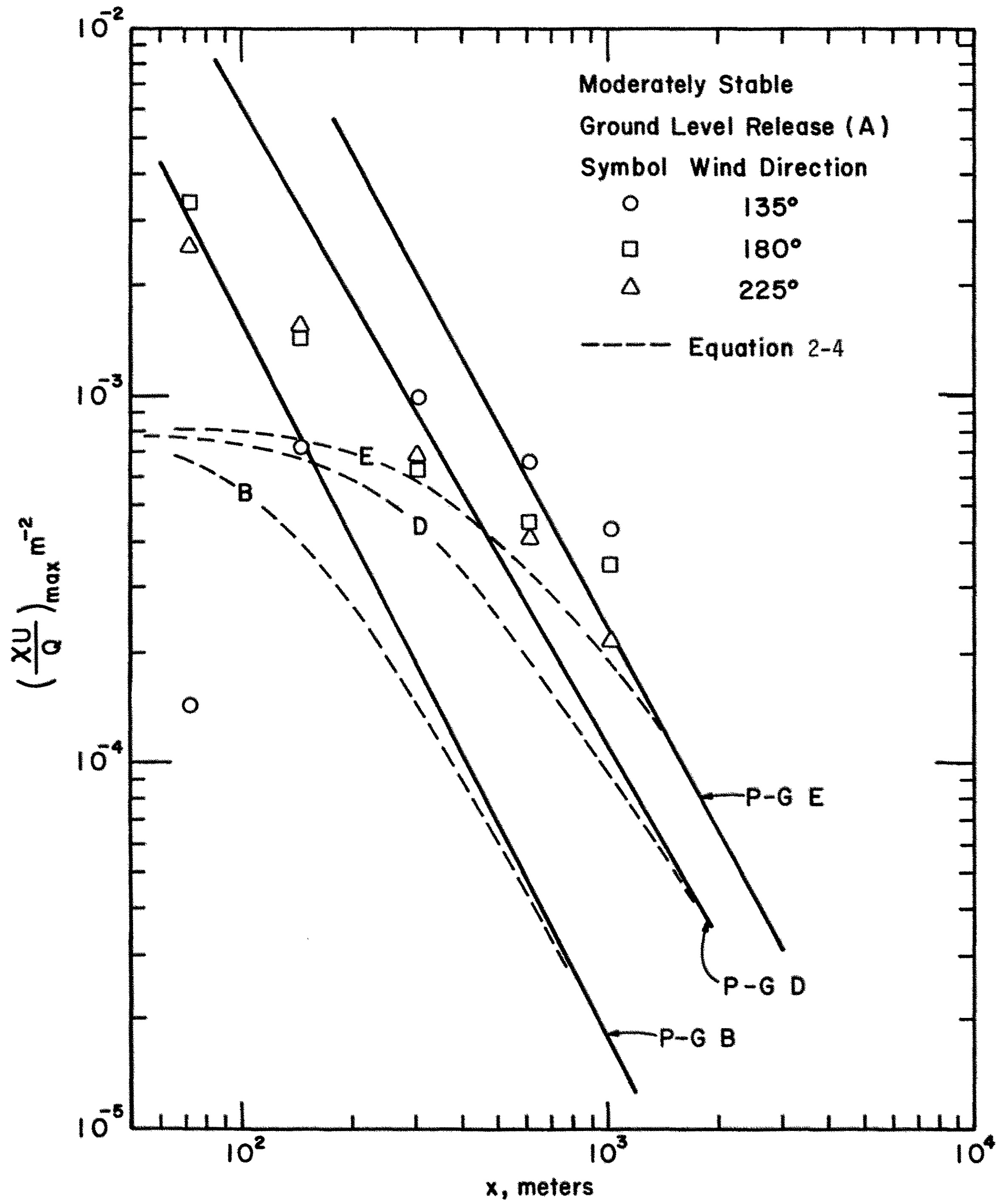

Figure 4. Plot of maximum ground level concentration coefficient, K_{c_1}, versus x.

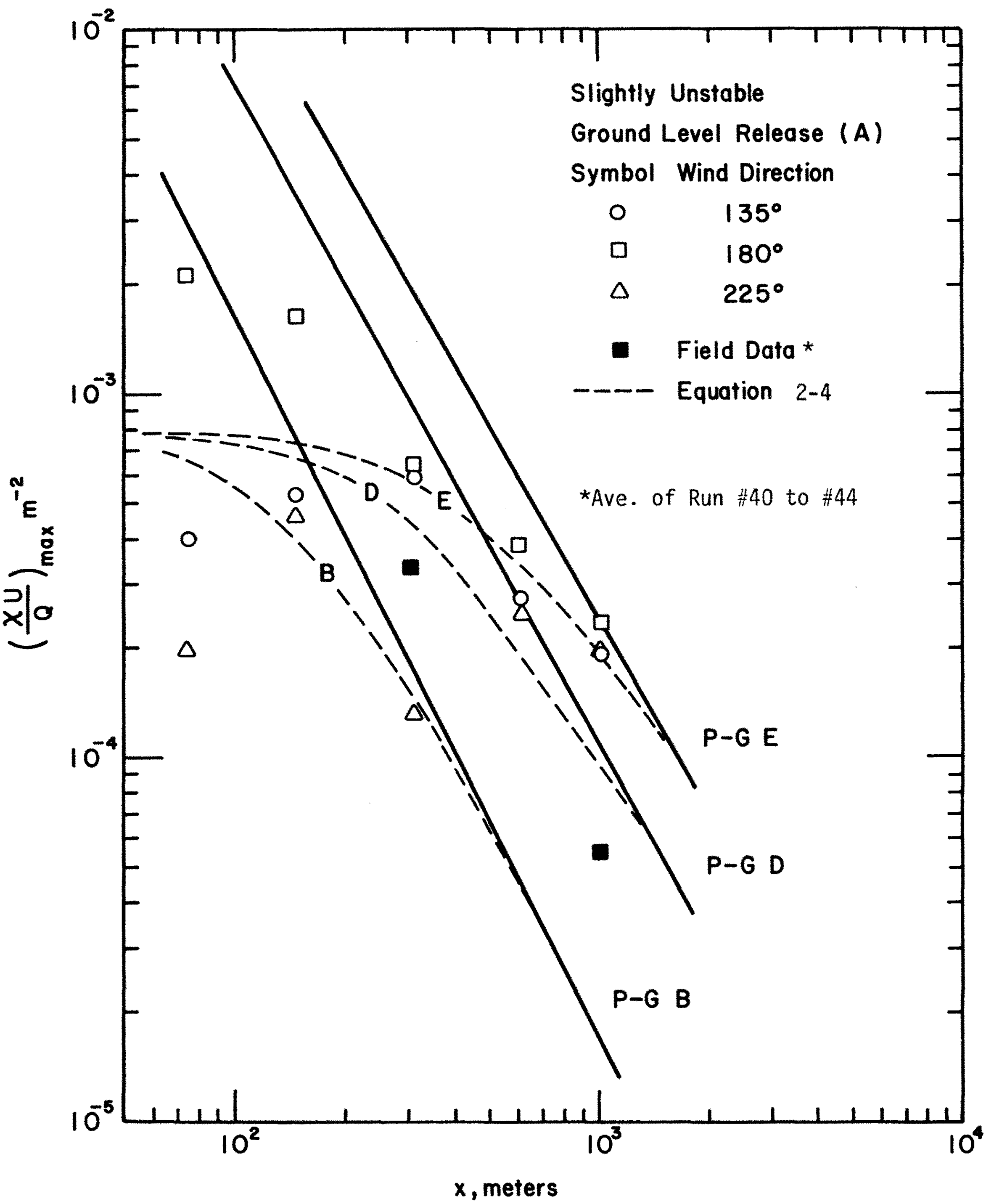

Figure 5. Plot of maximum ground level concentration coefficient, K_{c_1}, versus x.

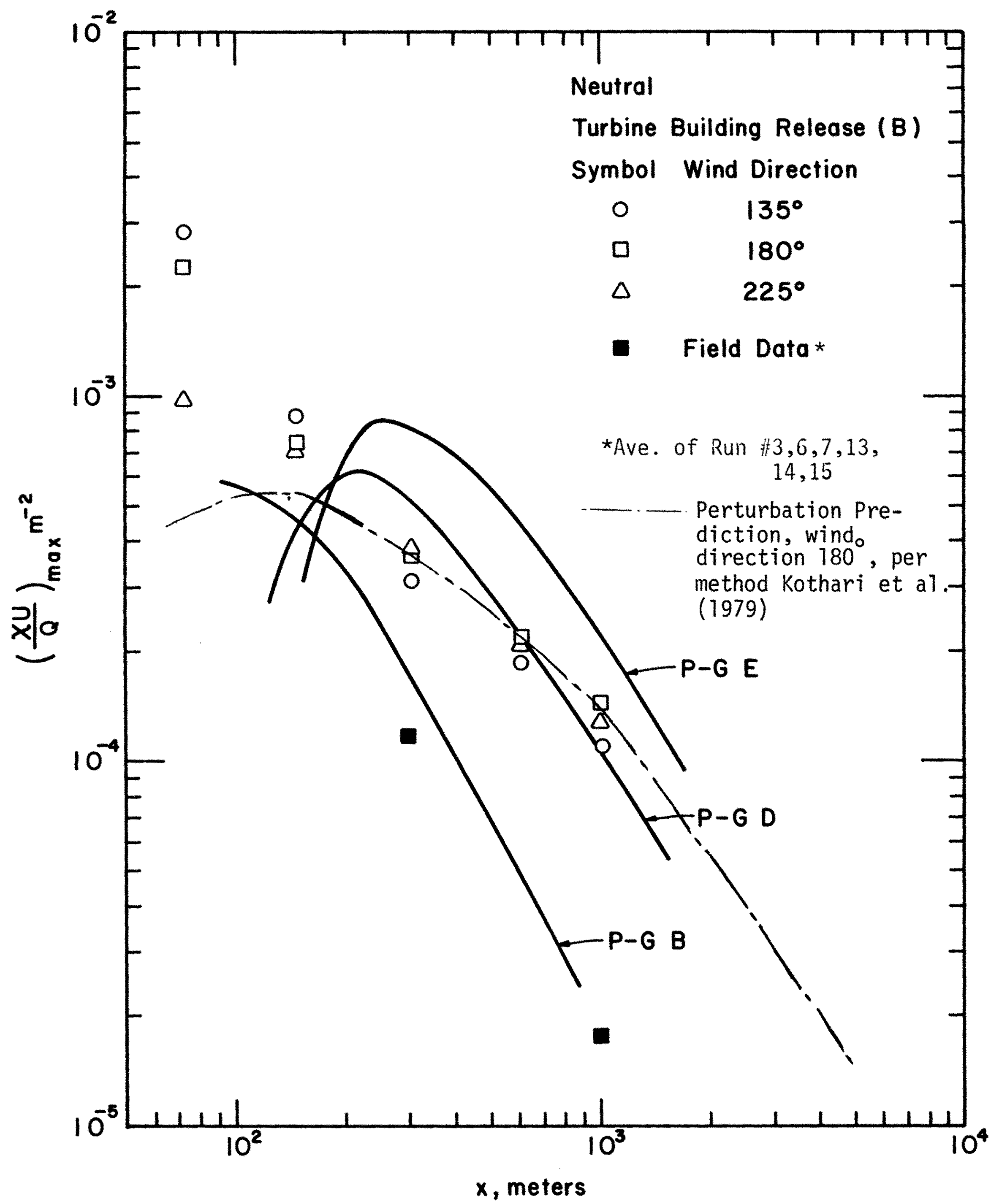

Figure 6. Plot of maximum ground level concentration coefficient, K_{c_1}, versus x.

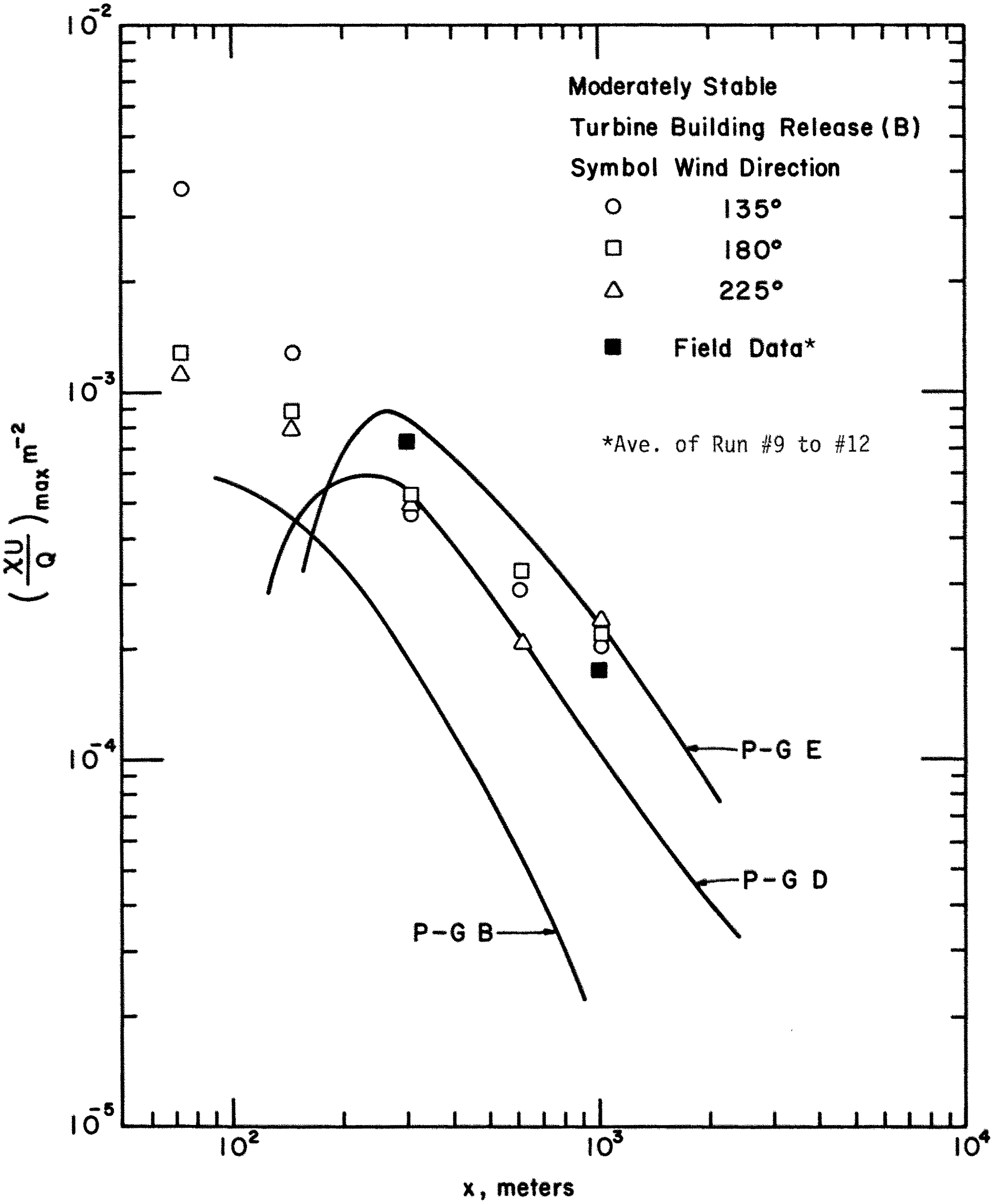

Figure 7. Plot of maximum ground level concentration coefficient, K_{c_1}, versus x.

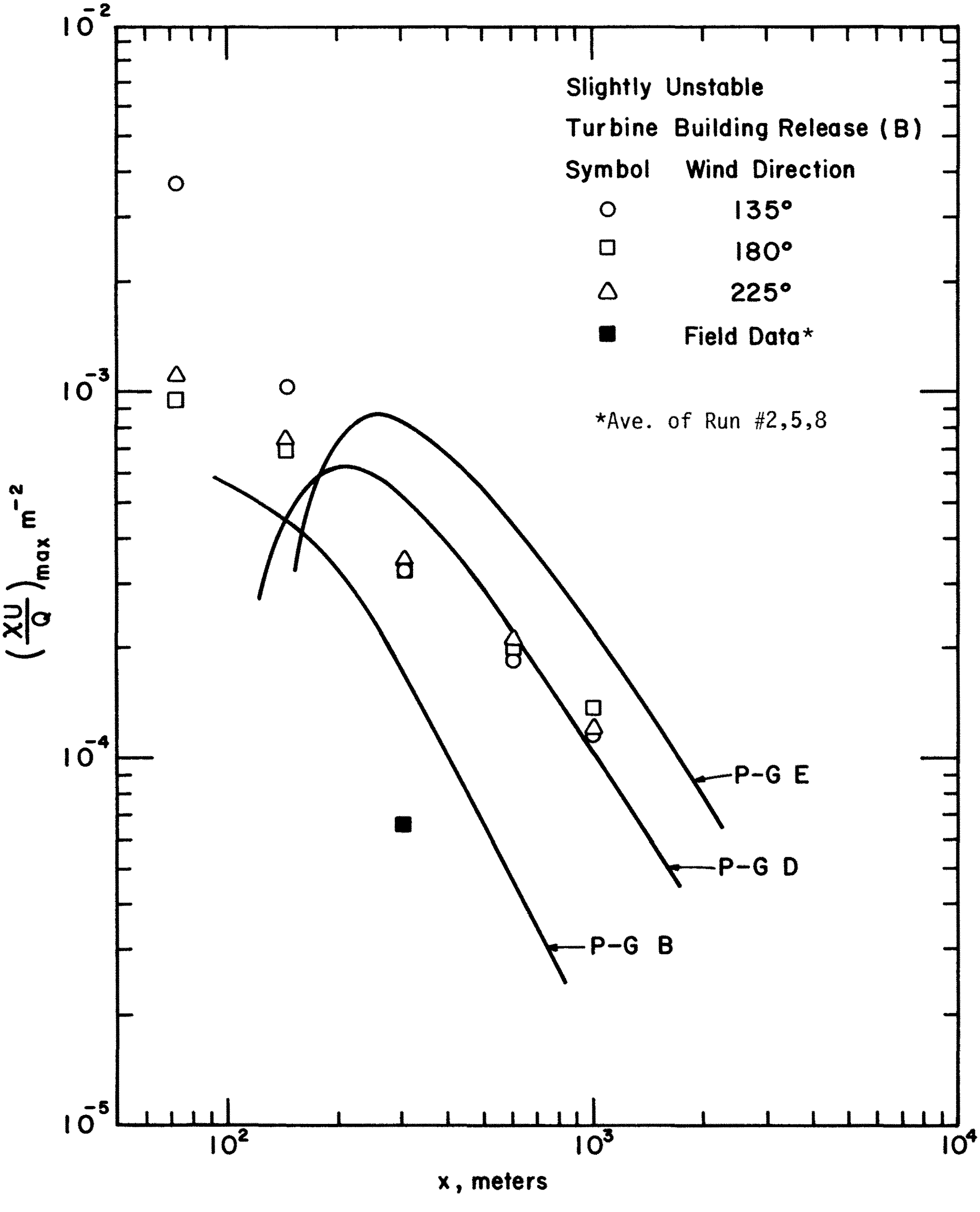

Figure 8. Plot of maximum ground level concentration coefficient, K_{c_1}, versus x.

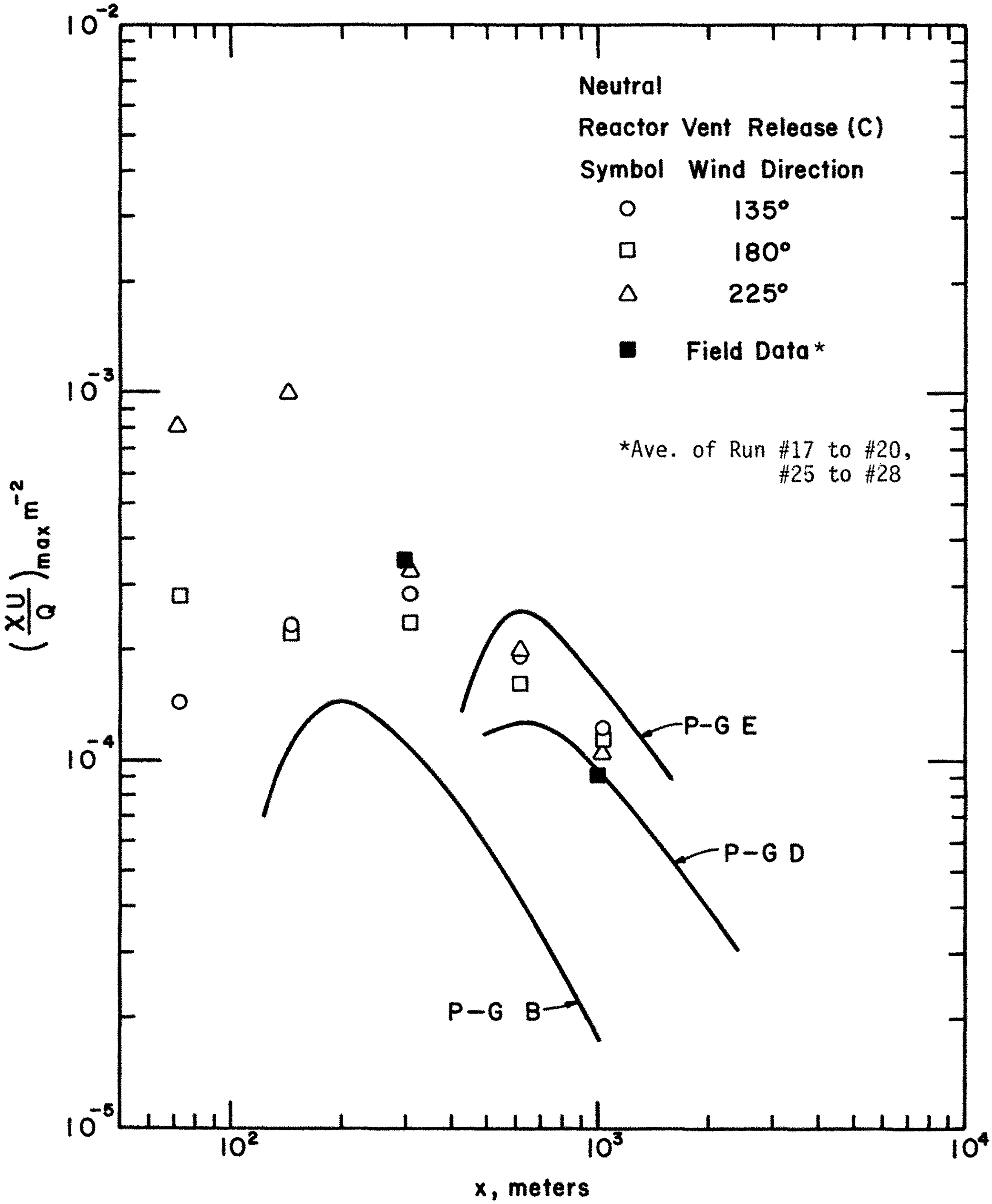

Figure 9. Plot of maximum ground level concentration coefficient, K_{c_1}, versus x.

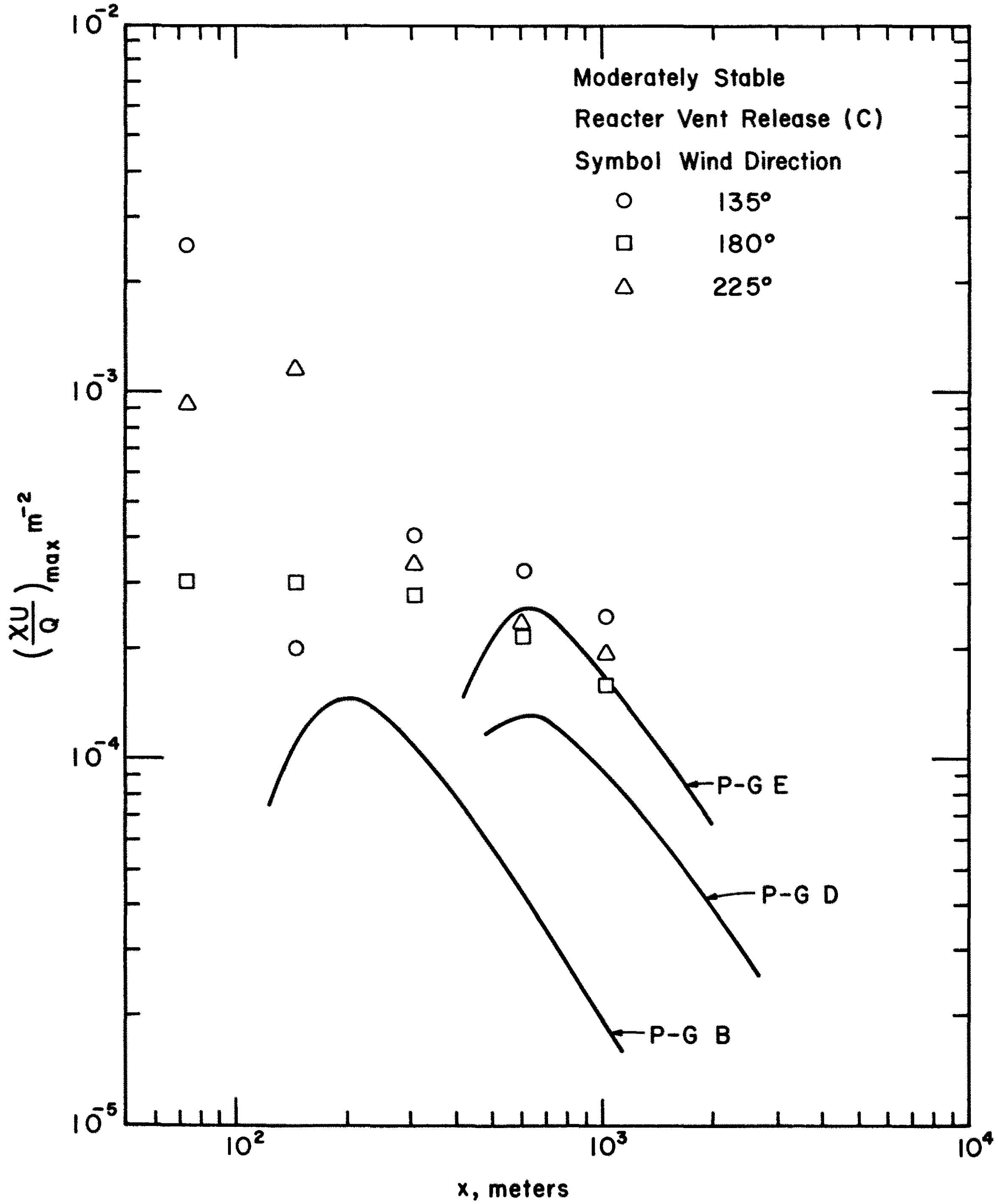

Figure 10. Plot of maximum ground level concentration coefficient, K_{c_1}, versus x.

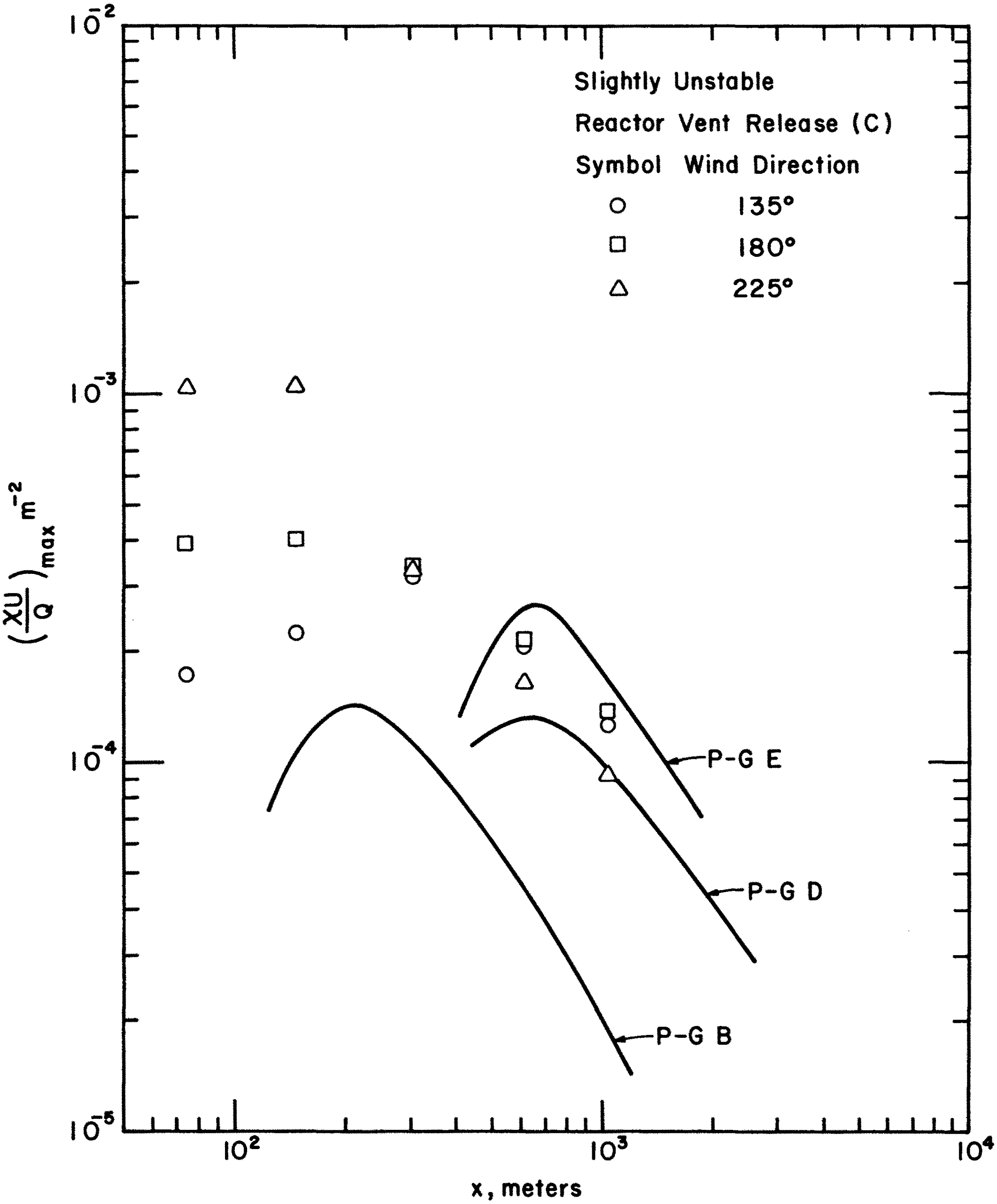

Figure 11. Plot of maximum ground level concentration coefficient, K_{c_1}, versus x.

et al. (1979) to account for building wake effect has been plotted (Figure 5) for neutral and 180° wind direction for release point B. The results of the theory compare very well with the observed concentration.

In Figures 3 to 11 are given comparisons of the wind-tunnel measured ground level axial concentration coefficient and the concentration coefficient determined from a modified Gaussian diffusion equation (Gifford, 1960, 1968). The comparison is also tabulated in Table 2. Wind directions 135°, 180° and 225° for a ground release point are considered. The Gaussian diffusion equation modified by Gifford to account for dispersion in building wakes is

$$\frac{\chi U}{Q} = \frac{1}{\pi\sigma_y\sigma_z + CA} \qquad (2\text{-}4)$$

where C was chosen to be 1/2 (Gifford, 1975). The area A in the above formula was evaluated as the area of the complex buildings perpendicular to flow for wind direction equal to 180°. The results show that on an average the Modified Gaussian equation underpredicts the measured concentration.

The near wake concentration measurements were converted to non-dimensional concentration coefficient, K_c. The isopleths were contoured at each of the four downwind locations, three releases and neutral stability for wind direction 180° and are presented in Appendix C. From all of the figures it is apparent that the building wake significantly alters the concentration pattern.

HORIZONTAL DISPERSION COEFFICIENT AND COMPARISON WITH PASQUILL-GIFFORD PREDICTED VALUES

The horizontal dispersion coefficient, σ_y, was determined using the method described by Whaley (1974). Only the ground level concentration data was used. First, the mass of pollutant per unit area of plume, q, was determined, where:

$$q = \int K_c \, dy \quad . \qquad (2\text{-}5)$$

Second, the center of pollutant mass, $\bar{y}$, which is the first moment was calculated:

Table 2

COMPARISON OF THE MEASURED CONCENTRATION COEFFICIENT, K_{c_1}, FOR GROUND LEVEL RELEASE WITH PREDICTION ACCORDING TO EQUATION 2-4

Arc Distance Meters	Stability*	$(\frac{\chi U}{Q})_{max} \times 10^4 m^{-2}$ Experimental for Wind Direction 135°	180°	225°	$(\frac{\chi U}{Q})_{max} \times 10^4 m^{-2}$ Equation 2-4	$\frac{(\frac{\chi U}{Q})_{max} \text{ Experimental}}{(\frac{\chi U}{Q})_{max} \text{ Equation 2-4}}$ for Wind Direction 135°	180°	225°
73.7	x	5.15	33.69	19.77	7.65	0.67	4.40	2.58
	y	1.43	33.95	25.52	7.98	0.18	4.25	3.20
	z	4.0	21.50	1.98	6.43	0.62	3.34	0.31
147.3	x	8.06	11.20	17.03	6.57	1.22	1.70	2.59
	y	7.12	14.13	15.04	7.43	0.96	1.90	2.02
	z	5.29	16.76	4.62	3.95	1.33	4.24	1.17
304.8	x	6.20	4.73	5.66	4.21	1.47	1.12	1.34
	y	9.92	6.28	6.93	5.87	1.69	1.06	1.18
	z	5.82	6.41	1.32	1.48	3.93	4.33	0.89
609.6	x	2.70	3.34	2.44	1.93	1.39	1.73	1.26
	y	6.54	4.54	4.06	3.38	1.93	1.34	1.20
	z	2.76	3.90	2.50	0.44	6.27	8.86	5.68
1031.2	x	0.89	1.98	1.30	0.93	0.95	2.12	1.39
	y	4.29	3.47	2.14	1.78	2.41	1.95	1.20
	z	1.94	2.38	1.91	0.16	12.13	14.88	11.94

*x neutral
y moderately stable
z slightly unstable

$$\bar{y} = \frac{1}{q} \int K_c \, y dy \tag{2-6}$$

Then, the second moment, σ_y^2, was determined:

$$\sigma_y^2 = \frac{1}{q} \int K_c \, (y - \bar{y})^2 dy \tag{2-7}$$

σ_y then is the square root of the variance σ_y^2. All of the integrals were evaluated using trapezoidal rule.

Table 3 lists the σ_y values for the 135°, 180° and 225° wind directions for the ground level release point under neutral, slightly unstable and moderately stable cases.

Figures 12, 13 and 14 present the plots of σ_y versus x for wind directions 135°, 180° and 225° for three different stabilities respectively. The Pasquill-Gifford values of σ_y for different stabilities are also displayed on these figures. It should be noted again that for the three different wind directions plotted, for each stability and at each x, the σ_y values are approximately constant, similar to the plots of concentration coefficients K_{c_1}. This again suggests that slight changes in the wind direction do not alter the concentration pattern. The slightly unstable case results show that beyond 600 m, the σ_y corresponds to one category less unstable. For the neutral and stable cases, the σ_y observed were much larger than that predicted by P-G category. This demonstrates the enhanced dispersion due to building wake effects. The field data for σ_y for ground release at two arcs are also shown in Figure 12. The σ_y values compare satisfactory at 300 m arc but at 1000 m arc wind-tunnel data underpredicts the σ_y values. A possible reason could be inadequate lateral arc extent.

MAXIMUM GROUND LEVEL CONCENTRATIONS FOR IDEALIZED BUILDING WAKE DIFFUSION TESTS

Table 4 provides a list of the maximum ground level concentration coefficient, K_c, for each of the six downwind distances. The cylindrical and hemispherical building wake concentration tests were performed for two vent heights and four release locations. The cubical building tests were for all four vent heights and various release locations.

Table 3

CALCULATED HORIZONTAL DISPERSION COEFFICIENT, σ_y, FOR GROUND LEVEL RELEASE FROM WIND-TUNNEL DATA

Wind Direction Degrees	Arc Distance Meters	Neutral σ_y Meters	Moderately Stable σ_y Meters	Slightly Unstable σ_y Meters
135	73.7	17.3	10.5	18.0
135	147.3	36.2	35.1	37.8
135	304.8	53.1	51.8	63.0
135	609.6	61.9	64.2	71.4
135	1031.2	--	76.4	106.7
180	73.7	15.1	14.4	13.3
180	147.3	21.3	26.5	28.0
180	304.8	43.8	46.3	48.5
180	609.6	48.5	60.0	63.6
180	1031.2	51.9	84.4	101.9
225	73.7	17.2	15.9	18.0
225	147.3	29.5	30.1	41.1
225	304.8	41.1	45.0	65.8
225	609.6	59.6	62.7	68.1
225	1031.2	60.2	93.7	107.4

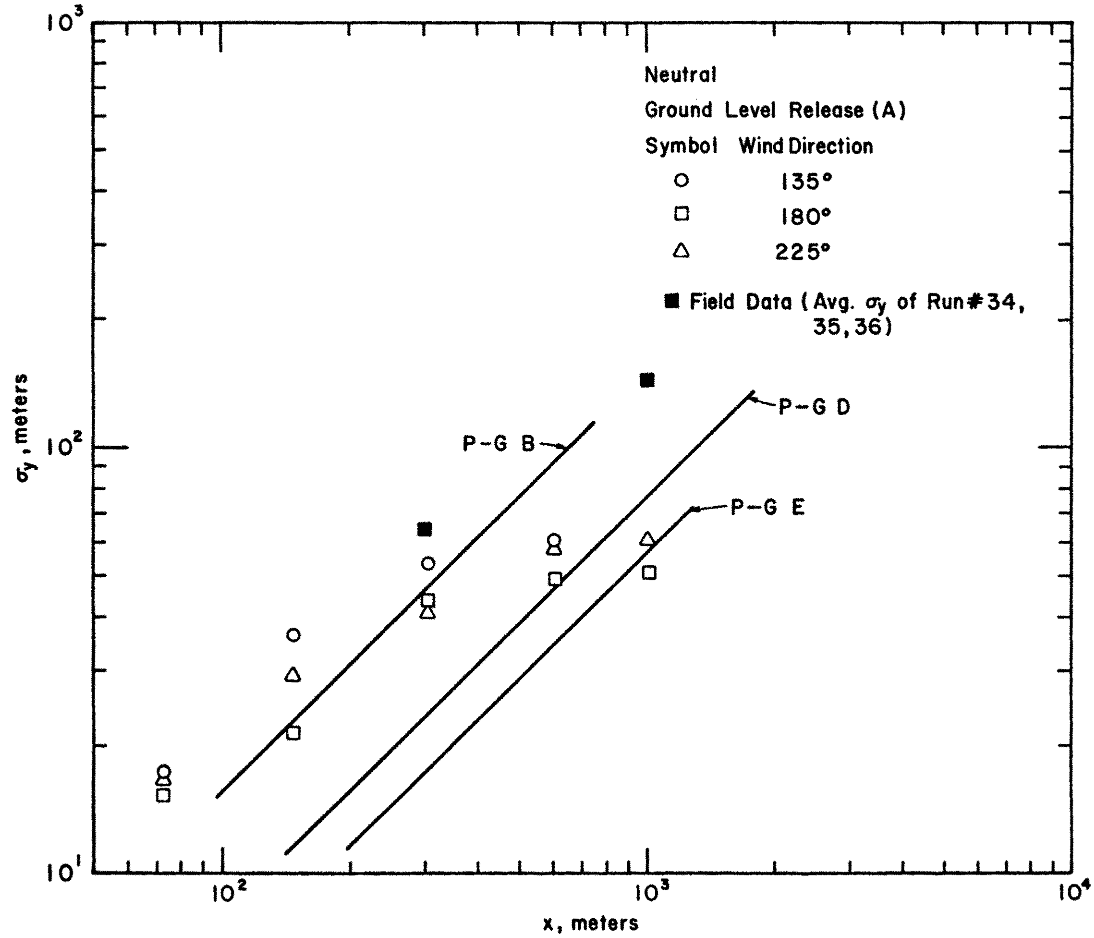

Figure 12. Plot of lateral dispersion, σ_y, versus x.

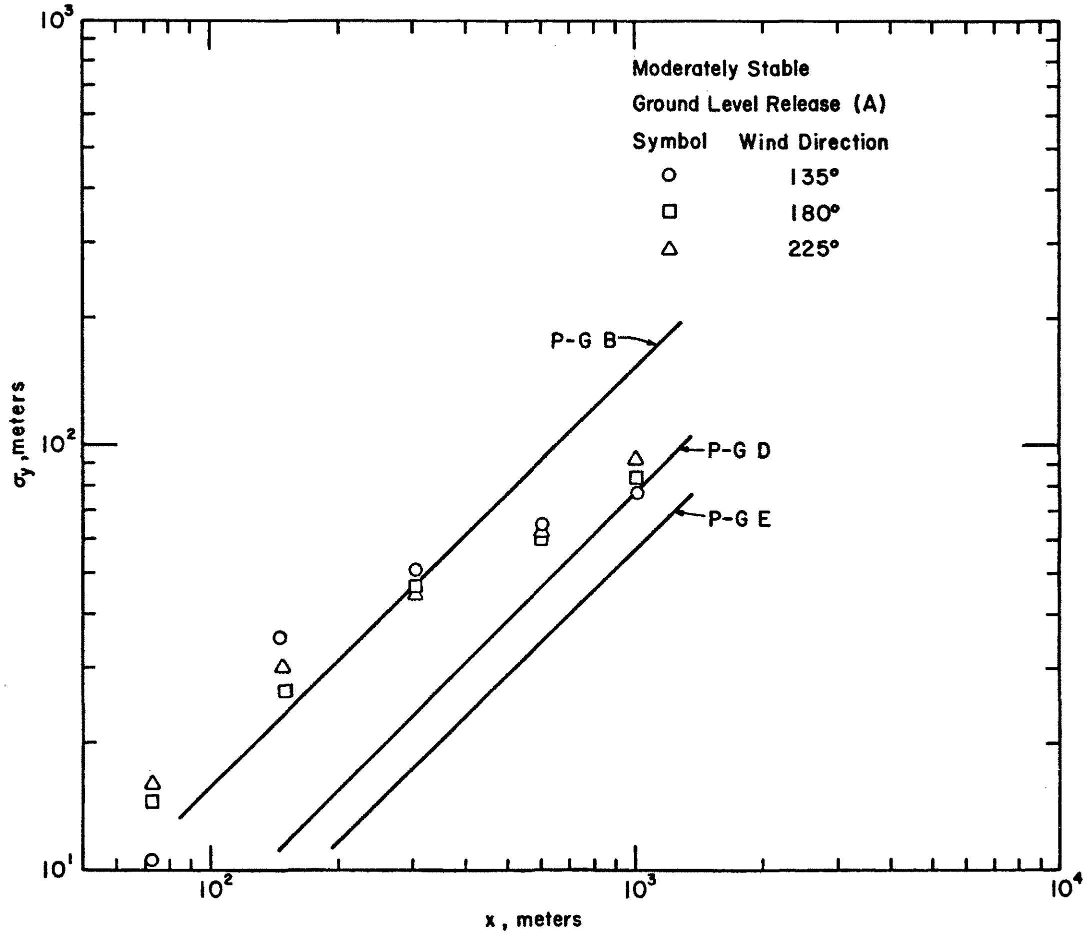

Figure 13. Plot of lateral dispersion, σ_y, versus x.

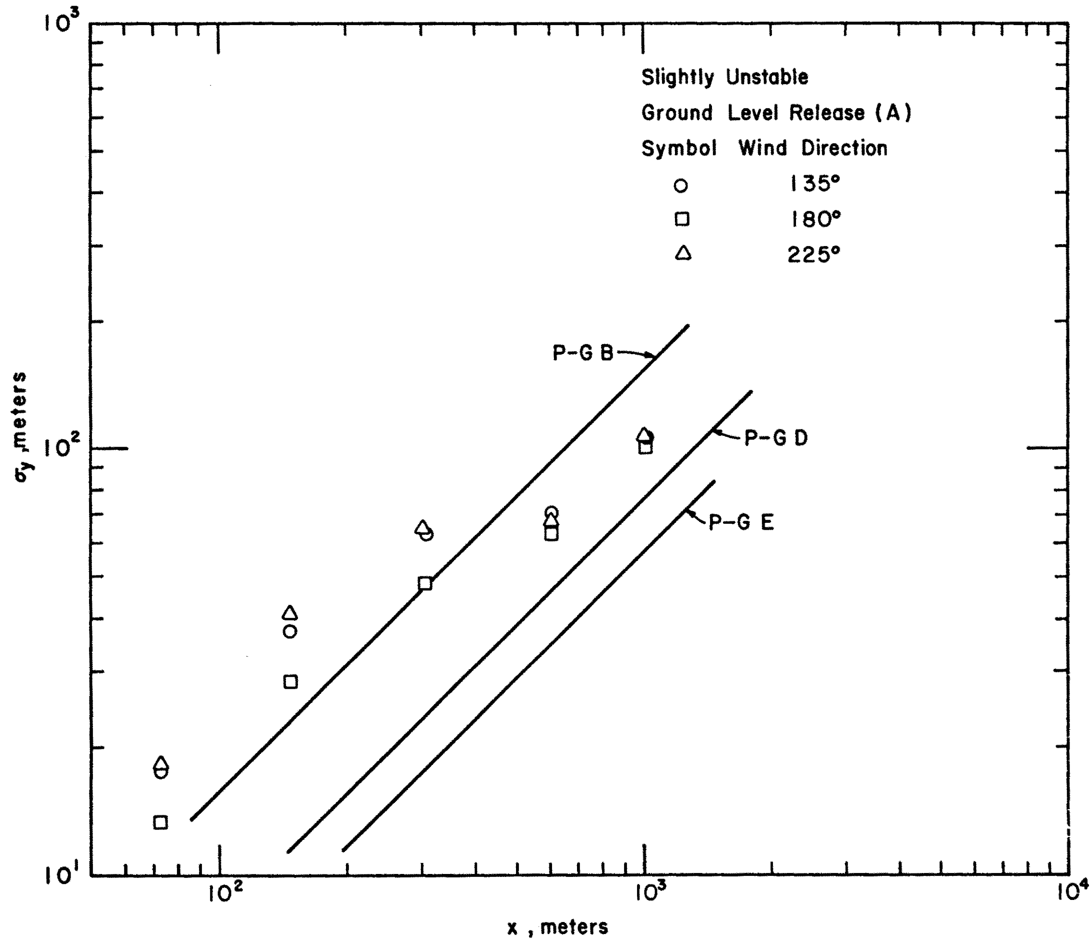

Figure 14. Plot of lateral dispersion, σ_y, versus x.

Table 4

MAXIMUM GROUND LEVEL CONCENTRATION COEFFICIENT, K_c , FOR IDEALIZED BUILDING WAKE RUNS

Obstacle Shape	Height H cm	Distance x/H	Release* Height Identification	Source Release Location 1	2	3	4
Cylindrical	7.6	1	A	.43	.34	.44	.34
		3	A	1.38	1.07	1.26	1.06
		5	A	1.29	1.06	1.10	1.01
		10	A	.71	.56	.61	.58
		20	A	.35	.28	.30	.28
		30	A	.20	.16	.17	.17
Cylindrical	7.6	1	B	.27	.13	.27	.10
		3	B	.53	.33	.51	.24
		5	B	.71	.54	.62	.36
		10	B	.56	.46	.51	.35
		20	B	.28	.23	.24	.21
		30	B	.18	.14	.16	.14
Cubical	7.6	1	A	.22	.18	.18	.17
		3	A	.43	.32	.40	.38
		5	A	.61	.43	.56	.45
		10	A	.45	.32	.21	.36
		20	A	.27	.21	.12	.22
		30	A	.17	.14	.08	.14
Cubical	7.6	1	B	.10	.08	.10	.03
		3	B	.25	.20	.24	.12
		5	B	.32	.26	.29	.20
		10	B	.32	.25	.28	.19
		20	B	.19	.17	.19	.15
		30	B	.14	.11	.12	.11
Cubical	7.6	1	C	--	--	--	--
		3	C	--	--	--	--
		5	C	.01	--	--	--
		10	C	.17	--	--	--
		20	C	.17	--	--	--
		30	C	.13	--	--	--
Cubical	7.6	1	D	--	--	--	--
		3	D	--	--	--	--
		5	D	0.0	--	--	--
		10	D	.02	--	--	--
		20	D	.08	--	--	--
		30	D	.08	--	--	--

Table 4. (Continued)

Obstacle Shape	Height H cm	Distance x/H	Release* Height Identification	Source Release Location 1	2	3	4
		1	A	.32	.28	.38	.42
		3	A	.47	.39	.47	.47
Hemispherical	7.6	5	A	.51	.43	.48	.47
		10	A	.40	.32	.35	.32
		20	A	.22	.18	.19	.17
		30	A	.14	.12	.12	.11
		1	B	.08	.20	.19	.10
		3	B	.18	.36	.31	.15
Hemispherical	7.6	5	B	.32	.41	.41	.23
		10	B	.33	.32	.34	.21
		20	B	.20	.18	.19	.15
		30	B	.15	.14	.14	.12
		1	A	1.26	1.22	1.10	.69
		3	A	1.90	1.65	1.58	1.04
Cylindrical	13.6	5	A	1.59	1.24	1.25	1.07
		10	A	.77	.59	.68	.55
		20	A	.26	.29	.23	.22
		30	A	.25	.19	.21	.20
		1	B	.45	.15	.49	.14
		3	B	1.19	.82	1.44	.43
Cylindrical	13.6	5	B	1.32	1.05	1.22	.67
		10	B	.77	.63	.63	.55
		20	B	.39	.33	.31	.31
		30	B	.25	.19	.21	.31
		1	A	.46	.31	.37	.31
		3	A	.51	.40	.47	.46
Cubical	13.6	5	A	.61	.48	.59	.49
		10	A	.42	.32	.39	.36
		20	A	.29	.21	.24	.25
		30	A	.28	.20	.22	.22
		1	B	.10	.13	1.22	.62
		3	B	.34	.25	.31	.25
Cubical	13.6	5	B	.38	.34	.41	.36
		10	B	.32	.24	.26	.25
		20	B	.24	.22	.23	.24
		30	B	.26	.21	.24	.21
		1	C	--	--	--	--
		3	C	--	--	--	--
Cubical	13.6	5	C	.27	--	--	--
		10	C	.27	--	--	--
		20	C	.19	--	--	--
		30	C	.17	--	--	--

Table 4. (Continued)

Obstacle Shape	Height H cm	Distance x/H	Release* Height Identification	Source Release Location 1	2	3	4
		1	D	--	--	--	--
		3	D	--	--	--	--
Cubical	13.6	5	D	0.0	--	--	--
		10	D	.03	--	--	--
		20	D	.09	--	--	--
		30	D	.13	--	--	--
		1	A	--	--	--	--
		3	A	.69	.56	.60	.97
Hemispherical	13.6	5	A	.66	.53	.58	.78
		10	A	.46	.37	.41	.44
		20	A	.26	.21	.23	.23
		30	A	.17	.14	.15	.15
		1	B	.15	.23	.17	.13
		3	B	.38	.45	.36	.33
Hemispherical	13.6	5	B	.46	.52	.43	.50
		10	B	.52	.45	.43	.48
		20	B	.35	.29	.29	.29
		30	B	.26	.21	.22	.22

* A = Roof top release
B = Stack height of 0.25 H above building
C = Stack height of 0.5 H above building
D = Stack height of 1.0 H above building
H = Building height

The maximum ground level concentration occurred for the vent height equal to building height indicating the maximum downwash induced by the buildings. An increase in the vent height resulted in lower concentrations as expected. For cubical shaped buildings, the building effects were reduced considerably for the vent height of 0.5 H above the building and there was no building influences for the vent height of 1.0 H above the building for release location 1. Hence, for cylindrical and hemispherical buildings only two lower vent heights were investigated.

The maximum ground level concentration coefficients, K_c, are plotted against x/H for two lower vent heights in Figures 15, 16 and 17 for cylindrical, cubical and hemispherical buildings, respectively. The approach boundary layer velocity profile and source gas exit velocity were the same for all experiments. However, the velocity ratio, defined as a ratio of source exit velocity to approach velocity at vent height, is smaller for larger building shape. This result in larger plume entrainment and higher concentrations is shown in Figures 15 through 17 for the same shape but larger building. This difference in concentration disappeared around 20 to 30 heights downstream of the building.

Figures 18, 19, 20 and 21 display the maximum ground level concentrations against x/H for the three different building shapes but the same size building and vent height. The ground level concentrations were maximum downwind of the cylindrical building, minimum in the wake of the cubical building, and in between downwind of the hemispherical building. There are two possible reasons for the building shape effects. The first one is related to the flow separation line on the building. The flow separation is delayed maximum for the cylindrical building and somewhat less delayed for the hemispherical building. The flow separation lines on the cubical building are defined by the geometry. Thus, it is expected to have the largest recirculating cavity zone behind the cubical building and smallest recirculating cavity in the wake of the cylindrical building. Thus, the initial plume dilution in the wake of the cylindrical building is less as compared with the cubical building. Secondly, two counterclockwise rotating horseshoe vortices have been observed by Kothari et al. (1979), Hansen et al. (1975) and Kothari et al. (1981) in the wakes of cubical, hemispherical and cylindrical buildings deeply submerged in the turbulent boundary layer, respectively. The horseshoe vortices were the strongest in the wake of

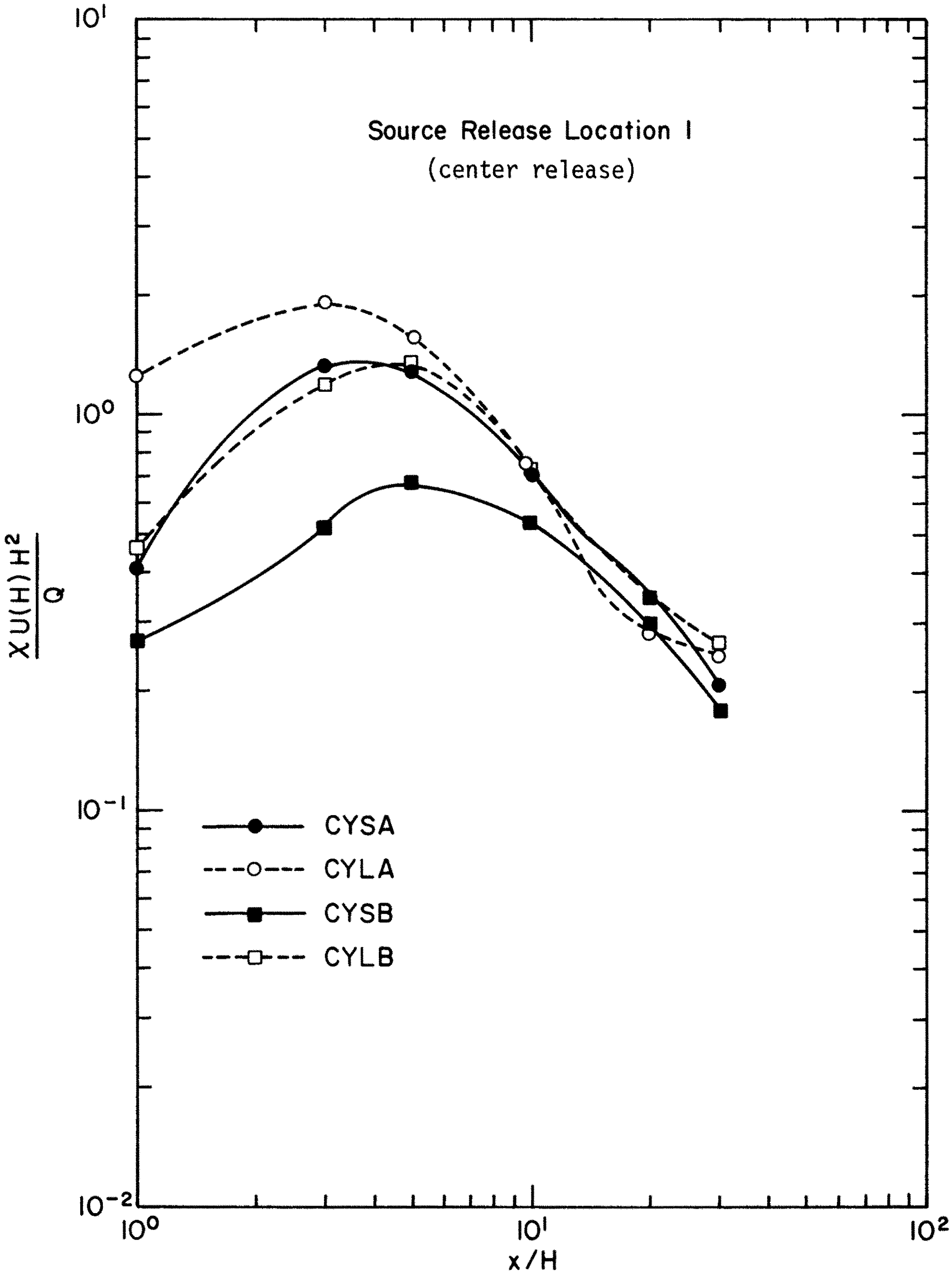

Figure 15. Plot of maximum ground level concentration coefficient, K_c versus x/H for cylindrical buildings CYSA, CYLA, CYSB and CYLB.

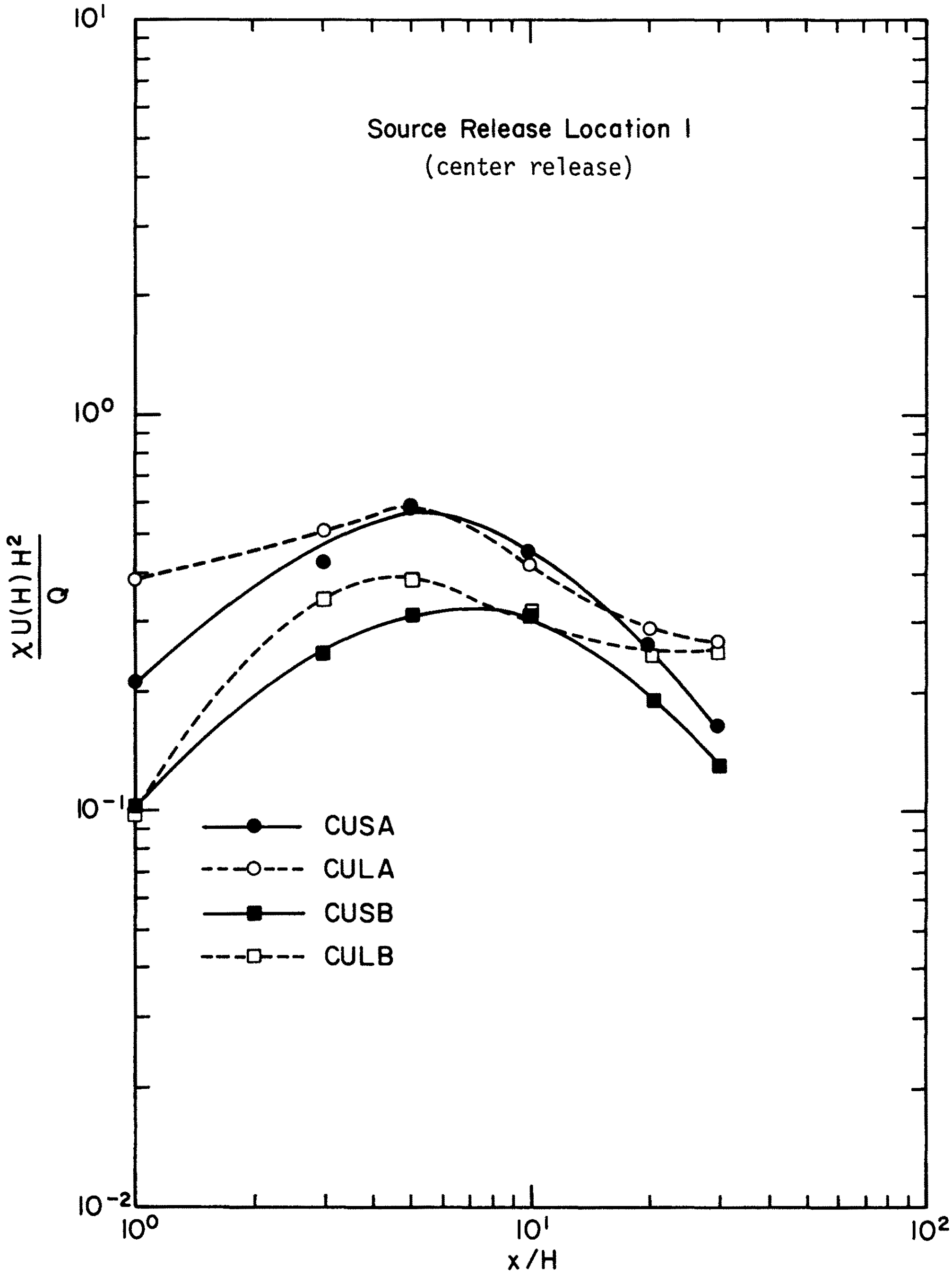

Figure 16. Plot of maximum ground level concentration coefficient, K_c versus x/H for cubical buildings CUSA, CULA, CUSB and CULB.

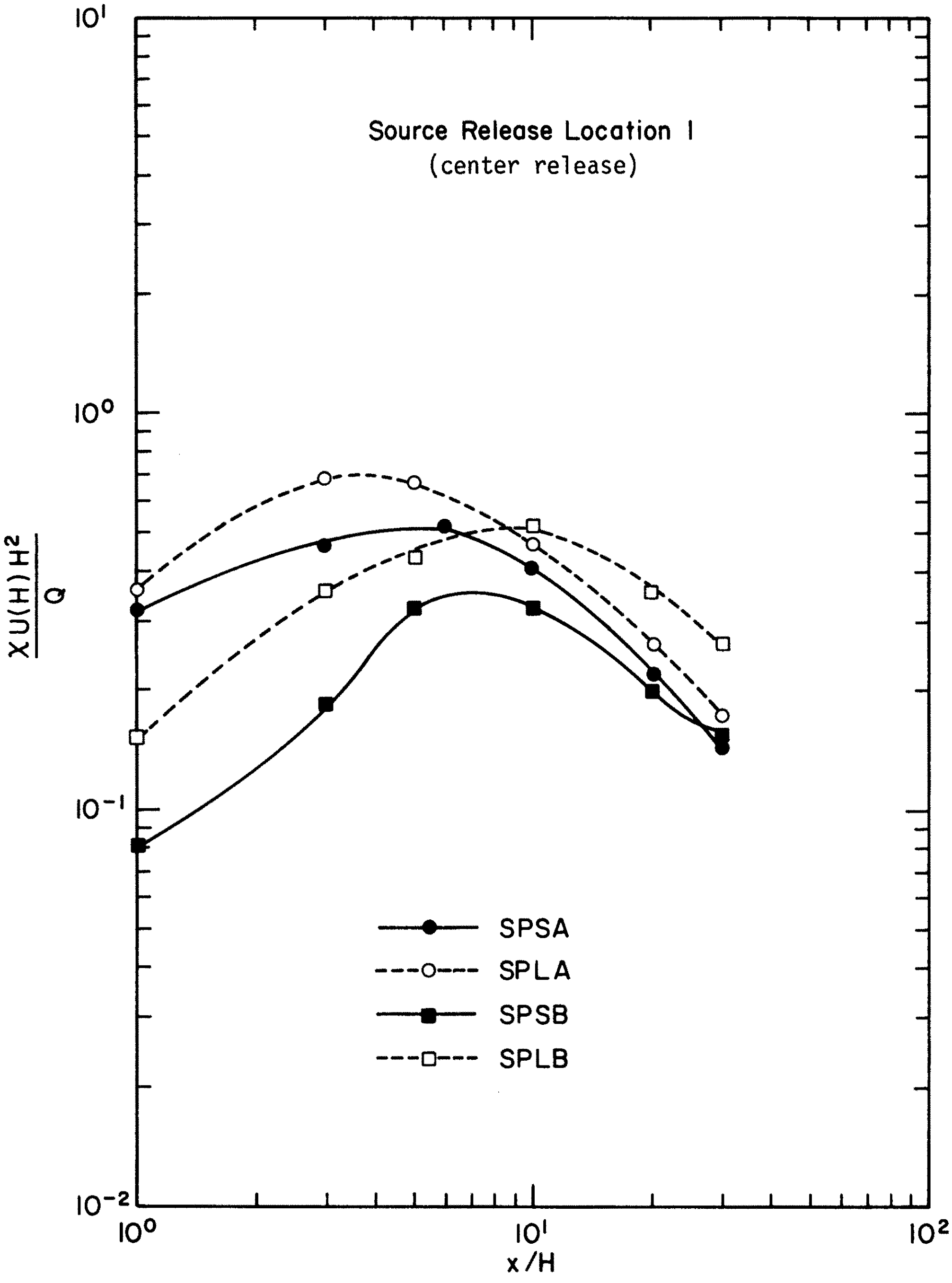

Figure 17. Plot of maximum ground level concentration coefficient, K_c versus x/H for hemispherical buildings SPSA, SPLA SPSB and SPLB.

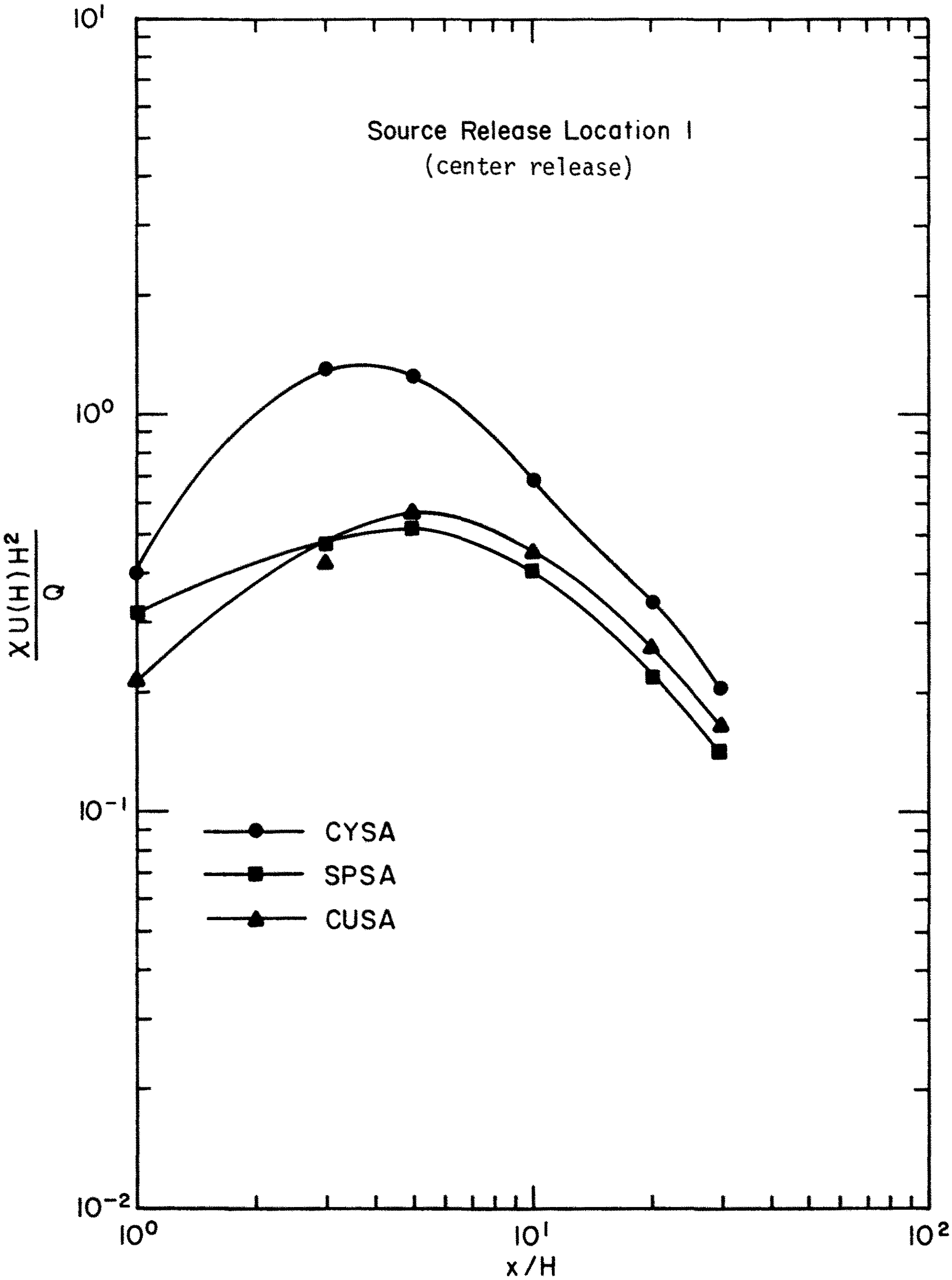

Figure 18. Plot of maximum ground level concentration coefficient, K_c versus x/H for buildings CYSA, SPSA and CUSA.

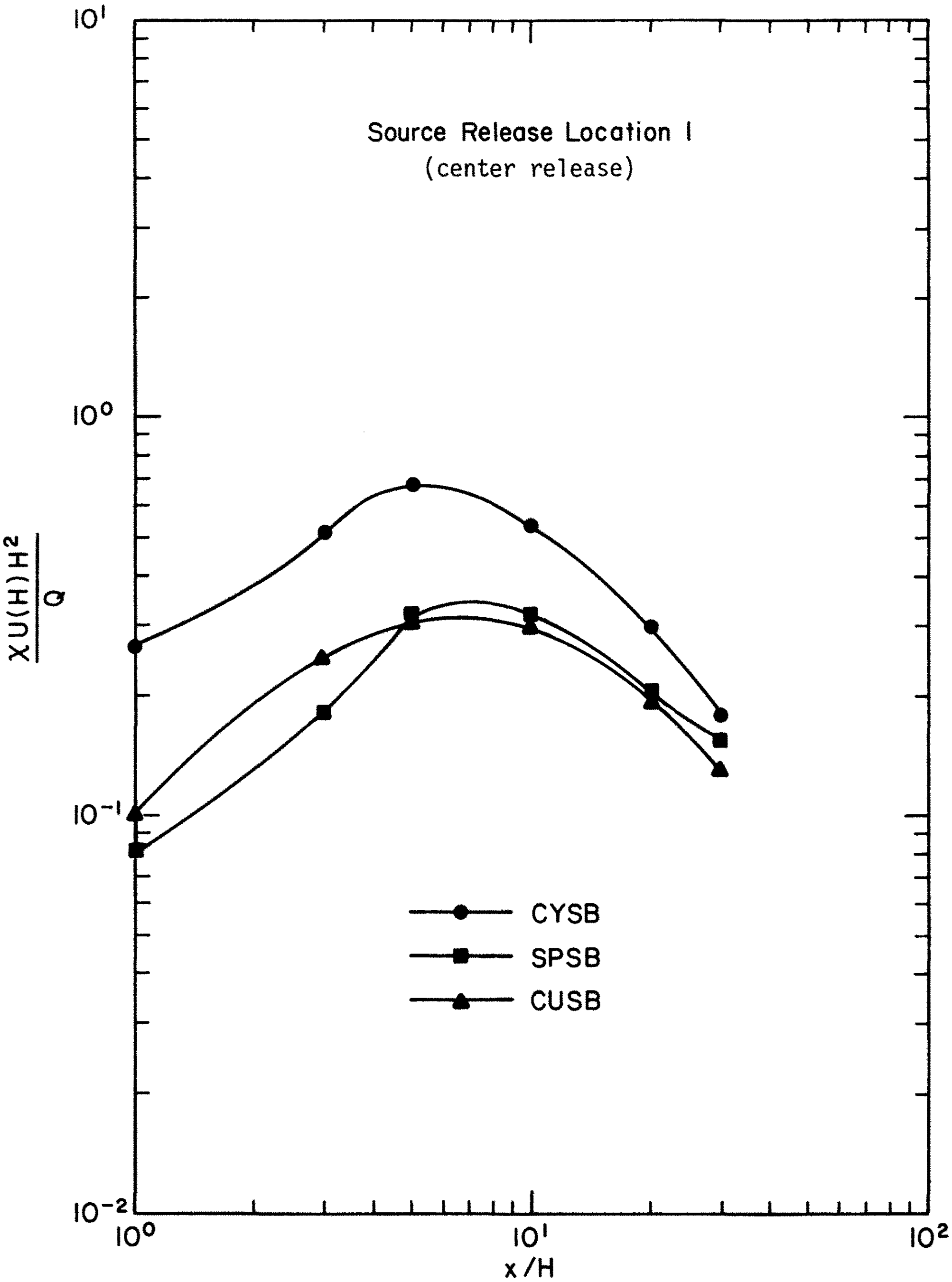

Figure 19. Plot of maximum ground level concentration coefficient, K_c versus x/H for buildings CYSB, SPSB and CUSB.

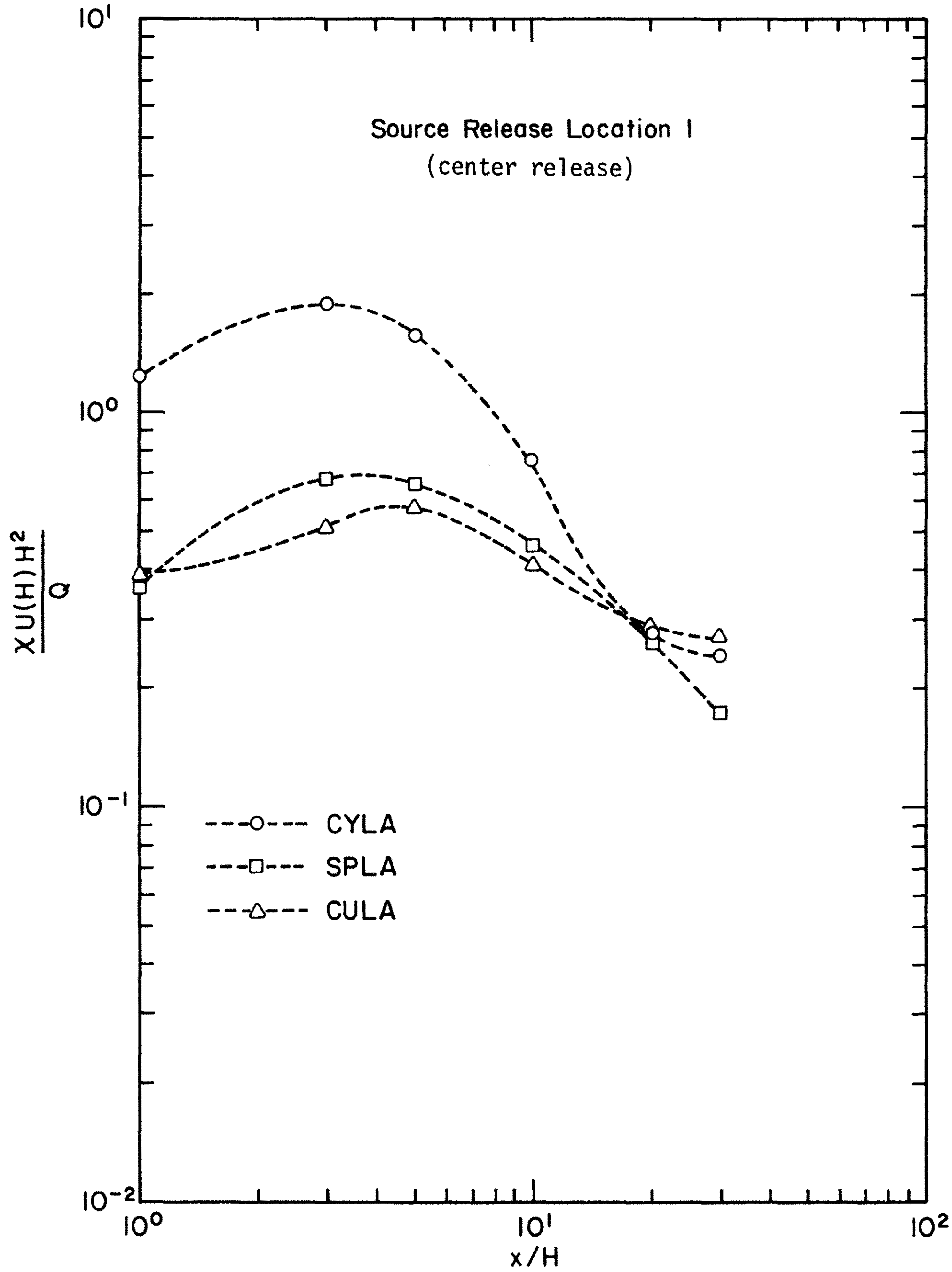

Figure 20. Plot of maximum ground level concentration coefficient, K_c versus x/H for buildings CYLA, SPLA and CULA.

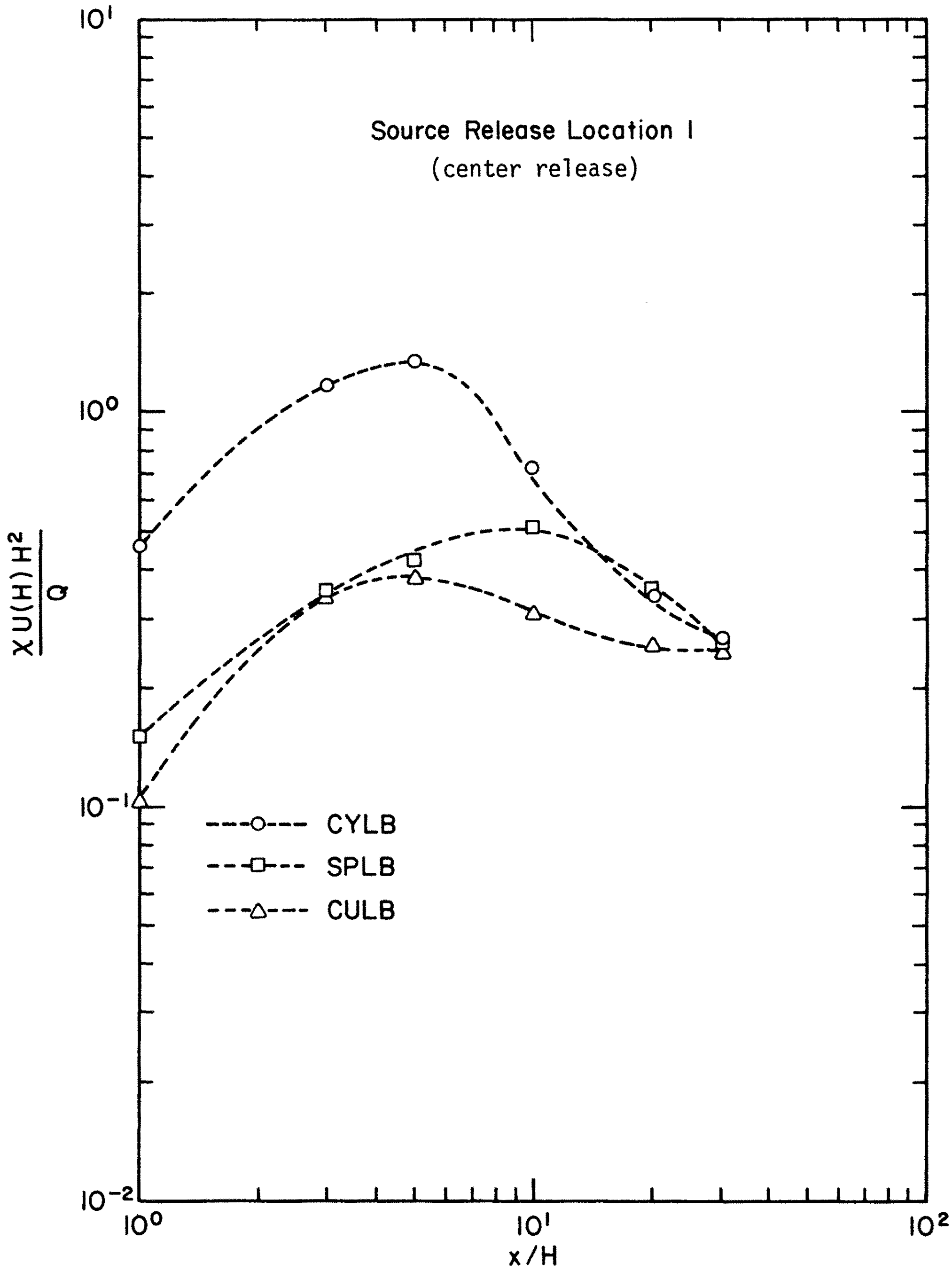

Figure 21. Plot of maximum ground level concentration coefficient, K_c versus x/H for buildings CYLB, SPLB and CULB.

cylindrical buildings and the weakest in the cubical building wake. These vortices bring the plume downward towards the ground along the centerline of the building and result in higher concentration. Thus, the strong horseshoe vortices and lesser initial plume dilution results in higher concentrations in the cylindrical building wake.

Figures 22 and 23 show the maximum ground level concentration versus x/H for the cylindrical building and vent heights for four release locations on the building. For the roof top release, the maximum ground level concentrations are about the same for release locations 1, 2 and 3, whereas release location 4 shows slightly less concentration in the near wake. At the vent height of 0.25 H above the building, the near wake concentrations are highly dependent on the release location. However, this concentration difference disappeared within about ten heights downwind of the building. The similar results were obtained for the cubical and hemispherical buildings.

FLOW VISUALIZATION

Black and white stills, color slides and 16 mm movie were exposed and provided satisfactory visual documentation of the plume drift. Titanium tetrachloride was used to make the plume visible. Wind directions 0, 45, 90, 112.5, 135, 157.5, 180, 202.5, 225, 247.5 and 270 were investigated with neutral flow conditions for each of the three release locations. For the idealized building wake runs, the flow visualization study was performed with all six buildings, four vent heights and a center release location (location 1). The pictures, slides and movie were furnished under a separate cover.

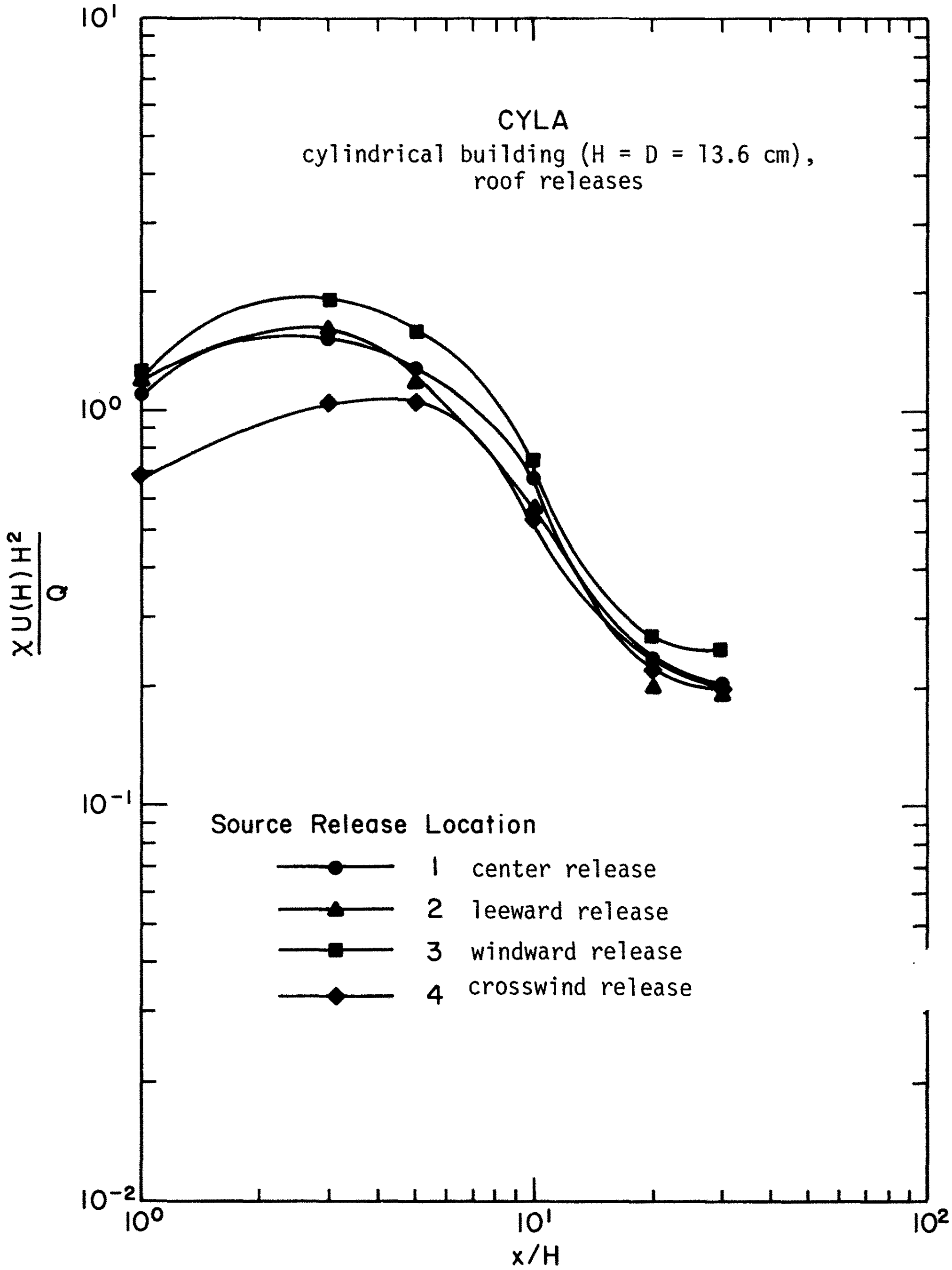

Figure 22. Plot of maximum ground level concentration coefficient, K_c versus x/H for building CYLA and all four release locations.

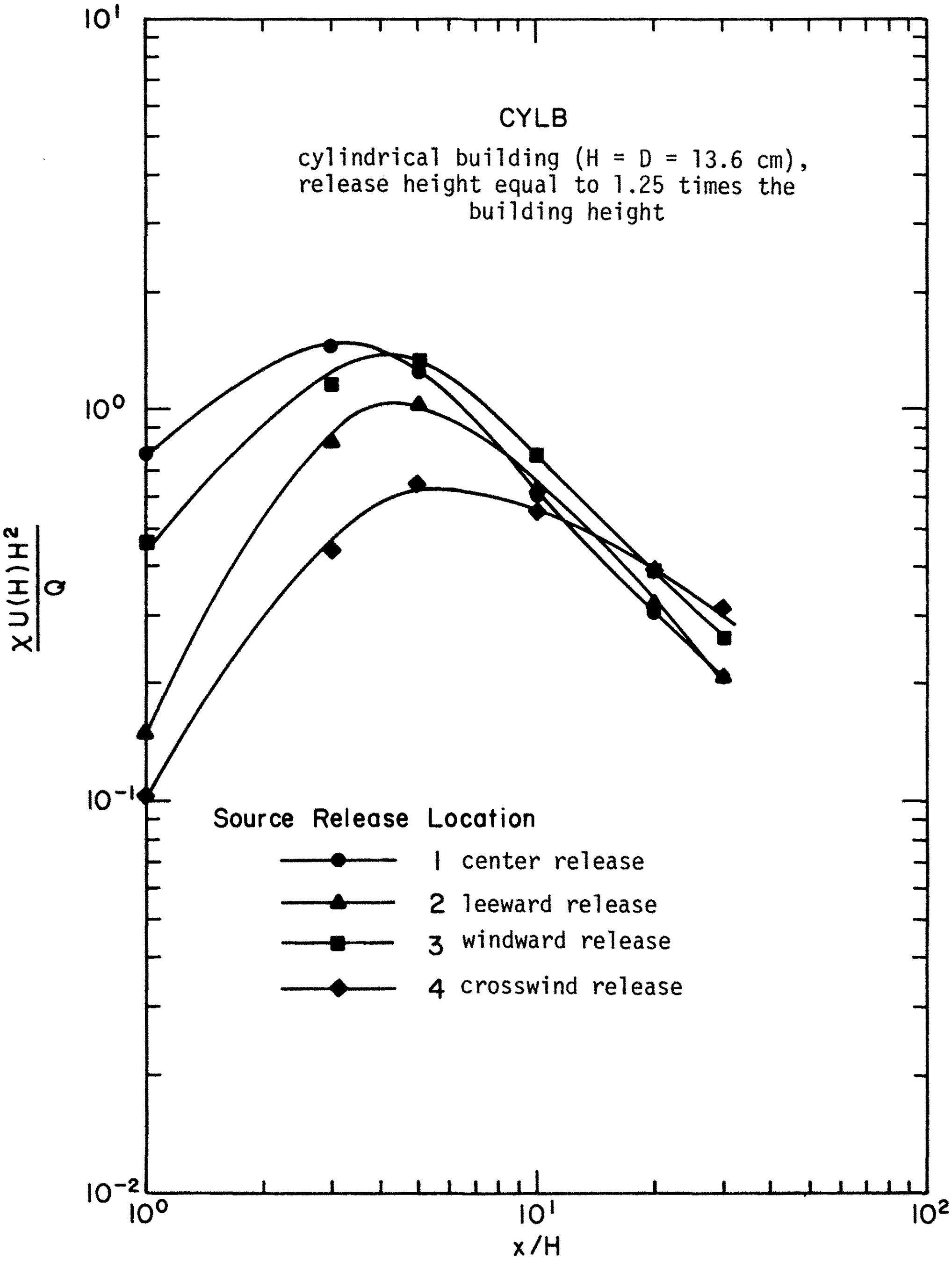

Figure 23. Plot of maximum ground level concentration coefficient, K_c versus x/H for building CYLB and all four release locations.

Chapter 3

COMPARISON OF FIELD AND WIND-TUNNEL EXPERIMENTS

The chapter describes the weighted algorithm method developed by Kothari et al. (1980) to estimate field concentrations under nonsteady meteorological conditions from wind-tunnel experiments. The weighted algorithm method is applied to the present nuclear power experiments and the results of it are compared against the direct field measurements of Thuillier (1979).

TIME-WEIGHTED LABORATORY MEASUREMENT ALGORITHM

Laboratory measurements of dispersion are generally scheduled for a number of combinations of wind direction, wind speed, and thermal stratification conditions. This matrix must be large enough to reasonably reproduce the range of expected situations; however, the number must remain finite to be economical. It is proposed that the measured concentration fields may also be combined in a time-weighted manner which reflects the influence of gustiness, meandering, and thermal structure.

Halitsky (1969) proceeded in this spirit when he compared rooftop concentration patterns detected during field experiments with patterns obtained by weighting wind-tunnel measurements made over a model placed at a series of wind orientations. The weighted laboratory data reproduced the magnitude and distribution of concentrations quite well.

General Formulation

It is generally accepted that the concentration, χ, measured at some sample location r and ϕ will be a function of source strength Q, speed U, wind direction orientation, θ and thermal stratification, Ri. The time average value of a fluctuating concentration over a time interval T may then be expressed as

$$\bar{\chi}(r,\phi) = \frac{1}{T} \int_{t}^{t+T} \chi(Q(t),\ U(t),\ \theta(t),\ Ri(t);\ r,\phi)\ dt \qquad (3\text{-}1)$$

Alternatively given a constant source strength one might construct a value for $\bar{\chi}$ by utilizing the joint probability distribution of U, θ and Ri over the test period. Let the joint probability distribution be $p(U,\phi,Ri)$, then

$$\bar{\chi}(r,\phi) = \int_{Ri} \int_{\theta} \int_{U} p(U,\theta,Ri)\chi(U,\theta,Ri;r,\phi)\, dUd\theta dRi \qquad (3\text{-}2)$$

In the above formulations it is assumed that:

Concentration wind-tunnel data are continuously available for any combination of wind speed, direction, and stability.

Mean wind and temperature characteristics are available from the field site at any instant during the test period, T.

Meteorological data available from a single site near the proposed field release are characteristic of the flow over the entire site.

The meteorological characteristics are quasi-steady over a period longer than the time it takes a particle to travel from the release point to a sample position. This implies that directional changes of the trajectory of an air parcel between the release point and the sample location are insignificant.

Segmented Time Approximation

Similarity theory suggests that for nonbuoyant plumes the dimensionless concentration coefficient, K, for equivalent field and laboratory conditions should be equal. This coefficient is defined as

$$K = \frac{\chi UA}{Q} \qquad (3\text{-}3)$$

where U, A, and Q, are characteristic velocity, area, and source scales. Prior laboratory experience confirms that these parameters are indeed equal when sampling times are less than 10 minutes; hence,

$$K_f = K_m \qquad (3\text{-}4)$$

and

$$\chi_f = (\frac{Q_f}{U_f A_f})\ Km \qquad (3\text{-}5)$$

where f and m subscripts indicate field and model situations respectively. Note that it is unnecessary to run laboratory tests for all source strength and velocity combinations since a single normalized concentration parameter defines such conditions. Frequently, however, field or laboratory data are reported with different characteristic length scales or velocity reference height. In such cases the comparison algorithm must incorporate scale and velcity profile adjustments.

Given a field test for every 2-minute average combination of the variables θ and Ri, one may represent an hour average version of Eq. (3-5) by the sum

$$\bar{\chi}_f(r,\phi) = \sum_{i=1}^{30} \frac{(Q_f)_i}{(U_f)_i A_f} (K_m)_i \qquad (3\text{-}6)$$

or

$$C_f(r,\phi) = \frac{\bar{\chi}_f(r,\phi)\bar{U}_f}{Q_f} = \sum_{i=1}^{30} \frac{(Q_f)_i}{Q_f} \frac{\bar{U}_f}{(U_f)_i} \frac{(K_m(r,\phi))_i}{A_f} \qquad (3\text{-}7)$$

where the overbar represents an hour average value.

Unfortunately it is not economically credible to run a laboratory test for every potential combination of Q, U, θ, and Ri; hence, there is always a finite number of discrete conditions among which data must be interpolated. An approximation has been prepared to estimate mean average concentration based on the summation of such a discrete data set.

Typically laboratory data may be available for a matrix of one to NS thermal stratification conditions for each of one to NW wind orientations. An interpolation method is proposed to estimate $(K_m)_i$ for the non-incremental 2-minute average values of $(\theta_f)_i$ and $(Ri_f)_i$. The following notation is introduced:

$$(K_m(r,\phi))_i = \sum_{j=1}^{NS} \sum_{k=1}^{NW} W_{ijk} K_{jk}(r,\phi) \tag{3-8}$$

where K_{jk} is a set of model concentration data measured for a specific member of the thermal stratification and wind orientation model test matrix, W_{ijk} is a weight function varying in magnitude from 0 to 1.0.

The determination of the weight factors for the ith interval of a given hour period is accomplished in three steps. First, the influence of wind orientation and stratification are assumed linearly independent; thus

$$W_{ijk} = WS_{ij}\ WW_{ik} \tag{3-9}$$

where WS and WW are contributions due to stratification and orientation, respectively.

The stability effects are estimated in the second step by a simple linear interpolation on bulk Richardson number, that is

a) if $(Ri_f)_i < (Ri_m)_1$, then $WS_{i1} = 1.0$

$$WS_{ij} = 0.0,\ j \neq 1$$

b) if $(Ri_m)_j \leq (Ri_f)_i \leq (Ri_m)_{j+1}$, then

$$WS_{ij} = \frac{(Ri_m)_{j+1} - (Ri_f)_i}{(Ri_m)_{j+1} - (Ri_f)_j}$$

$$WS_{i(j+1)} = \frac{(Ri_f)_i - (Ri_m)_j}{(Ri_m)_{j+1} - (Ri_m)_j}\ , \text{ otherwise}$$

$$WS_{ij} = 0.0,$$

c) if $(Ri_m)_{NS} < (Ri_f)_i$, then

$$WS_{i(NS)} = 1.0$$

$$WS_{ij} = 0.0,\ j \neq NS$$

Although the adequacy of such linear interpolation may be questionable, it does not appear a more sophisticated interpolation scheme is appropriate at this time. Among those stratification classification schemes proposed for predictive schemes the bulk Richardson number was judged by Hanna et al. (1977) and Weber et al. (1977) to be reasonably reliable.

The wind orientation weight factor is also estimated by simple linear interpolation. That is, if

$(\theta_m)_k \le (\theta_f)_i \le (\theta_m)_{k+1}$ then

$$WW_{ik} = \frac{(\theta_m)_{k+1} - (\theta_f)_i}{(\theta_m)_{k+1} - (\theta_m)_k}$$

$$WW_{i(k+1)} = \frac{(\theta_f)_i - (\theta_m)_k}{(\theta_m)_{k+1} - (\theta_m)_k} \text{ , otherwise}$$

$$WW_{ik} = 0.0$$

Of course the recommended interpolation scheme is not yet adequate to fully account for wind direction variation. It is proposed to assign a revised bearing to the wind-tunnel data. The concentration at grid point r, ϕ is given the value of the model concentration of the grid point closest to $r, \phi - (\theta_f)_i + (\theta_m)_k$. This device prevents the appearance of lobbed surface concentration contours which result when one simply superimposes orientation unmodified data.

If the velocity reference height stipulated for field measurements is Z_f, whereas the equivalent reference height utilized for reference velocities for model data is Z_m, then a correction factor must be applied to laboratory results based on the laboratory measured velocity profiles. Hence if

$$f_j = \left(\frac{Z_f}{Z_m}\right)^{p_j} \qquad (3\text{-}10)$$

where p_j is the velocity profile power-law coefficient. Then incorporating the weight factors, the rotation, and the reference height corrections in Eq. (3-8) produces

$$(K_m(r,\phi))_i = \sum_{j=1}^{NS} f_j WS_{ij} \sum_{k=1}^{NW} WW_{ik} K_{jk}(r,\theta-(\theta_f)_i + (\theta_m)_k) \tag{3-11}$$

The final laboratory-weighting algorithm proposed herein incorporates Eq. (3-11) into Eq. (3-7) such that

$$\bar{C}_f(r,\phi) = \sum_{i=1}^{30} \frac{(Q_f)_i}{Q} \frac{\bar{U}_f}{(U_f)_i} \frac{1}{A_f} \sum_{j=1}^{NS} f_j WS_{ij}$$

$$X \sum_{k=1}^{NW} WW_{ik} K_{jk}(r,\phi-(\theta_f)_i + (\theta_m)_k) \tag{3-12}$$

Equation (3-12) presented above is the basis for a computer program to calculate 1-hour mean field concentration using wind-tunnel data. The details of the program are described by Bouwmeester, Kothari and Meroney (1979).

FIELD EXPERIMENTS

A series of 44 tests was conducted at the nuclear power plant located in the midwest in the summer of 1978. During each test period a tracer gas was released from the nuclear power plant, gas samples were taken at arc distances of 300 m and 1000 m downwind, and meteorological conditions were recorded at a nearby meteorological tower. The run numbers 1 to 16, 17 to 33 and 34 to 44 in the field tests corresponds to releases from turbine building roof top, reactor building stack and ground level, respectively. The release locations are the same as in the corresponding wind-tunnel experiments.

The sampling grid for this study consisted of two circular arcs centered on the reactor containment vessel with radii of 300 m and 1000 m. Samplers were spaced every 12 degrees (approximately) and every 6 degrees (approximately) at the arc distance of 300 m and 1000 m respectively and started from west to east in clockwise direction. Meteorological data was obtained from the instrumentation mounted on a 50 m nearby tower. Sensors to measure temperatures, horizontal wind velocities and horizontal and vertical wind angles were mounted at heights of 10 m and 50 m. One-hour average values of the meteorological data were reported by Thuillier (1979). Meteorological data averaged over successive 2-minute increments during the 1-hour test periods were also supplied by Thuillier directly to the authors. The latter information was used to define the meteorological condition utilized in construction of time-weighted concentration averages from the wind-tunnel data. For each 2-minute interval, bulk Richardson numbers were calculated based on measurements taken at 10 m and 50 m levels. The wind direction data sometimes show substantial variation of the wind direction with height; nevertheless, the characteristic wind direction was selected at the release height. For some field test runs fewer number of velocity and temperature data were reported and hence the weighted algorithm was applied for fewer number of points.

COMPARISON OF WEIGHTED WIND TUNNEL AND FIELD MEASUREMENTS

The algorithm developed in the previous section has been incorporated into a computer program to predict hour average concentrations as measured at the nuclear power plant. Wind-tunnel measurements of concentration fields downwind of a 1:400 scale model of the nuclear power plant facility were combined with 2-minute interval meteorological records taken during the field tests to produce a series of synthesized 1-hour average concentration data.

Figure 24 shows the typical results of the weighted laboratory data calculations corresponding to field test number 44. The wind-tunnel data were also weighted for two additional arcs at 147 m and 609 m as shown in Figure 24. This model shows considerable improvement over direct comparison of 1-hour average field data to 10-minute equivalent laboratory measurements. The weighting algorithm is generally more realistic in predicting centerline values as well as the horizontal spread of the plume. The maximum ground level concentration coefficients, $\frac{\chi U}{Q}$ for the field data and algorithm calculated values are compared in Table 5 for the 300 m and 1000 m arc distances. If one considers the ratios c/a and d/b it is evident that on an average the algorithm slightly underpredicts at the 300 m arc and overpredicts by two times at the 1000 m arc the observed maximum field concentration. These weighted predictions are 50 percent better than direct comparison to wind-tunnel data.

If physical modeling is expected to be a useful means to predict concentrations in the field, there must be a linear relationship between measurements in the laboratory and field. The best estimate of the population correlation coefficients is the sample correlation coefficient commonly calculated as:

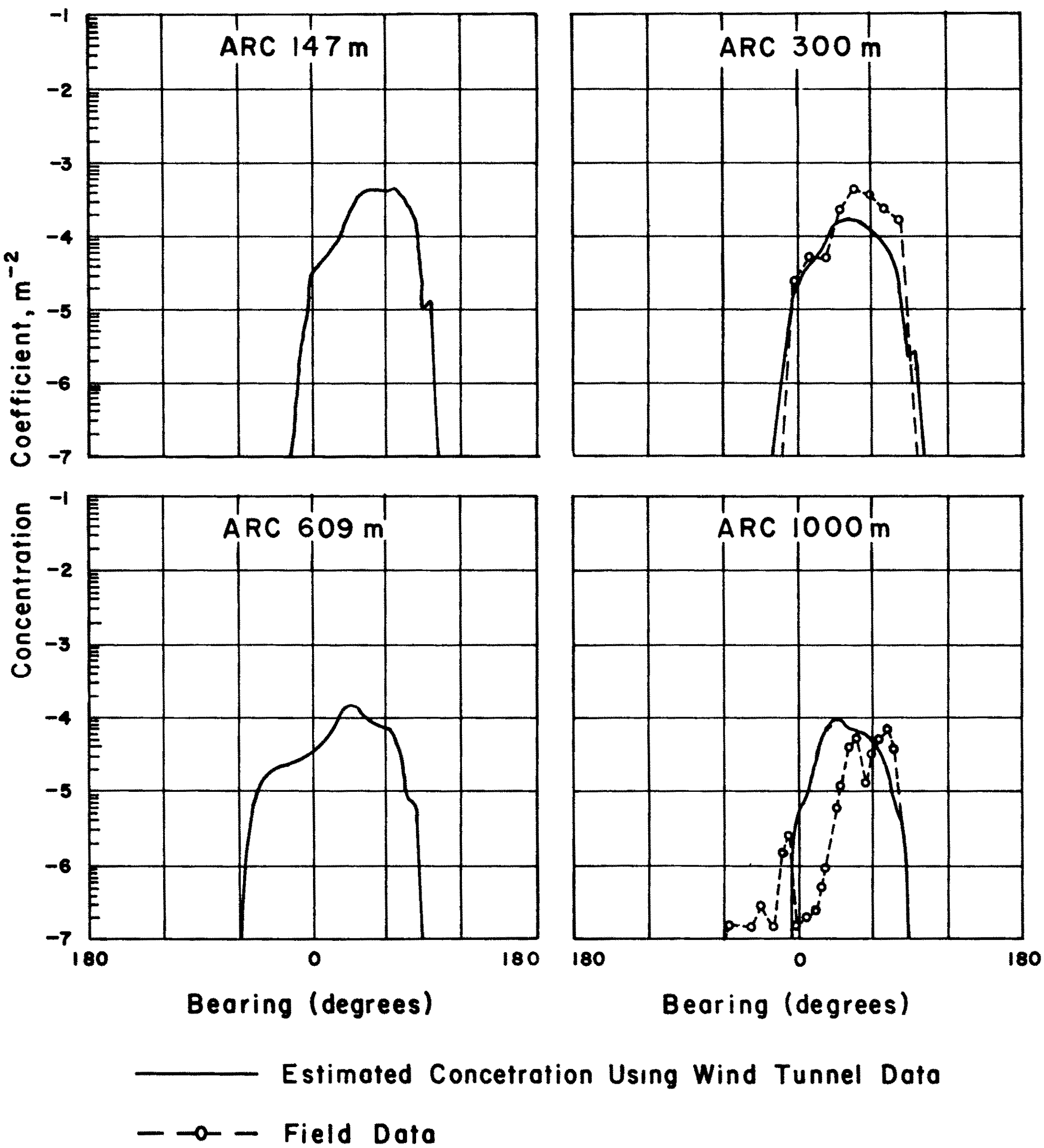

Figure 24. Comparison of $\frac{\chi U}{Q}$ (power of ten) for run number 44.

Table 5

COMPARISON OF FIELD DATA WITH WEIGHTED WIND-TUNNEL DATA USING ALGORITHM

Field run number	Release* location	U_f m/sec	θ_f degree	Field Stability (Golder)	Field $\frac{\chi U}{Q}$ x 10^4 m^{-2} maximum @ 300 m a	Field $\frac{\chi U}{Q}$ x 10^4 m^{-2} maximum @ 1000 m b	Algorithm $\frac{\chi U}{Q}$ x 10^4 m^{-2} maximum @ 300 m c	Algorithm $\frac{\chi U}{Q}$ x 10^4 m^{-2} maximum @ 1031 m d	Wind Tunnel $\frac{\chi U}{Q}$ x 10^4 m^{-2} maximum @ 300 m e	Wind Tunnel $\frac{\chi U}{Q}$ x 10^4 m^{-2} maximum @ 1031 m f	$\frac{c}{a}$	$\frac{d}{b}$	$\frac{e}{a}$	$\frac{f}{b}$
1	B	1.1	171	-	0.96	0.13	1.47	0.45	-	-	1.53	3.46	-	-
2	B	2.0	184	B	1.10	0.16	1.49	0.74	3.37	1.39	1.35	4.62	3.06	8.68
3	B	2.2	167	C	1.50	0.21	1.67	1.27	3.69	1.42	1.11	6.04	2.46	6.76
4	B	1.5	118	-	2.55	0.53	1.46	0.47	-	-	0.57	0.89	-	-
5	B	1.7	170	B	0.60	0.08	1.12	0.42	3.37	1.39	1.87	5.25	5.61	17.38
6	B	2.2	171	C	0.90	0.14	1.19	0.88	3.69	1.42	1.32	6.29	4.10	10.14
7	B	2.8	139	C	1.96	0.30	1.40	0.54	3.06	1.10	0.71	1.80	1.56	3.66
8	B	1.7	112	B	0.44	0.08	1.20	0.31	4.10	1.39	2.72	3.88	9.31	17.37
9	B	4.0	157	E	16.69	1.67	1.87	0.82	5.36	2.15	0.11	0.49	0.32	1.28
10	B	4.5	164	E	1.61	2.07	1.66	0.77	5.36	2.15	1.03	0.37	3.32	1.04
11	B	4.6	164	E	5.80	2.24	1.82	1.48	5.36	2.15	0.31	0.66	0.94	0.96
12	B	4.3	157	E	8.41	3.00	1.52	1.29	5.36	2.15	0.18	0.43	0.64	0.72
13	B	2.2	185	C	1.74	0.41	1.88	0.96	3.69	1.42	1.08	2.34	2.12	3.46
14	B	1.8	200	C	0.51	0.11	2.11	0.66	3.21	1.44	4.14	6.00	6.29	13.09
15	B	1.6	239	C	2.29	0.22	2.06	0.52	4.32	1.47	0.90	2.36	1.88	6.68
16	B	1.8	296	-	0.86	0.27	1.59	0.42	-	-	1.85	1.56	-	-
17	C	4.3	153	C	2.41	0.30	1.40	0.61	2.12	1.19	0.58	2.03	0.88	3.97
18	C	4.4	160	C	3.48	0.48	1.02	0.70	2.12	1.19	0.29	1.46	0.61	2.48
19	C	4.1	166	C	2.50	0.44	1.43	1.08	2.12	1.19	0.57	2.45	0.85	2.70
20	C	4.3	149	C	1.84	0.36	1.21	0.59	2.12	1.19	0.66	1.64	1.15	3.30
25	C	4.5	188	C	5.18	1.69	1.89	1.54	2.38	1.16	0.36	0.91	0.46	0.69
26	C	4.5	182	C	2.88	1.25	1.10	0.90	2.38	1.16	0.38	0.72	0.83	0.93
27	C	4.6	183	C	4.31	1.73	1.13	1.28	2.38	1.16	0.26	0.74	0.55	0.67
28	C	5.1	203	C	4.14	1.08	1.92	0.87	3.80	1.38	0.46	0.81	0.92	1.28
34	A	3.3	169	D	7.87	3.27	3.66	0.87	4.70	1.98	0.47	0.27	0.60	0.61
35	A	2.7	171	D	5.37	3.43	3.19	1.35	4.70	1.98	0.59	0.39	0.88	0.58
36	A	2.0	156	D	4.43	1.68	3.05	1.14	5.16	2.00	0.69	0.68	1.16	1.19
37	A	4.6	226	C	8.67	1.01	1.39	1.99	5.66	1.30	0.16	1.97	0.65	1.29
38	A	3.5	217	C	8.56	1.60	1.94	1.33	5.66	1.30	0.23	0.83	0.66	0.81
39	A	3.5	216	C	7.15	1.58	2.10	1.03	5.66	1.30	0.29	0.65	0.79	0.82
40	A	2.2	199	B	2.37	0.32	3.21	1.11	4.03	1.61	1.35	3.47	1.70	5.03
41	A	3.2	214	B	2.63	0.77	2.08	1.27	1.32	1.91	0.79	1.65	0.50	2.48
42	A	3.1	224	B	4.47	0.48	1.48	0.81	1.32	1.91	0.33	1.69	0.30	3.98
43	A	3.1	216	B	2.74	0.52	1.76	0.85	1.32	1.91	0.64	1.63	0.48	3.67
44	A	3.1	223	B	3.57	0.74	1.83	0.99	1.32	1.91	0.51	1.34	0.37	2.58
									Average		0.87	2.04	1.75	4.07
									Average without run numbers 9,10,11,12		0.93	2.24	1.81	4.51

*A--ground level release, U_f and θ_f at 10 m height.

B--turbine building release, U_f at 23.5 m height and θ_f at 10 m height.

C--reactor vent (stack height) release, U_f and θ_f at 50 m height.

$$r = \frac{n\Sigma xy - \Sigma x\Sigma y}{[n\Sigma x^2-(\Sigma x)^2]^{\frac{1}{2}}[n\Sigma y^2-(\Sigma y)^2]^{\frac{1}{2}}} \qquad (3\text{-}13)$$

For the present case x and y represent wind-tunnel algorithm calculated data and field data respectively and n is number of data points. The correlation coefficient r always lies between -1 and +1. If, and only if, all points lie on the regression line, the $r = \pm 1$. If $r = 0$, the regression line does not explain anything about the variation of y.

If it is assumed that there are only two variables of interest, an "independent" variable x, and a "dependent" variable y, then the equation of the sample regression line of y on x is:

$$y = a + bx \quad . \qquad (3\text{-}14)$$

Note that coefficients a and b are defined in normal least squares manner for a two variable linear regression; that is:

$$b = \frac{n\Sigma xy - \Sigma x\Sigma y}{n\Sigma x^2 - (\Sigma x)^2} \quad , \qquad (3\text{-}15)$$

$$a = \frac{\Sigma y - b\Sigma x}{n} \quad . \qquad (3\text{-}16)$$

Figure 25 is a scatter diagram of all field data (y) versus wind-tunnel data as modified by the weighting algorithm (x). The correlation coefficient is 0.52 and $y = -0.51 + 2.14x$ using all data of Table 5. It was noticed that for field tests 9 through 12 wind speed, stability and wind direction were approximately the same; however, the concentration coefficients varied from 1.61 to 16.69 and no explanation was given for this variation. Hence, when these four runs are removed from the calculation, the average concentration slightly underpredicts at the 300 m arc and overpredicts by 2.24 times at the 1000 m arc. The correlation coefficient r is 0.62 and $y = -0.51 + 1.88x$ when runs 9 through 12 are excluded.

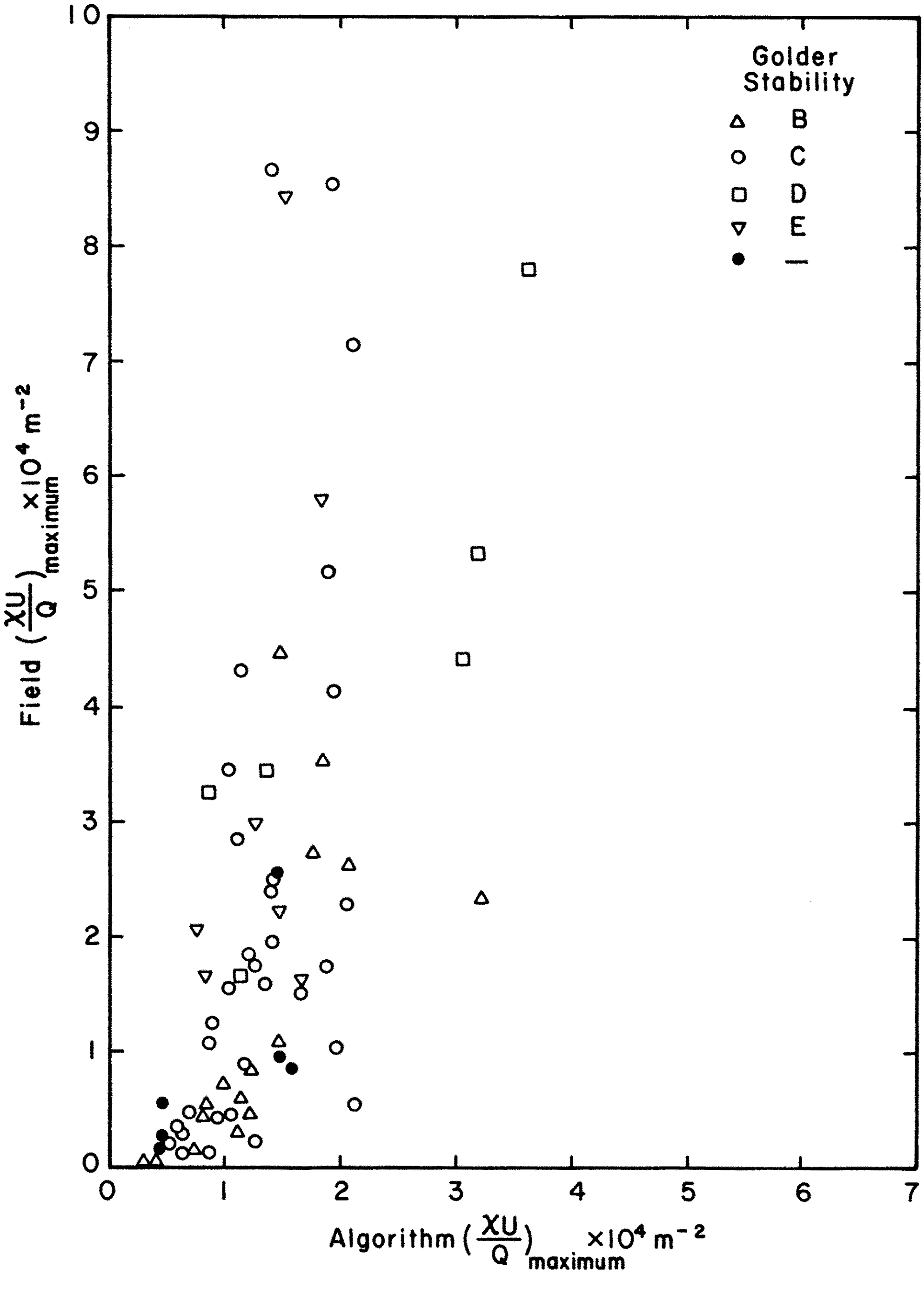

Figure 25. Comparison of field data with weighted wind-tunnel data using algorithm.

Chapter 4

CONCLUSIONS

Forty-eight wind-tunnel tests were performed for diffusion around a 1:400 scale model of the nuclear power plant located in the midwest. Three atmospheric stabilities, viz., neutral, moderately stable and slightly unstable, were investigated. Three different tracer gases were released from the three different release points on and near the containment vessel and concentration field downwind was measured. Eight wind directions for far wake region and six wind directions for near wake region were investigated for turbulent diffusion from the nuclear power plant.

The bulk Richardson numbers set in the wind tunnel were 0.0, 0.25 and -0.28, corresponding to the neutral, moderately stable and slightly unstable conditions when the wind profile power-law exponents are 0.13, 0.24 and 0.12 respectively. The smooth floor was used for the development of the approach boundary layer.

The maximum ground level concentration for each of the sampling arcs occurred during the moderately stable stratification for the turbine building release. Similar results were obtained for the ground level release and stack height release (reactor vent) except for the 73.7 m downwind arc. It was also observed that the maximum ground level concentration at each arc occurred for wind direction of 135° except at 147.3 m arc. At the arc distance of 147.3 m the maximum ground level concentration was obtained for a 157.5° wind direction.

A thorough examination of dispersion characteristics was carried out for the 135°, 180° and 225° wind directions. The following conclusions were based on the selected three wind directions.

The concentration distributions were about the same at each arc, for the three wind directions investigated. The surface level PasquillGifford approach over-predicts concentrations up to about 300 m downwind. This implies that the excess turbulence created by the building complex plays a much more important role than the wind direction.

The present results were also compared with a modified Gaussian diffusion equation for the ground level release. The results show that on an average the modified Gaussian equation underpredicts the measured concentration.

The σ_y values are approximately constant, at each arc distance and for each of the stabilities, for the above mentioned wind directions. This again implies that building wake effects are more dominant than the slight changes in the wind direction. The slightly unstable case results also show that beyond 600 m downwind, the observed σ_y corresponds to one category less untable. For neutral and stable case, the measured σ_y were larger than that predicted by Pasquill-Gifford category indicating enhanced dispersion due to building wake effects. The weighted data algorithm was realistic in both predicting the centerline concentration values as well as the horizontal spread of the plume.

Sixteen wind-tunnel tests were performed for diffusion downwind of six idealized buildings deeply submerged in a neutral turbulent boundary layer. The three building shapes, four vent heights and four gas release locations were investigated to determine concentration downwind of these idealized buildings. Four different neutrally buoyant tracer gases were released simultaneously from the four release locations and concentration fields downwind of the buildings were measured. The smooth floor with the spires and trip at the test section entrance were used to obtain a fully developed turbulent boundary layer at the test location. The velocity power-law exponent was 0.13.

The maximum ground level concentrations occurred for the vent height equal to building height indicating the maximum downwash induced by the buildings. Increase in the vent height resulted in the lower concentrations, as expected. For cubical buildings, the building effects were reduced considerably for the vent height of 0.5 H above the building and there was no building influence for the vent height 1.0 H above the building. The slight decrease in the velocity ratio resulted in higher concentrations in the near wake of the building. However, the effect of the velocity ratio on the concentration field disappeared in 20 to 30 heights downstream of the building. The highest ground level concentrations were observed in the wake of cylindrical buildings and lowest in the wake of cubical buildings. The ground level concentrations for the hemispherical building wake were in between those of the cylindrical and cubical building. For the roof top release, the maximum ground level concentrations are about the same for release locations 1, 2 and 3 and slightly lower for release location 4. At the vent height of 0.25 H above the building, the near wake concentrations were highly dependent on the release location. However, this concentration difference disappeared within about 10 heights downwind of the building.

Chapter 5

REFERENCES

Allwine, K. J., Meroney, R. N. and Peterka, J. A., 1978, "Rancho Seco Building Wake Effects on Atmospheric Diffusion: Simulation in a Meteorological Wind Tunnel," Fluid Dynamics and Diffusion Laboratory Report CER77-78KJA-RNM-JAP25.

Bouwmeester, R. J. B., Kothari, K. M. and Meroney, R. N., 1977, "An Algorithm to Estimate Field Concentrations under Nonsteady Meteorological Conditions from Wind-Tunnel Experiments," FDDL Report CER78-79RJBB-KMK-RNM43, Colorado State University, Fort Collins, June.

Cermak, J. E., 1971, "Laboratory Simulation of the Atmospheric Boundary Layer," AIAA Journal, Vol. 9, No. 9, pp. 1746-1754.

Cermak, J. E., 1975, "Applications of Fluid Mechanics to Wind Engineering--A Freeman Scholar Lecture," Journal of Fluids Engineering, Trans. of the ASME, Vol. 97, pp. 9-38.

Gifford, F. A., Jr., 1960, "Atmospheric Dispersion Calculations Using the Generalized Gaussian Plume Model," Nuclear Safety, Vol. 2, pp. 56-59, pp. 67-68.

Gifford, F. A., Jr., 1968, "An Outline of the Theories of Diffusion in the Lower Layers of the Atmosphere," in Meteorology and Atomic Energy - 1968, edited by D. H. Slade, USAEC Report No. TID 24190, pp. 65-116.

Gifford, F. A., 1975, "Turbulent Diffusion Typing Schemes: A Review," Environmental Research Laboratories, ATDL Report No. 75/2, or 1976, Nuclear Safety, Vol. 17, No. 1, pp. 68-86.

Golden, J., 1961, "Scale Model Techniques," M.S. Thesis, New York University, Department of Meteorology and Oceanography.

Halitsky, J., 1969, "Validation of Scaling Procedures for Wind Tunnel Model Testing of Diffusion near Buildings," New York University, Report No. TR-69-8.

Hanna, S. R., Briggs, G. A., Deardorff, J., Egan, B. A., Gifford, F. A. and Pasquill, F., 1977, "AMS Workshop on Stability Classification Schemes and Sigma Curves--Summary of Recommendations," Bulletin of the American Meteorological Society, Vol. 58, No. 12, pp. 1305-1309.

Hansen, A. C. and Cermak, J. E., 1975, "Vortex-Containing Wakes of Surface Obstacles," FDDL Report CER75-76-ACH-JEC16, Colorado State University, Fort Collins, December.

Hatcher, R. V., Meroney, R. N., Peterka, J. A. and Kothari, K. M., 1977, "Dispersion in the Wake of a Model Industrial Complex," FDDL Report CER76-77RVH-RNM-JAP-KMK35, Colorado State University, Fort Collins, June 1977.

Hinds, W. T., 1967, "On the Variation of Concentration in Plumes and Building Wakes," USAEC Meteor. Information Meeting, September 11-14, 1967, pp. 105-131.

Hino, M., 1968, "Maximum Ground Level Concentration and Sampling Time," Atmospheric Environment, Vol. 2, pp. 149-165.

Hino, M., 1968, "Computer Experiment on Smoke Diffusion Over a Complicated Topograph," Atmospheric Environment, Vol. 2, pp. 543-558.

Huber, A. H. and Snyder, W. H., 1976, "Building Wake Effects on Short Stack Effluents," Preprint Volume, Third Symposium on Atmospheric Turbulence, Diffusion and Air Quality.

Kothari, K. M., Bouwmeester, R. J. B. and Meroney, R. N., 1980, "An Algorithm to Estimate Field Concentrations Under Nonsteady Meteorological Conditions from Wind-Tunnel Experiments," Submitted for publication to Journal of Applied Meteorology.

Kothari, K. M., Meroney, R. N. and Peterka, J. A., 1981, "The Flow and Diffusion Structure in the Wakes of Cylindrical Obstacles," a paper submitted to the 4th U.S. National Conference on Wind Engineering Research to be held July 26-29, 1981 in Seattle, Washington.

Kothari, K. M., Peterka, J. A. and Meroney, R. N., 1979, "An Analytical Method for Determination of Dispersion in the Wake of a Power Plant," to be published.

Meroney, R. N. and Yang, B. T., 1971, "Wind-Tunnel Study on Gaseous Mixing Due to Various Stack Heights and Injection Rates above an Isolated Structure," FDDL Report CER71-72RNM-BTY16, Colorado State University, Fort Collins.

Ogura, Y., 1959, "Diffusion from a Continuous Source in Relation to a Finite Observation Interval," Adv. Geophysics, Vol. 6, pp. 149-159.

Plate, E. J. and Cermak, J. E., 1963, "Micro-Meteorological Wind-Tunnel Facility: Description and Characteristics," FDDL Report CER63-EJP-JEC9, Colorado State University, Fort Collins.

Snyder, W. H., 1972, "Similarity Criteria for the Application of Fluid Models to the Study of Air Pollution Meteorology," Boundary Layer Meteorology, 3(2), pp. 113-134.

Start, G. E., Cate, J. H., Dickson, C. R., Ricks, N. R., Ackermann, G. R. and Sagendorf, J. F., 1977, "Rancho Seco Building Wake Effects on Atmospheric Diffusion," National Oceanic and Atmospheric Administration Technical Memorandum ERL ARL-69, p. 185.

Thuillier, R. H., 1979, "Building Effects on Effluent Dispersion from Roof Vents at Nuclear Plants," Standford Research Institute Report 6888.

Turner, D. B., 1969, "Workbook of Atmospheric Dispersion Estimates," U.S. Department of Health, Education and Welfare, Public Health Service, Cincinnati, Ohio.

Weber, A. H., McDonald, K. R. and Briggs, G. A., 1977, "Turbulence Classification Schemes for Stable and Unstable Conditions," Joint conference on Applications of Air Pollution Meteorology, November 29-December 2, 1977, Salt Lake City, Utah, American Meteorological Society, pp. 91-102.

Whaley, H., 1974, "The Derivation of Plume Dispersion, Parameters from Measured Three-dimensional Data," Atmospheric Environment, Vol. 8, pp. 281-290.

Appendix A

MODELING REQUIREMENTS

The atmosperic surface layer can be modeled in a meteorological wind tunnel at Colorado State University. This is accomplished by maintaining equality between pertinent prototype and model dimensionless quantities determined by the governing equations of motion. This appendix itemizes the similarity parameters important to this study (also, see Hatcher et al., 1977 and Allwine et al., 1978). A detailed presentation of modeling criteria for the atmospheric surface layer has been prepared by Cermak (1971, 1975) and Snyder (1972).

APPROACH FLOW

Similarity of neutral flow conditions in the atmospheric surface layer may be accomplished through equality of the dimensionless parameters

$$\frac{U_*}{U_r} \quad \text{and} \quad \frac{z_o}{z_r}$$

where U_* is friction velocity, U_r is reference velocity, z_o is the characteristic surface roughness height and z_r is a reference height. The equality of these dimensionless parameters between model and prototype insure similar logarithmic wind profiles for model and prototype. The logarithmic wind profile, which holds only for a neutral boundary layer and $z > z_o$, is

$$\frac{U}{U_*} = \frac{1}{k} \ln \frac{z}{z_o} \tag{A-1}$$

where k is von Karman's constant.

For thermally stratified flow, the similarity between model and prototype requires the bulk Richardson number, Ri_b, and power-law exponent, p, of velocity profile to be equal. The bulk Richardson number is defined as,

$$Ri_b = \frac{g}{T} \frac{\Delta T \ \Delta Z}{(\Delta U)^2} \qquad \text{(A-2)}$$

where g is the acceleration due to gravity, ΔT is the temperature difference over a region of interest, ΔZ is the height of the region of interest, ΔU is the velocity difference over the same layer and T is the average temperature expressed in absolute units through the layer. The bulk Richardson number is a measure of the stability of the atmosphere over a finite layer. A positive Ri_b indicates stable stratification, a negative Ri_b indicates unstable stratification and a Ri_b equal to zero indicates a neutral condition.

The wind profile in terms of power law is defined as,

$$\frac{U}{U_r} = \left(\frac{z}{z_r}\right)^p \quad . \qquad \text{(A-3)}$$

The coefficient p ranges from 0.1 to 0.6 as stability varies from unstable through neutral to very stable. This relationship is valid for all stabilities.

It should be noted that large-scale atmospheric eddies and meandering associated with time scales of the order of one hour are not modeled in the wind tunnel. Generally wind-tunnel results are equivalent to 10-minute average or less for prototype conditions.

FLOW AROUND BUILDINGS

Geometric similarity between model and prototype was accomplished by undistorted scaling in the three dimensions. Exact Reynolds number ($Re = U \sqrt{A}/\nu$) similarity between model and prototype was not possible. Very high wind-tunnel velocities would be required in order to attain Reynolds number equality.

However, Reynolds number equality is not necessary when the flow is over sharp-edged geometries. Golden (1961) has shown that flows with Reynolds numbers above a certain critical number the concentration patterns change very little and determined that this critical Reynolds number as 11,000. Even when Reynolds number exceed about 3,500, there was little detectable variation in the far field plume behavior. The Reynolds number based on velocity at a reference height of 10.4 cm was 11,140 for the present study.

This study deals with the dispersion of slowly released pollutants in the wake of the nuclear power plant. Consequently, situations where the jetting of the emitted tracers from the building cavity region occurs were not considered. It is generally accepted that for $h_s/h_b > 2.5$ and $U/U_\infty > 1$, the effluent will escape the cavity region (Huber et al., 1976 and Meroney et al., 1971). U is the velocity at the release point and h_s is the height of the release point. For this study the h_s/h_b ratio for the three release points was approximately 1.0 or less and the U/U_∞ ratio was 0.71 or less.

CONCENTRATION MEASUREMENTS

Concentration measurements from the wind tunnel can be compared directly to the field levels by assuming equality of a dimensionless concentration parameters, K_c, between model and prototype (Halitsky, 1968). K_c, the nondimensional concentration coefficient, is defined as

$$K_c = \frac{\chi U H^2}{\chi_{source}\, Q_{source}} \qquad \text{(A-4)}$$

where χ is the local concentration, U is the characteristic velocity, H is a characteristic height, Q_{source} is the source flow rate, and χ_{source} is the source strength. K_c is a function of nondimensional space coordinates. The field measurements are reported as $K_{c_1} = \frac{\chi\, U}{\chi_{source}\, Q_{source}}$ and hence the present wind-tunnel concentration measurements are reported as K_{c_1}, which is determined by dividing K_c with field reference area (2500 m^2).

Appendix B

EXPERIMENTAL METHODS

WIND TUNNEL

This study was conducted in the Meteorological Wind Tunnel (MWT) at the Fluid Dynamics and Diffusion Laboratory (FDDL) of Colorado State University. A complete description of this wind tunnel (Figure 1) is given by Plate and Cermak (1963). The tunnel has a test section 26.8 meters long and a nominal cross-sectional area of 1.8 x 1.8 meters. Air velocities can be maintained from 0.5 to 35 meters per second with an ambient turbulence level of less than 0.1 percent. The ceiling is adjustable to eliminate any longitudinal pressure gradient.

The MWT was specifically designed to simulate the atmospheric boundary layer. Air inside the tunnel can be maintained at temperatures from 0°C to 80°C. Plates cooled with an ethylene glycol solution were installed on the floor of the first 12 meter portion of the test section. This permitted the test section to be cooled to 0°C over its entire length. The final 13 meters of the test section floor is equipped with heaters such that when the heaters are operational a temperature gradient of 122°C between the hot floor and cold air can be maintained.

The idealized building wake diffusion measurements were performed in the Industrial Aerodynamics Wind Tunnel (Figure 2) located in the Fluid Dynamics and Diffusion Laboratory at Colordo State University.

The wind tunnel is a closed circuit facility driven by a 75 h.p. single speed induction motor. A 16-blade variable pitch axial fan provides control of the speed in the wind tunnel. The contraction ratio at the entrance of the test section is 4:1. The square cross section of the tunnel is 3.3 m^2 and the length of the test section is 18.3 m. The roof of the last 7.3 m of the test section is adjustable to obtain zero pressure gradient along the test section. The test section velocities range from zero to 24.4 m/sec.

VELOCITY MEASUREMENTS

Measurements of mean velocity and turbulence intensity were accomplished with a single hot-wire anemometer with its axis horizontal. The instrumentation used was a Thermo-Systems constant temperature hot-wire anemometer model 1050 with a 2.54 x 10^{-3} cm diameter platinum film sensing element 0.0508 cm long. The output of the constant temperature hot-wire anemometer was fed to an on-line data acquisition system consisting of a Hewlett-Packard 21MX computer, disc unit, card reader, printer, Digi-Data digital tape drive and a Preston Scientific analog-digital converter. The data was processed immediately into mean velocity, turbulence intensity and corresponding height and stored on the computer disc for printout or further analysis. For stable and unstable velocity measurements a temperature compensated probe was used to account for the change in calibration and wind-tunnel temperatures.

Calibration of the hot-wire anemometer was performed using a facility developed by CSU staff. The calibration data were fit to a variable exponent King's law relationship,

$$E^2 = A + B\,U^n \tag{B-1}$$

where E is the hot-wire output voltage, U the velocity and A, B and n are coefficients selected to fit the calibration data. The measurements were performed with a sample rate of 250 samples per second for 20 seconds and the above relationship was used to determine the mean velocity. The fluctuating velocity in the form U_{rms} (root-mean-square velocity) was obtained from

$$U_{rms} = \frac{2E\,E_{rms}}{Bn\,U^{n-1}} \tag{B-2}$$

where E_{rms} is the root-mean-square of the voltage output from the anemometer. The local turbulence intensity, U_{rms}/U, was then evaluated.

TEMPERATURE MEASUREMENTS

Temperature measurements were made with a YSI model 44004, Fennal glass-coated bead thermistors. Manufacturer's specifications suggest an accuracy of ±0.2°C for this type thermistor. The thermistors ere connected to a YSI model 42 SC Tele-Thermometer with a range of -40°C to 150°C.

APPROACH FLOW

Thuillier (1979) reports various methods to determine the field stabilities for each of the runs for field data. It should be noted that the stabilities, for each run, were different depending on the method used. It was thought that the stabilities generated in the wind tunnel represent that determined by Golden's method for the field data. Hence, three of the representative stabilities from field data determined by Golden's method were selected for all of the wind-tunnel tests.

Three different approach flow conditions were utilized in the wind tunnel: one for neutral conditions ($Ri_b = 0$), one for moderately stable stratification ($Ri_b = 0.26$), and one for slightly unstable stratification ($Ri_b = -0.28$). The bulk Richardson number was set in the wind tunnel over the layer 2.5 to 12.5 cm corresponding to 10 to 50 meters for the prototype.

Approach Flow for Neutral Case

With the addition of spires at the test section entrance, the boundary layer developed naturally over the initial 13 meters of fetch upwind of the model to a depth of about 1.2 meters. The mean velocity and turbulence intensity profiles approaching the model are shown in Figure 26. A power-law exponent of 0.13 was determined by least squares fitting the velocity profile to a power-law curve. U_*/U_r and z_o/z_r values of 0.19 and 8.0×10^{-4}, respectively were also determined.

Approach Flow for Moderately Stable Case

For the moderately stable case the floor of the meteorological wind tunnel was cooled to 0°C and the air entering the test section was heated to approximately 60°C. The velocity was adjusted until a desired Ri_b was reached. The tunnel was allowed to come to equilibrium for 4 to 6 hours. Figure 27 shows the mean velocity, turbulence intensity and temperature profiles. The bulk Richardson number of 0.25 was determined over the layer 2.5 to 12.5 cm. The power-law exponent was 0.24 and arrived at by least square fitting the mean velocity profile to a power-law curve.

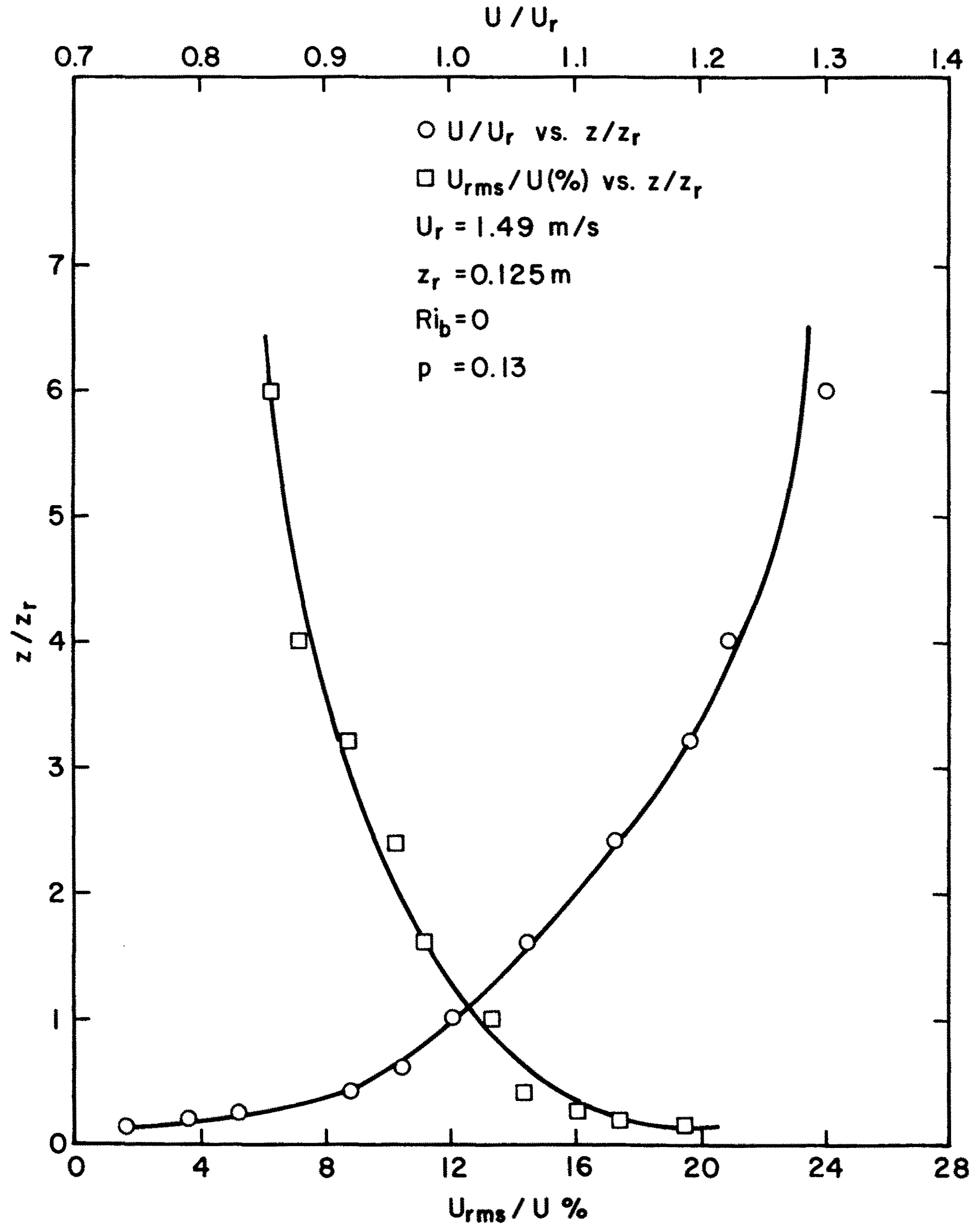

Figure 26. Mean velocity and turbulence profiles, neutral stratification.

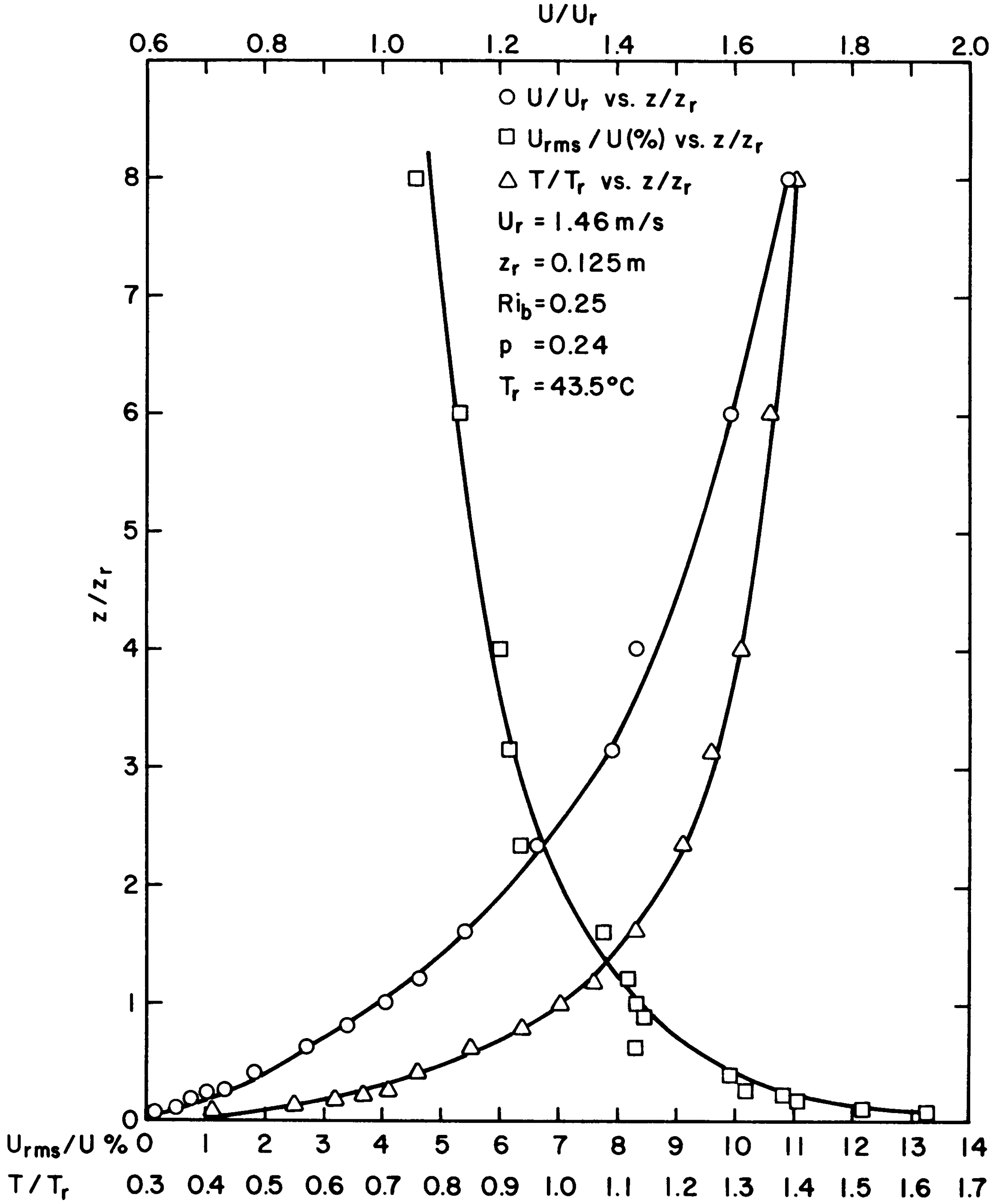

Figure 27. Mean velocity, temperature and turbulence profiles, moderately stable stratification.

Approach Flow for Slightly Unstable Case

The wind-tunnel floor was heated to approximately 20°C and the air entering the test section was cooled to approximately 0°C. The mean velocity, turbulence intensity and temperature profiles are displayed in Figure 28. The bulk Richardson number was -0.28 and the power-law exponent was 0.12.

Approach Flow for Idealized Building Wake Diffusion Tests

All the data reported for the idealized building wake diffusion tests were taken at a nominal velocity of 3.0 m/sec. The long smooth floor test section in conjunction with spires and trip at the test section entrance were used to generate a thick neutral turbulent boundary layer. The idealized buildings were located at 9.6 m from the test section entrance where a similarity profile was obtained. The mean velocity and turbulence intensity profiles approaching the idealized building wake diffusion tests are shown in Figure 29. A power-law exponent of 0.13 was determined by least squares fitting the velocity profile to a power-law curve.

MODEL

The 1:400 scale model of the nuclear power plant and surrounding area was constructed from wooden blocks and placed on a 3.2 mm masonite sheet as the base. The model then fit into the 1.8 m wide meteorological wind tunnel with ~2 m of terrain upwind and ~2 m of terrain downwind of the containment vessel. All of the model buildings were made to scale in the FDDL shop from plant drawings provided by EPRI. Figure 30 shows a view of the model in the wind tunnel. Idealized building models were constructed from plexiglass material. The three shapes of the building viz. cylindrical, hemispherical and cubical and two sizes of each shape building were constructed. The holes were drilled at the respective release locations on the buildings. The additional stack heights were made out of brass tubes. The idealized model dimensions and release locations are shown in Figures 31 and 32.

CONCENTRATION MEASUREMENTS

Three separate sets of wind-tunnel studies were performed. One set consists of the concentration measurements in the far wake of a nuclear power plant for eight wind directions and three stability classes. In the second set the concentration

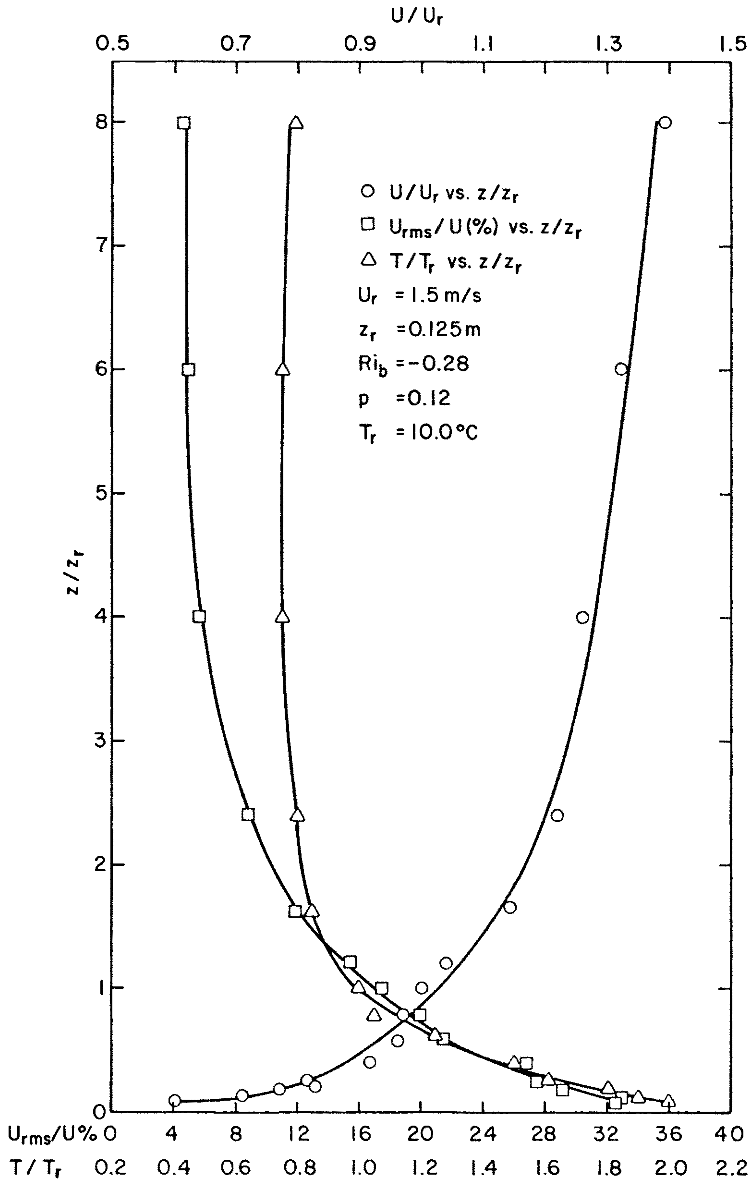

Figure 28. Mean velocity, temperature and turbulence profiles, slightly unstable stratification.

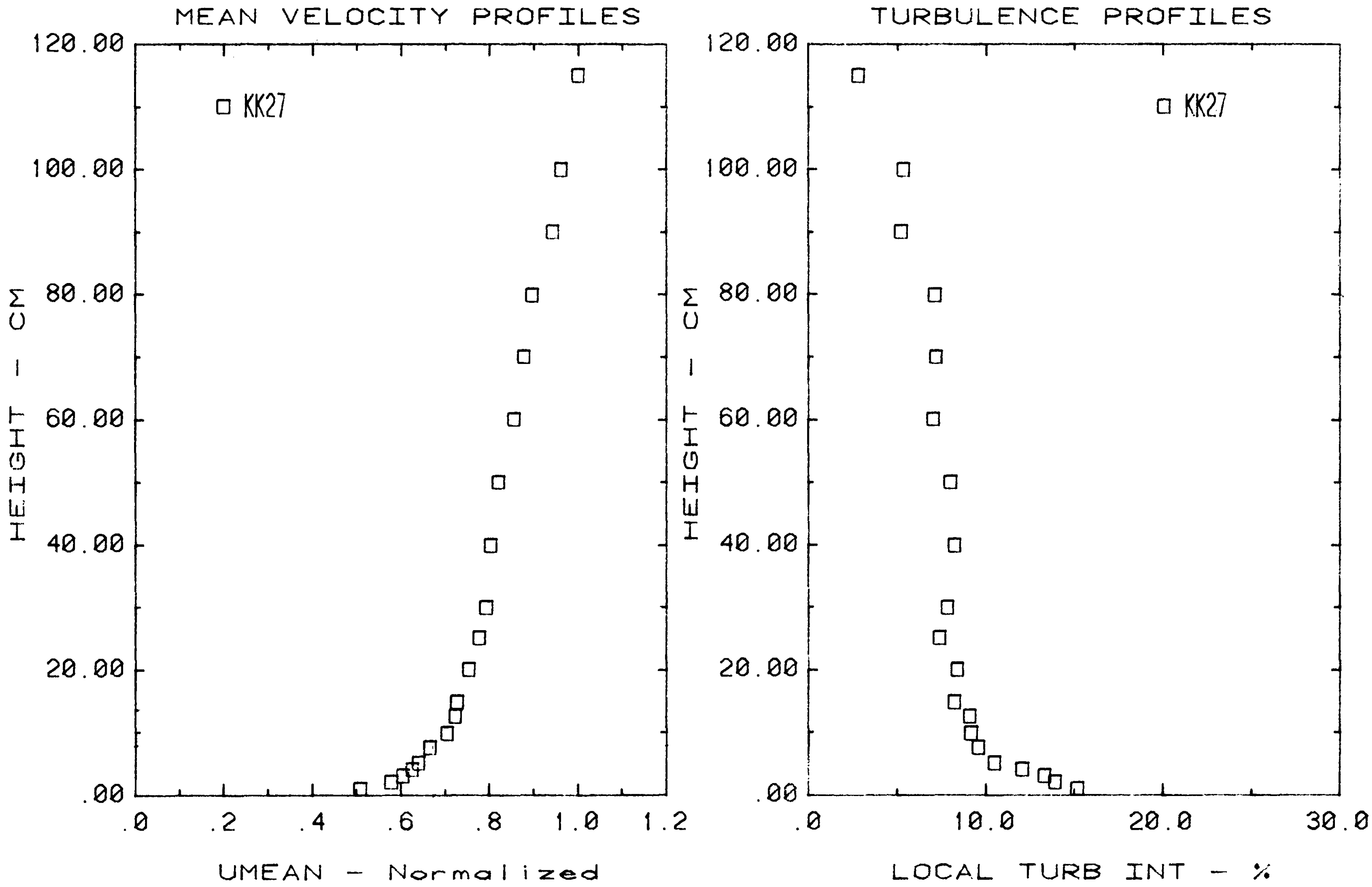

Figure 29. Approach mean velocity and turbulence profiles for idealized building wake runs with neutral stability.

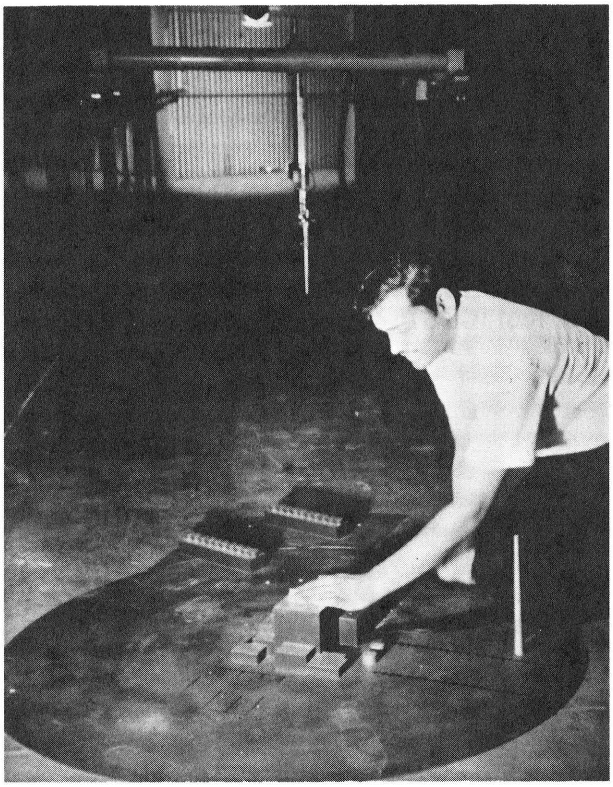

Figure 30. Nuclear Power Plant model in wind tunnel.

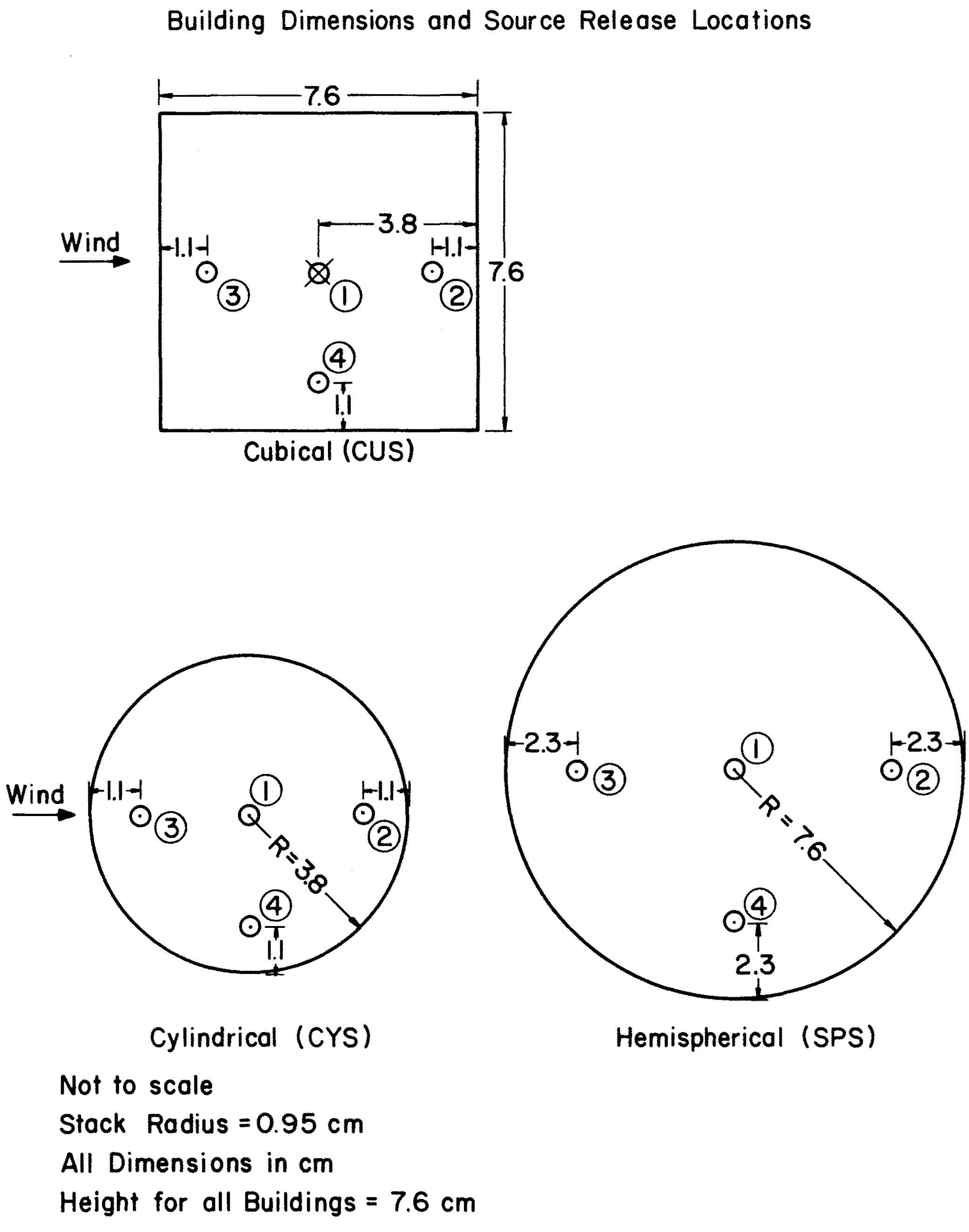

Figure 31. Building dimensions and source release locations for buildings of height 7.6 cm.

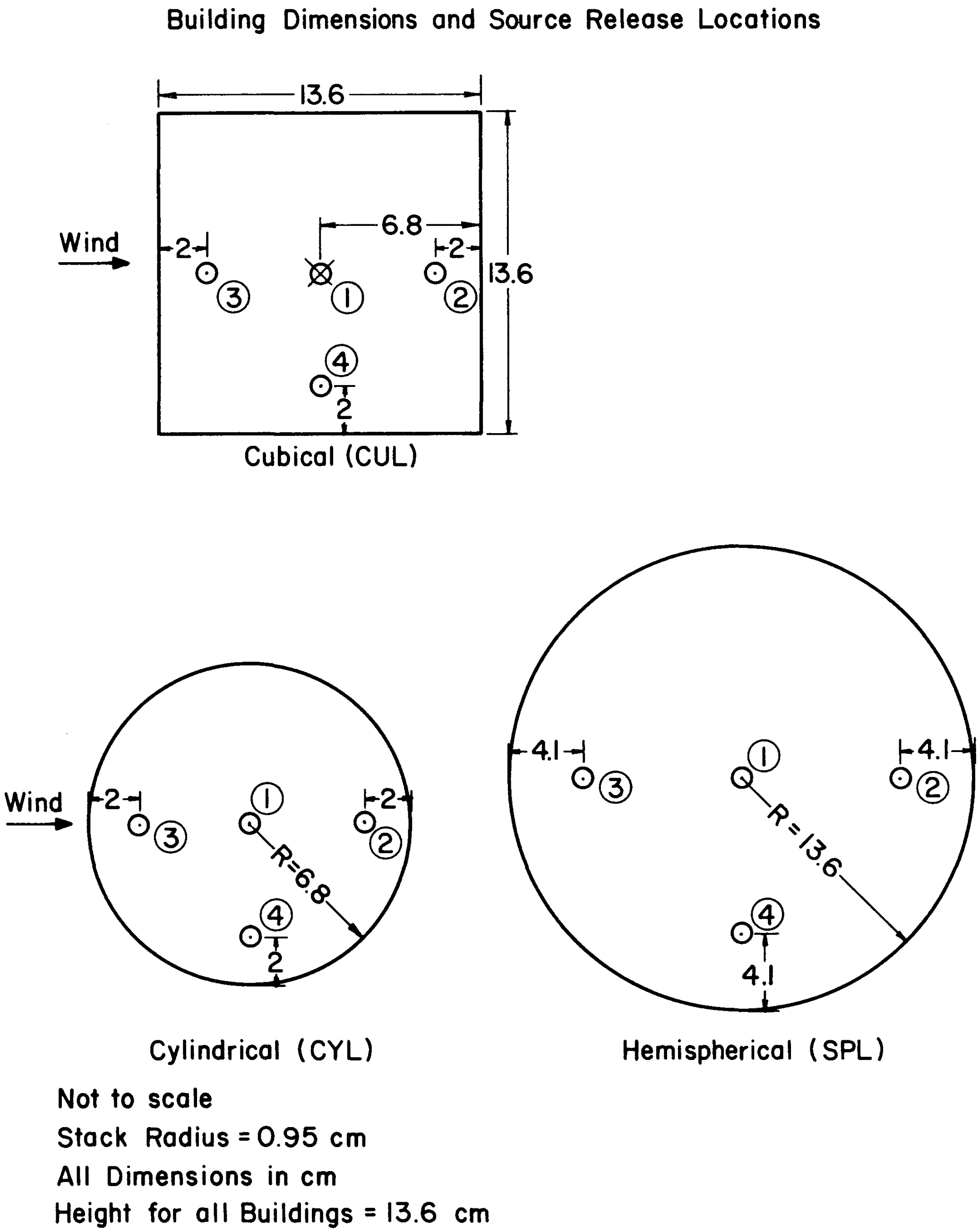

Figure 32. Building dimensions and source release locations for buildings of height 13.6 cm.

measurements were performed in the near wake of a nuclear power plant for six wind directions and neutral stability. Concentration measurements were also performed for three stability classes and three release heights with no buildings present. The third test consists of concentration measurements downwind of idealized buildings. Flow visualization tests were performed for eleven wind directions and three releases in neutral flow. Idealized tests were performed with neutral stability.

Three tracer gases were released, one from the top of a reactor vent at a height 11.4 cm (45.7 m, prototype), second from the top of the turbine building vent at a height 5.9 cm (23.5 m, prototype), and third from ground level at the center on the east side of the turbine building. The release locations and the building dimension are shown in Figure 33. The four gas release locations for idealized building wake diffusion runs are shown in Figures 31 and 32.

The tracer gases used were mixed such that the equivalent molecular weight of each mixture corresponds to approximate molecular weight of air. Four gases, methane (CH_4), ethane (C_2H_6), propane (C_3H_8) and butane (C_4H_{10}), were individually mixed with either nitrogen or nitrogen and carbon dioxide to obtain such mixtures.

After the release of the tracer gases began, the sample collection system was flushed several times. Then a final sample was drawn over a period of approximately 60 seconds and held for subsequent analysis. Once samples were isolated the tracer gas flows were immediately terminated to prevent background buildup in the wind tunnel.

Tracer Gases Release System

The tracer gases were fed to their respective release port via tygon tubes. Methane mixture was released from ground level, ethane mixture from the top of turbine building and propane mixture from the top of the reactor vent (stack height). Each gas came from a Matheson gas cylinder through a two-stage regulator, a flow controller and then on to the release port on the containment vessel. The tracer gases follow similar paths to the exit port and released at the rate of 37.6 cm^3/sec for idealized building wake diffusion tests. The flow rates were measured using a 100 cc soap film flow meter. The flow rates were set so that there was no appreciable plume rise.

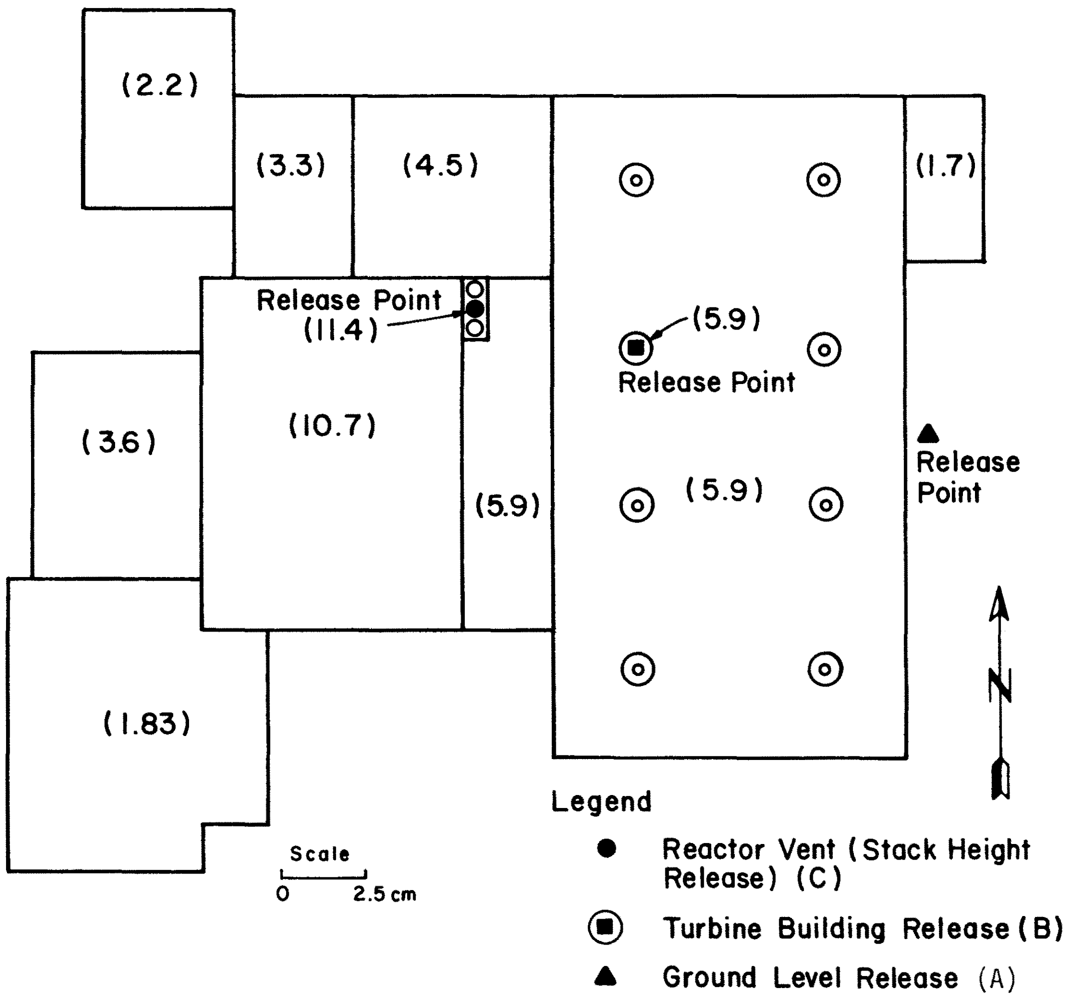

Figure 33. Release locations and building dimensions. Roof elevations, in cm, are in parentheses.

Sample Collection Locations

A total of 33 samples plus background concentration sample were collected per run for far wake data collection. These samples were taken on the 73.7, 147.3, 304.8, 609.6 and 1031.2 meter arcs (scaled) downwind of the containment vessel for eight different wind directions. For each arc the sampler locations were chosen to intersect where the plume was anticipated. Elevated samples were collected on the centerline of the 304.8 and 1031.2 meter arcs (scaled).

For near wake measurement of concentration, the sampling points were placed on a rack fixed to a traverse. The traverse can be raised or lowered using motor control from outside the wind tunnel and can be moved longitudinally along the rail in the wind tunnel. At each x locations 20 samples plus background were taken. The rack was moved vertically and another set of 20 plus background samples were observed. These actions resulted in 40 samples at each x location. The measurements were repeated for a total of six wind directions.

A total of 33 samples plus background samples were collected at each x/H location for idealized building runs. This resulted in a centerline vertical profile and ground level horizontal profile. The ground level horizontal and centerline vertical profiles were measured at x/H = 1, 3, 5, 10, 20 and 30 downstream from the center of each building.

Sample Collection System

Tygon tubes (3.2 mm diameter) approximately 8 m in length were fed through the wind-tunnel wall and each fastened at a sample grid location. The other ends of the tubes were connected to a sample withdrawal and containment system designed and built by the FDDL staff. In this system are four modules with each module able to hold eight samples. Each sample was insulated in a 30 cc plexiglas container by valves at the inlet and outlet sides. The air sample was drawn into or expelled from the plexiglas container using positive or negative pressure differentials across a flexible plastic diaphragm.

Sample Analysis System

A Hewlett-Packard 5700A gas chromatograph with a flame ionization detector (FID) was used to analyze the samples. The oven was maintained at 145°C, the detector at 250°C with a carrier flow rate through the column of approximately 55 cc/min.

The column was a 3.2 mm x 2 m Porapak-R column and the carrier gas was nitrogen. Good separation was achieved for the three desired compounds with methane coming off the column first after approximately 13 seconds, ethane after 20 seconds, propane after 42 seconds and butane after 75 seconds from injection. Consequently, each sample analysis took approximately two minutes.

The principle of operation of chromatograph is that the compounds are separated by molecular size as they pass through the column. As each hydrocarbon compound elutes from the column and into the FID it is burned in a hydrogen flame where it is ionized. The potential setup across the detector is measured by an electrometer, amplified and transmitted to a recorder or any other compatible data handling device.

For this study the analog output from the gas chromatograph was converted to a digital signal using a Preston A/D converter which was interfaced to a Hewlett-Packard 21MX computer system. Therefore, the concentration of each tracer was determined and stored on a disc file in the computer system.

Prior to each sample collection a background air sample was taken in the wind tunnel. This level for each compound was subtracted from the sample values. The gas chromatograph was calibrated prior to each day's operation.

It should be noted that the electrometer output is proportional to the number of carbon atoms (or methane molecules) that are ionized in the detector. Consequently, only one hydrocarbon compound of known concentration is needed to calibrate the electrometer response. For instance, 30 ppm of propane gives the same total integrated response as 82.5 ppm of methane [(44/16) x 30]. Therefore, the electrometer response can be calibrated based on one compound and all the other compounds can be expressed in terms of the known compound.

The minimum resolution for the entire sample collection-analysis system was determined to be approximately 1 to 2 ppm methane.

FLOW VISUALIZATION

Titanium tetrachloride added to the respective release mixture as a carrier was used as a visible tracer. The mixture, regulated by a flow controller, passed through a bottle of titanium tetrachloride and was carried through a 3.2 mm tygon tube to the release port. For 11 wind directions (0, 45, 90, 112.5, 135, 157.5, 180, 202.5, 225, 247.5, 270) for each release point under neutral stability, pictures were taken of the visible plume. These pictures included black and white stills and color slides. Also silent color 16 mm movies were taken for each nuclear power plant run. The flow visualization study was performed for center release, four vent heights and six idealized building shapes. The black and white stills and color slides were taken. The slides, movie and black and white slides, were submitted to EPRI under separate cover.

DATA ANALYSIS

The concentration data was reduced to a nondimensional concentration coefficient, K_c. The coefficient K_c is determined from

$$K_c = \frac{\chi U H^2}{\chi_{source}\, Q_{source}} \tag{B-3}$$

where χ is the local concentration (ppm), U is the reference velocity at release heights (m/s), H is the reference height which was chosen to be the height of the meteorological tower (12.5 cm model, 50 m prototype), χ_{source} is the source strength (ppm) and Q_{source} is the source flow rate (m^3/sec). The results were also tabulated as $K_{c_1} = \frac{\chi\, U}{\chi_{source}\, Q_{source}}$ m^{-2} by dividing K_c with prototype equivalent reference area (50 x 50 m^2).

It should be noted that for idealized building wake diffusion tests the building height was used as reference height and the velocity at building height in approach flow was used as the reference velocity in Eq. (B-3) to arrive at K_c.

EXPERIMENTAL PROCEDURE

The procedure for the experiment was as follows: 1) the model, velocity and temperature probes and sampling grid were installed in the wind tunnel; 2) wind-tunnel heating and cooling controls were adjusted to achieve the proper thermal stratification; 3) concentration measurements were taken; 4) flow visualization was performed; and 5) the data was processed.

Appendix C

NEAR WAKE CONCENTRATION COEFFICIENT, K_c, ISOPLETH

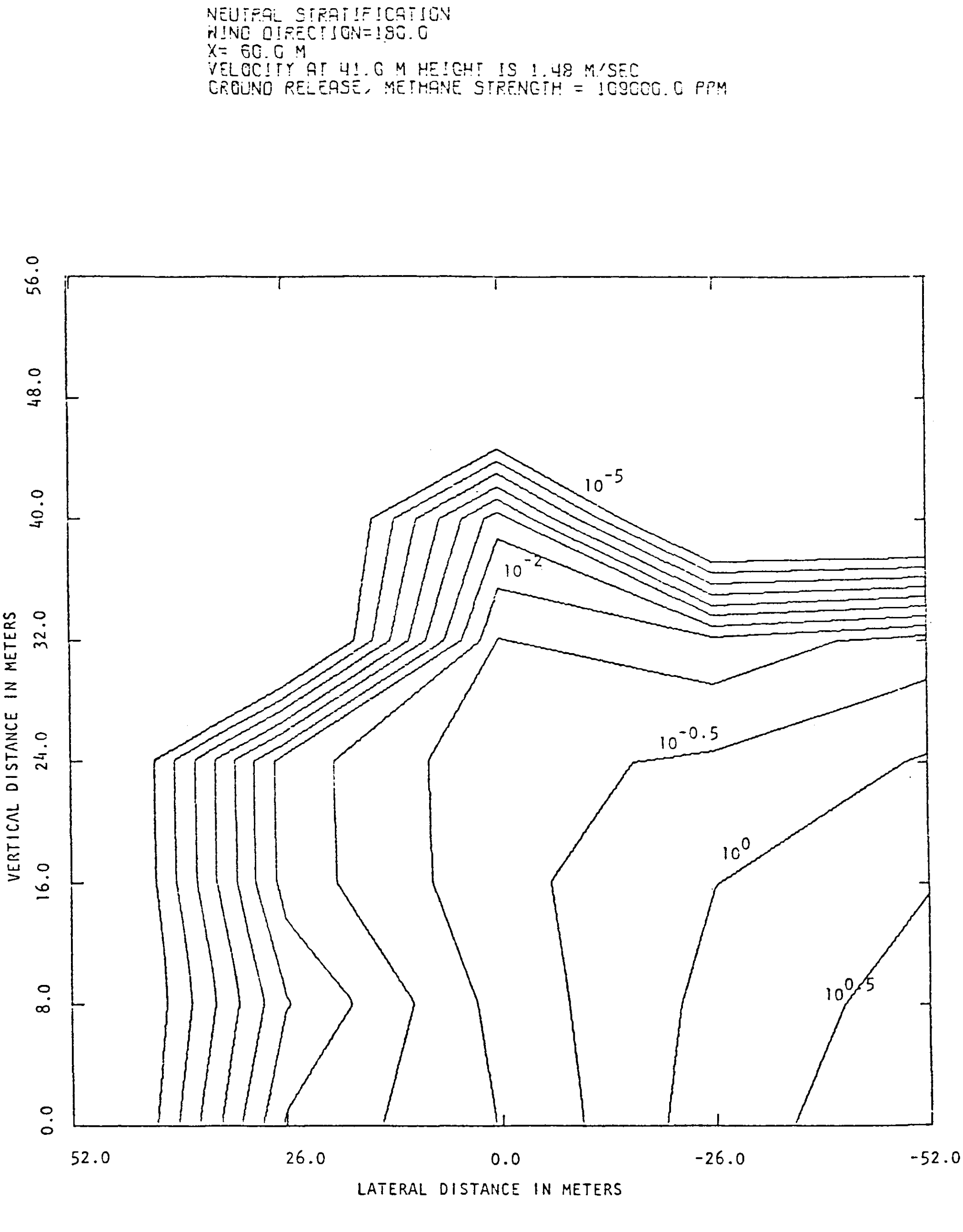

Figure 34. Nondimensional concentration coefficient, K_c, $\frac{\chi UH^2}{Q}$, isopleth.

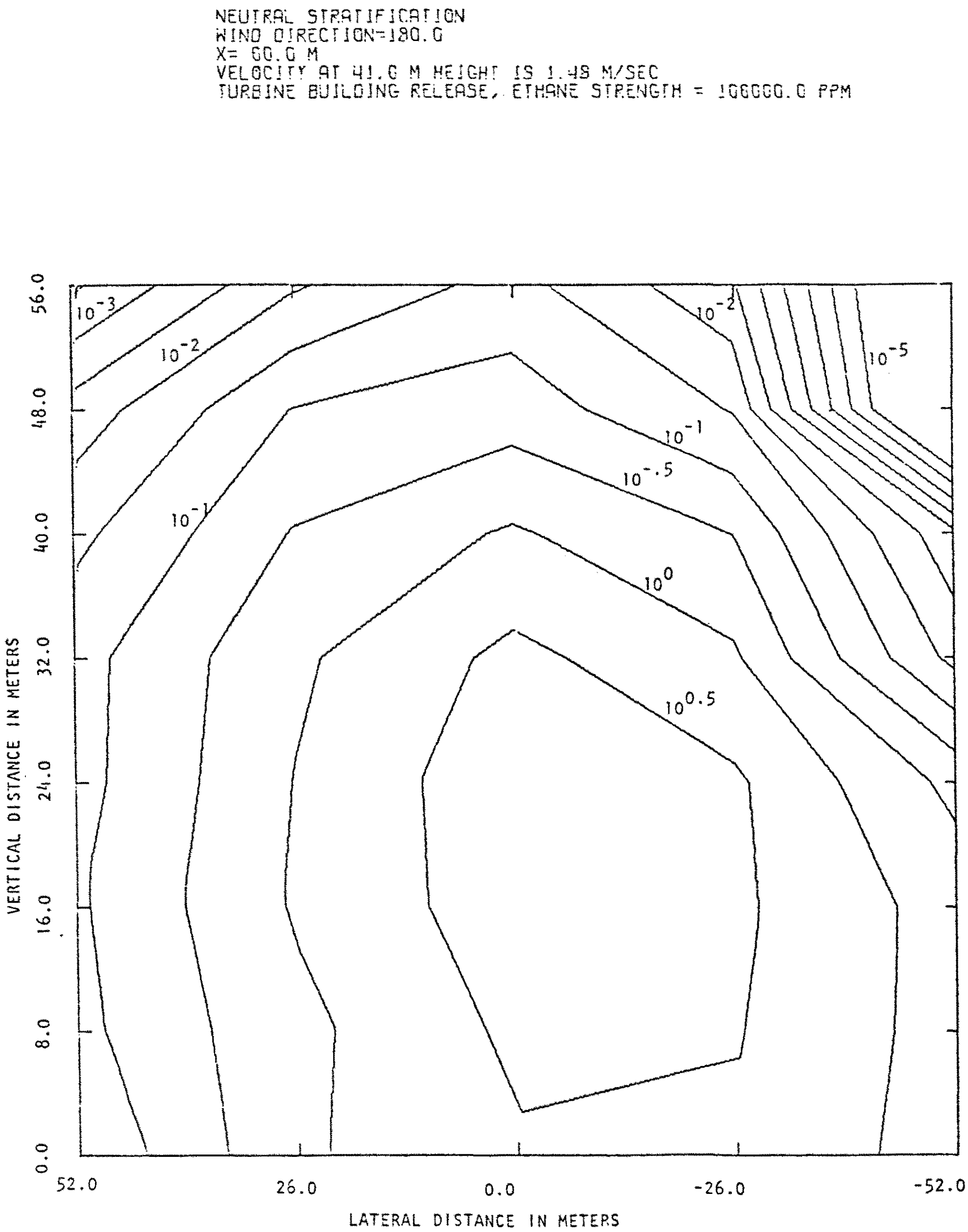

Figure 35. Nondimensional concentration coefficient, K_c, $\frac{\chi UH^2}{Q}$, isopleth.

NEUTRAL STRATIFICATION
WIND DIRECTION=180.0
X= 60.0 M
VELOCITY AT 41.6 M HEIGHT IS 1.48 M/SEC
STACK HEIGHT RELEASE, PROPANE STRENGTH = 59500.0 PPM

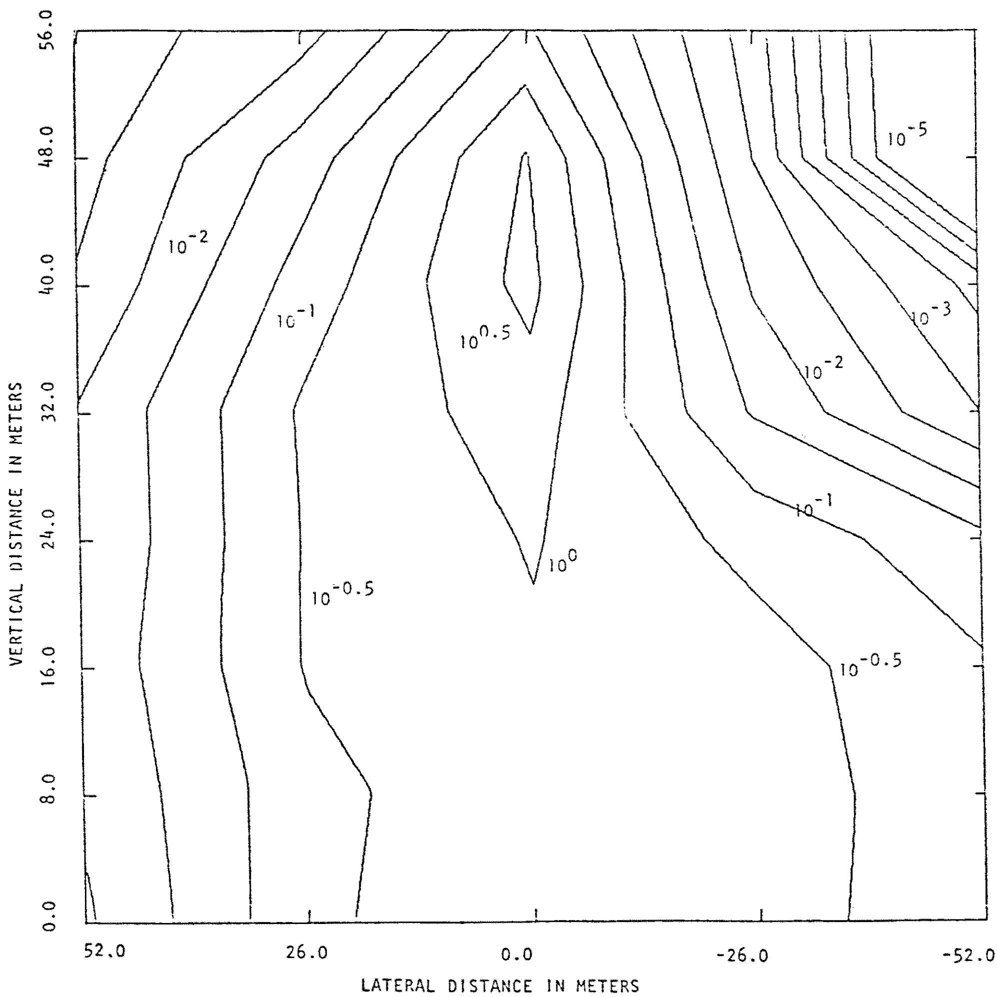

Figure 36. Nondimensional concentration coefficient, K_c, $\frac{\chi U H^2}{Q}$, isopleth.

NEUTRAL STRATIFICATION
WIND DIRECTION=180.0
X= 80.0 M
VELOCITY AT 41.0 M HEIGHT IS 1.48 M/SEC
GROUND RELEASE, METHANE STRENGTH = 100000.0 PPM

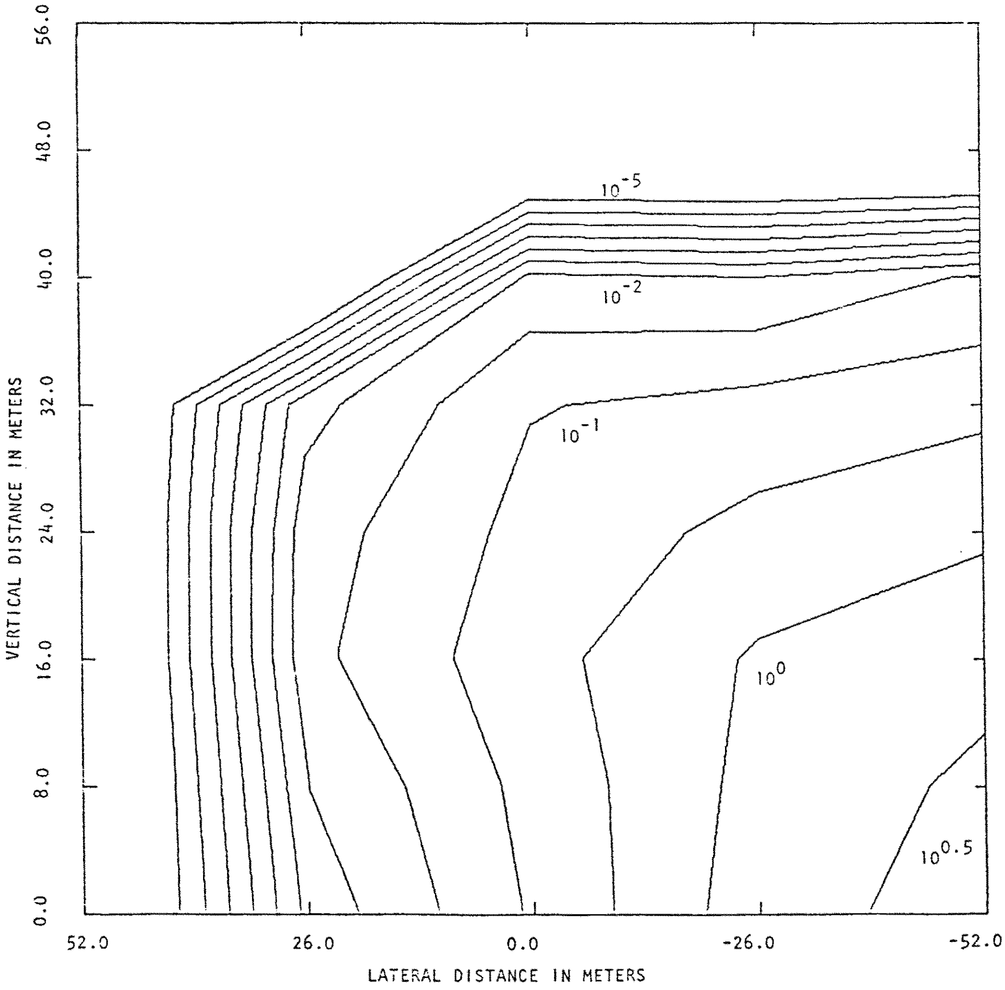

Figure 37. Nondimensional concentration coefficient, K_c, $\frac{\chi U H^2}{Q}$, isopleth.

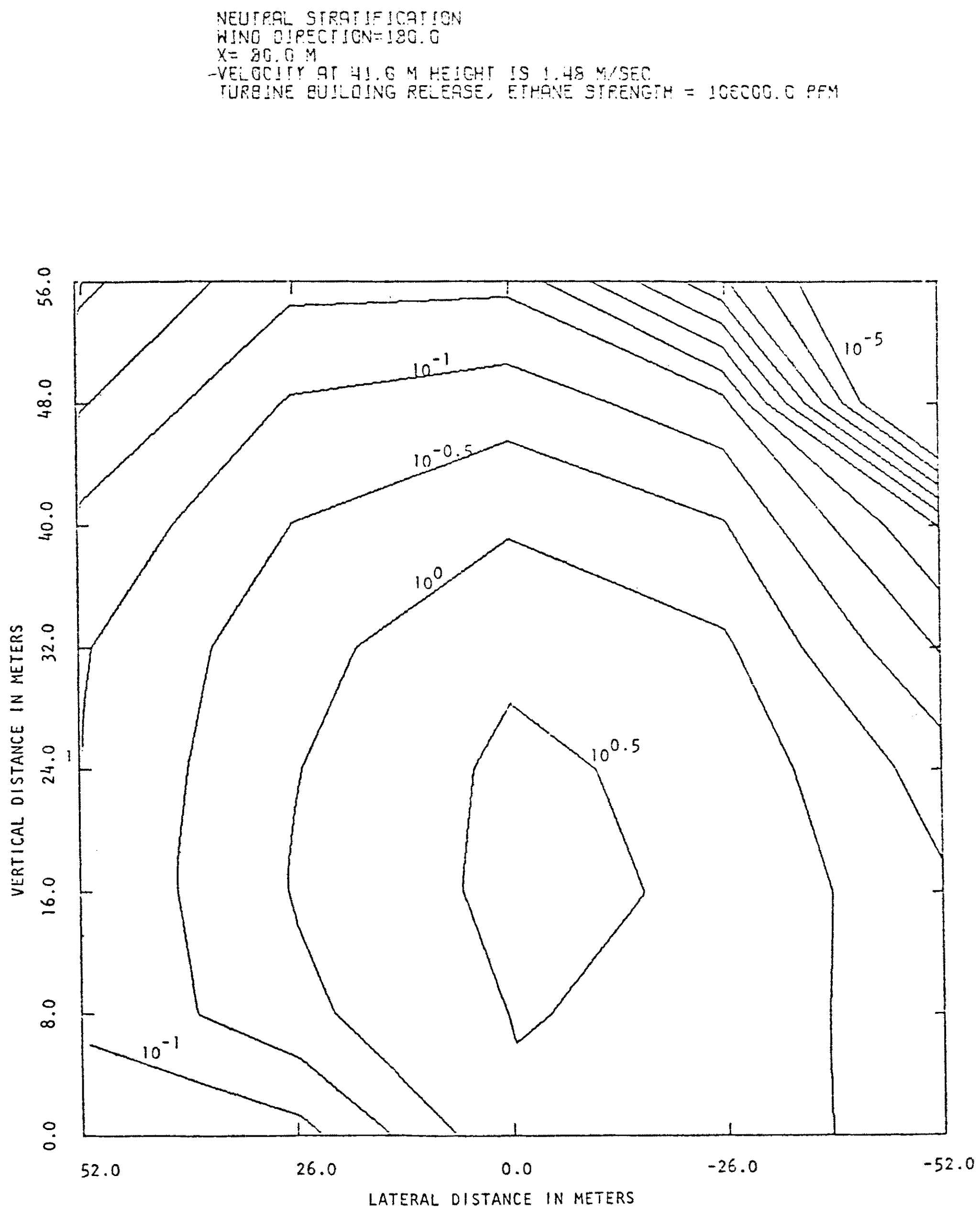

Figure 38. Nondimensional concentration coefficient, K_c, $\frac{\chi U H^2}{Q}$, isopleth.

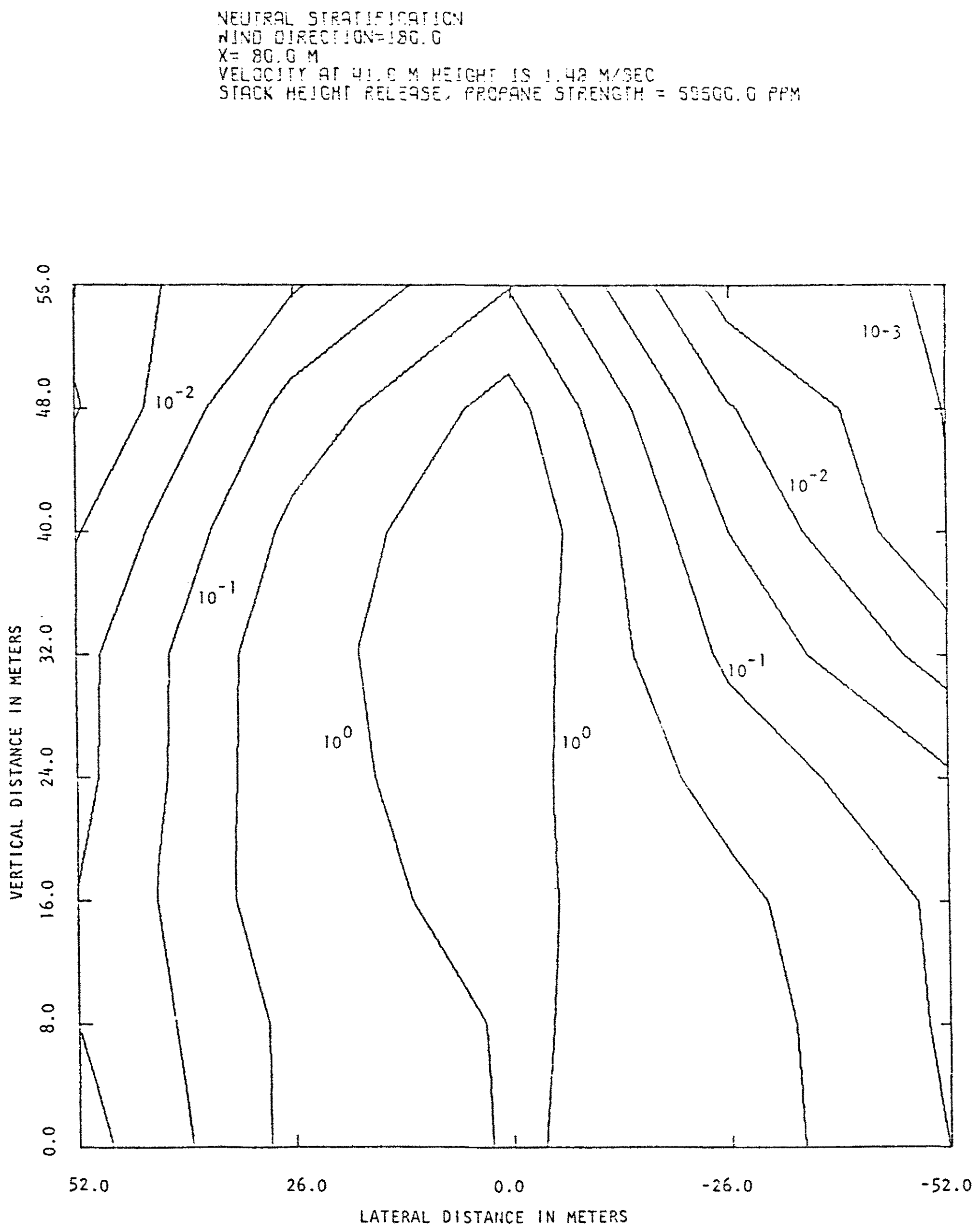

Figure 39. Nondimensional concentration coefficient, K_c, $\frac{\chi UH^2}{Q}$, isopleth.

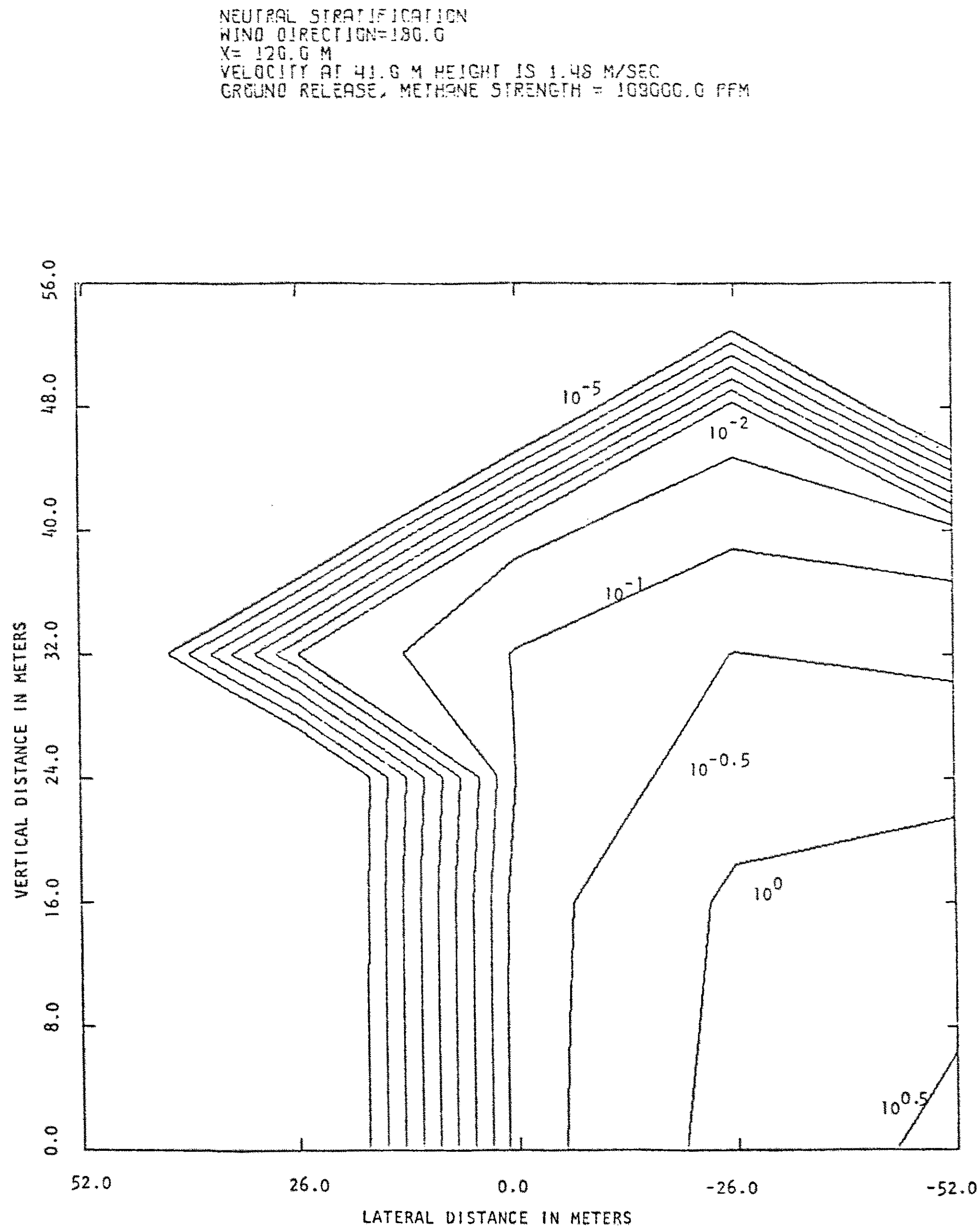

Figure 40. Nondimensional concentration coefficient, K_c, $\frac{\chi U H^2}{Q}$, isopleth.

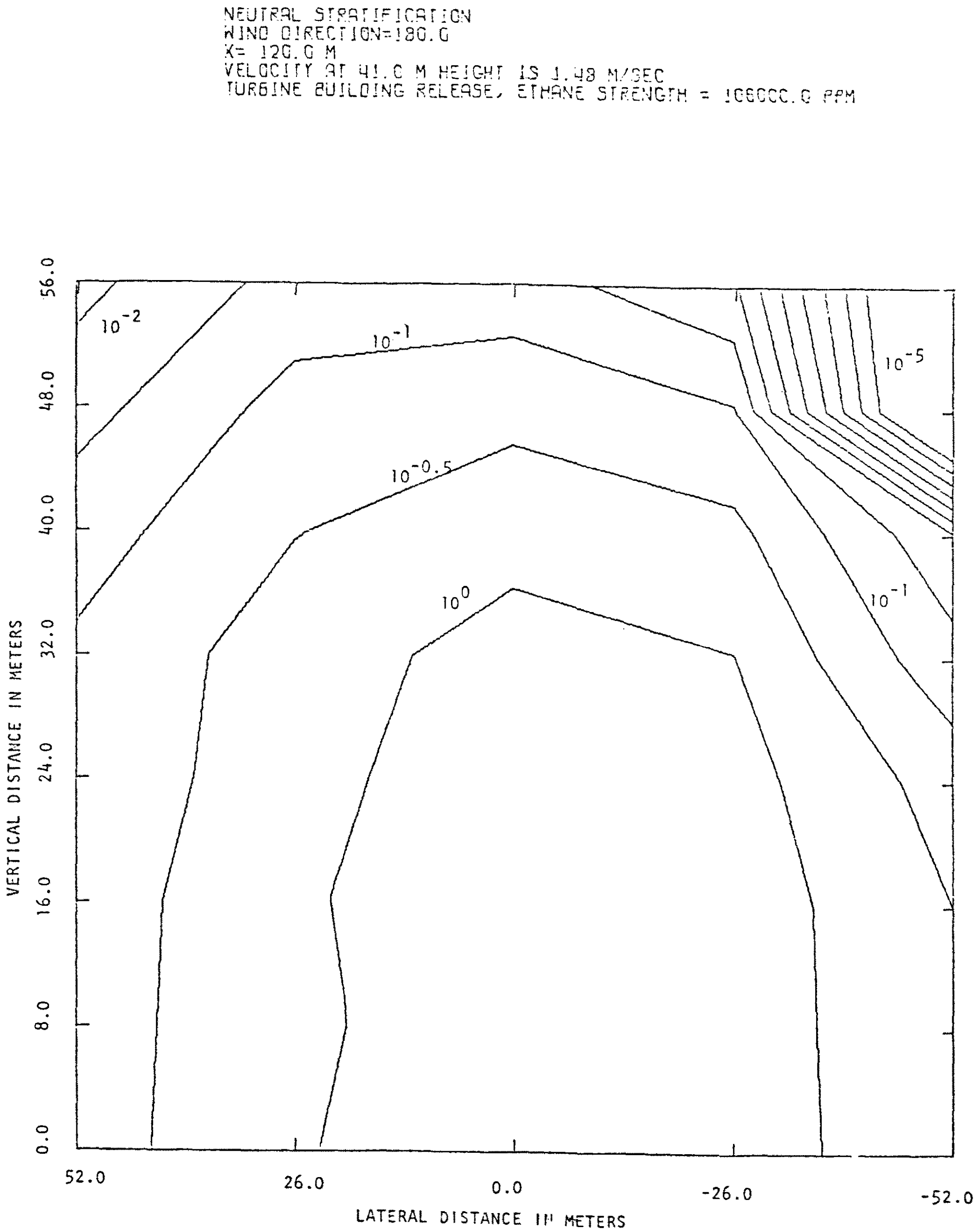

Figure 41. Nondimensional concentration coefficient, K_c, $\frac{\chi U H^2}{Q}$, isopleth.

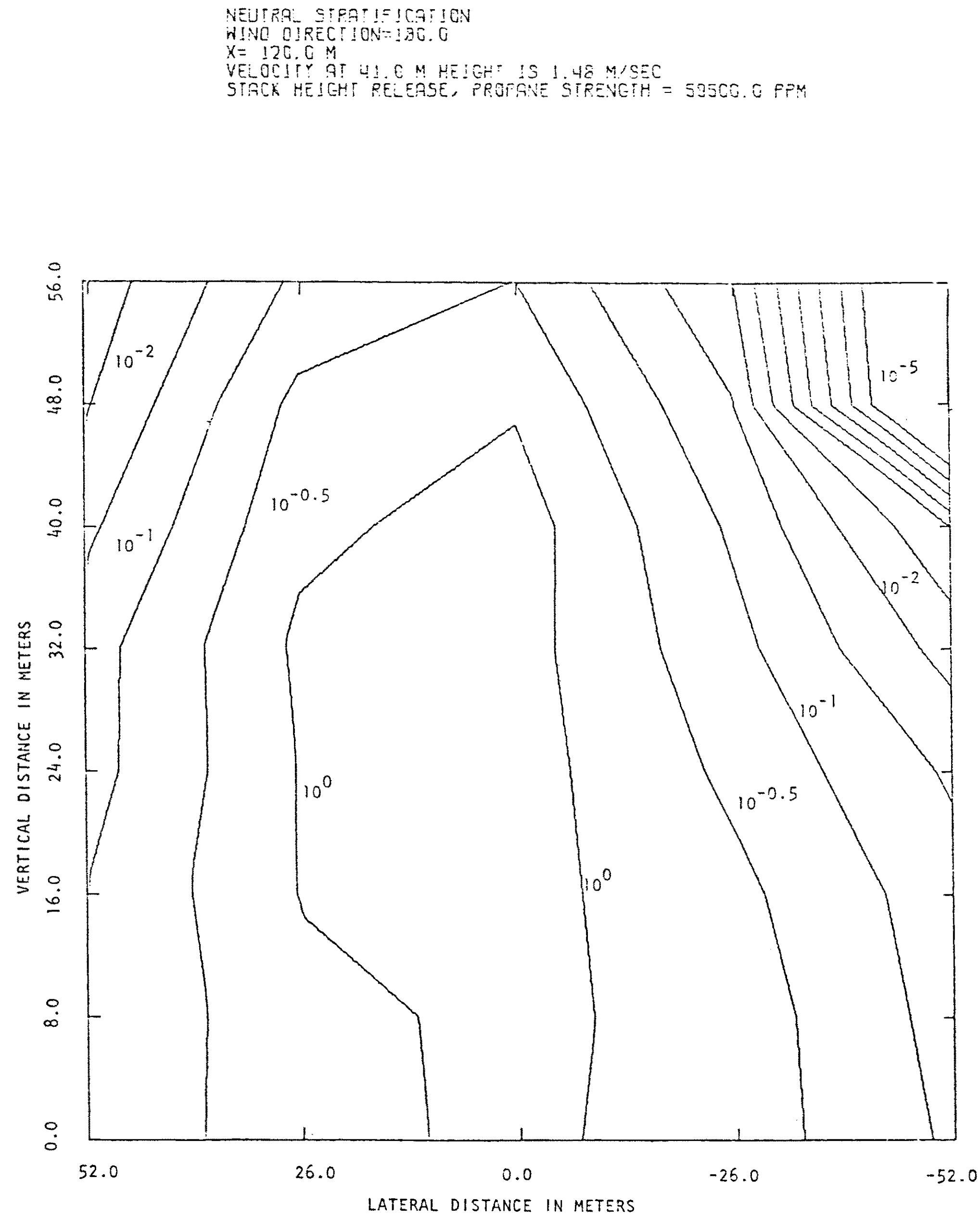

Figure 42. Nondimensional concentration coefficient, K_c, $\frac{\chi UH^2}{Q}$, isopleth.

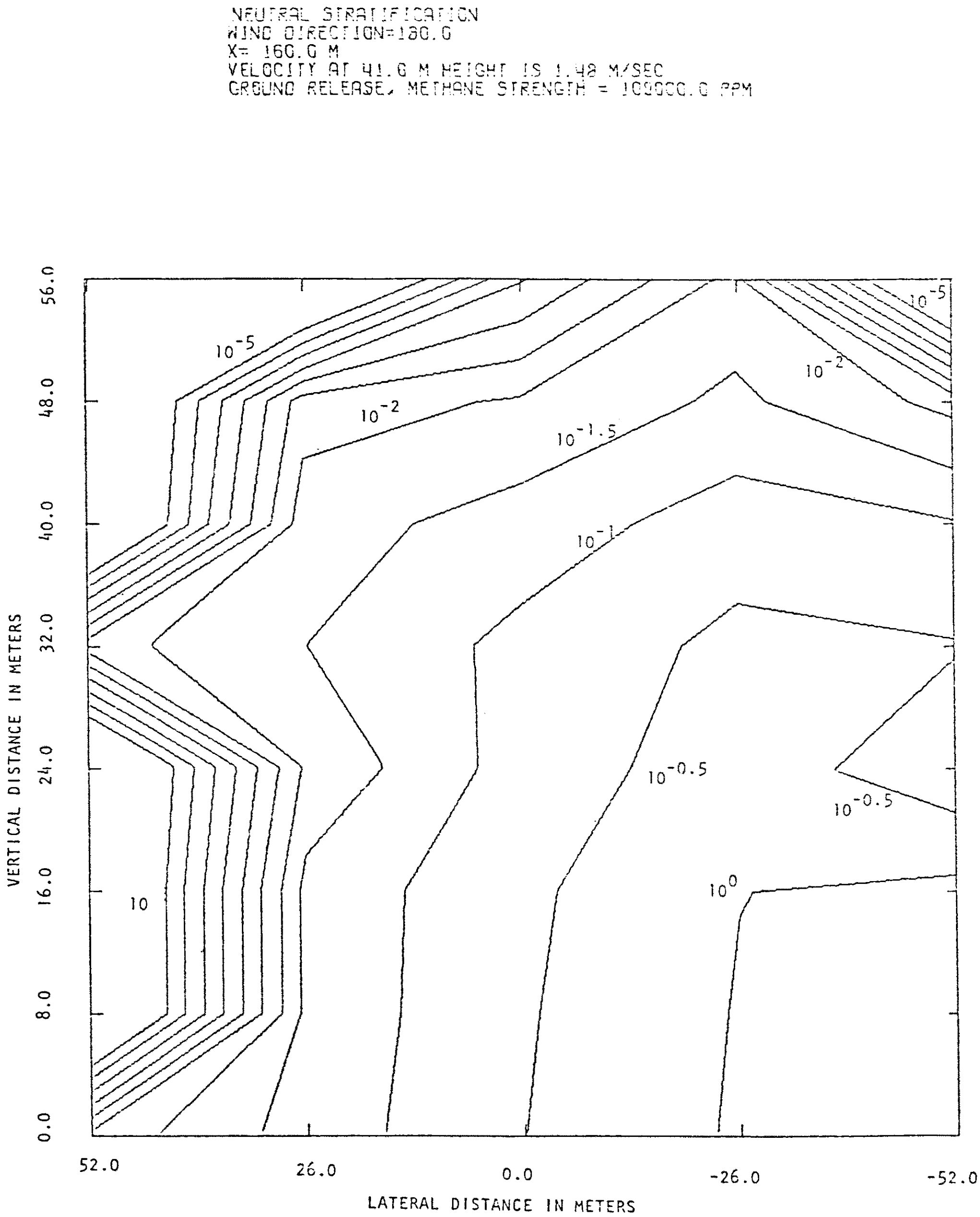

Figure 43. Nondimensional concentration coefficient, K_c, $\frac{\chi U H^2}{Q}$, isopleth.

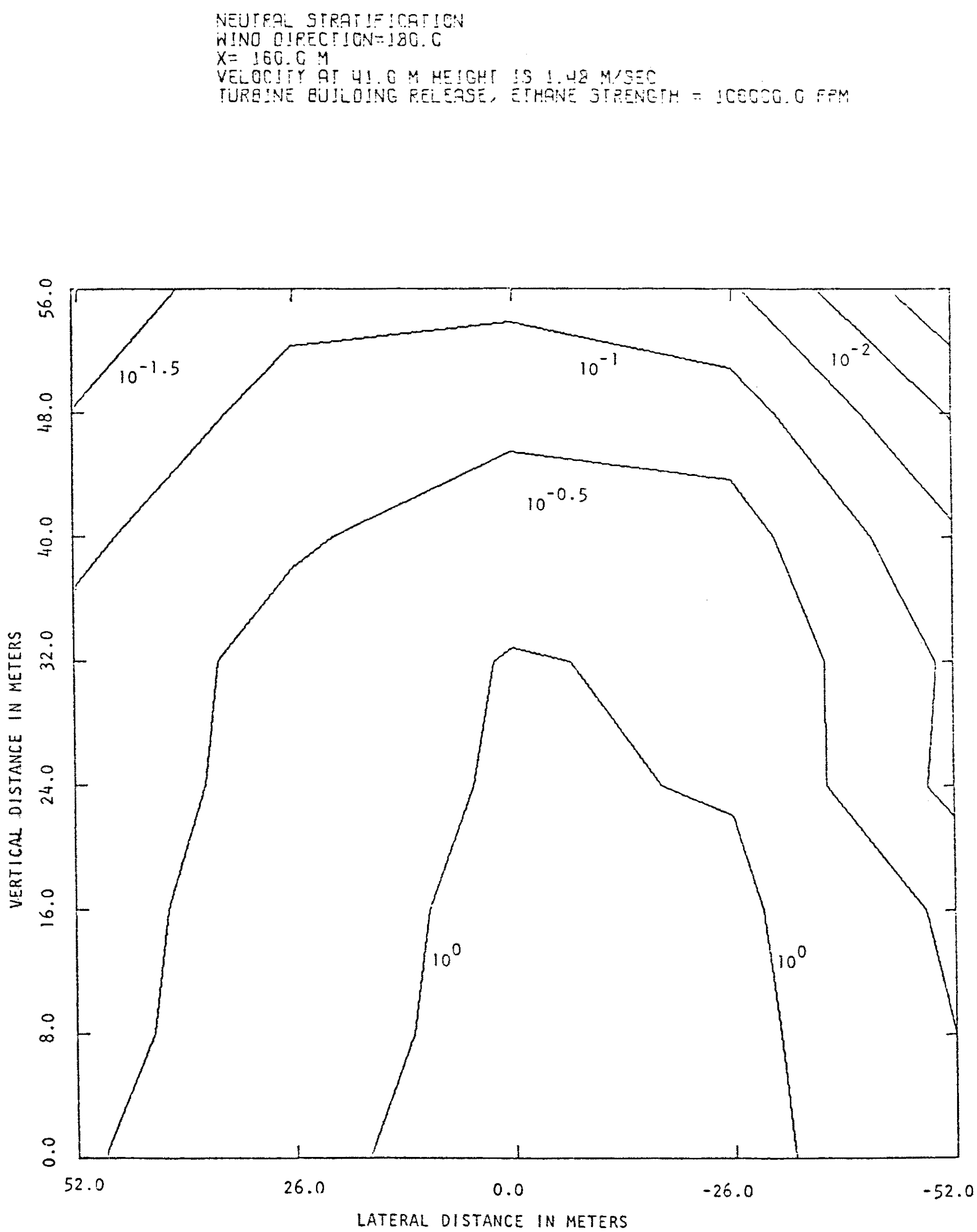

Figure 44. Nondimensional concentration coefficient, K_c, $\frac{\chi UH^2}{Q}$, isopleth.

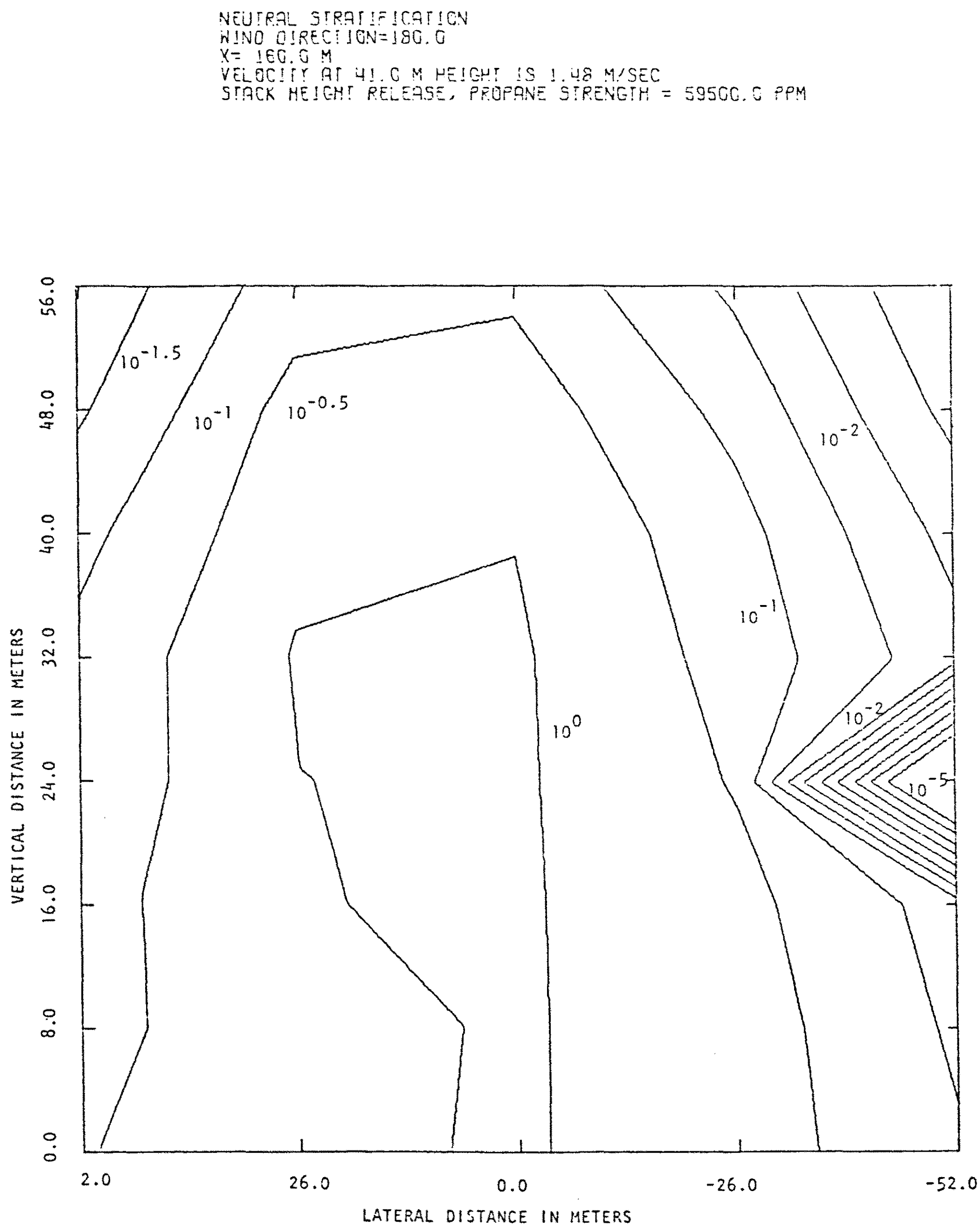

Figure 45. Nondimensional concentration coefficient, K_c, $\frac{\chi UH^2}{Q}$, isopleth.

Below are five index cards that allow for filing according to the four cross-references in addition to the title of the report. A brief abstract describing the major subject area covered in the report is included on each card. For information regarding index card subscriptions to past and future EPRI publications contact the Research Reports Center, P.O. Box 50490, Palo Alto, California 94303. Telephone (415) 965-4081.

EPRI

EPRI NP-1891
RP1073-2
Final Report
June 1981

Nuclear Power Plant Building Wake Effects on Atmospheric Diffusion: Simulation in Wind Tunnel

Contractor: Colorado State University

This report describes wind tunnel simulations conducted to determine the aerodynamic effects of large structures on the dispersion of atmospheric plumes. Results are reported of a wind tunnel mock-up test designed to simulate a previous field study (EPRI Final Report NP-1380) and to demonstrate the applicability of the mock-up to meteorological simulations. Methods for maximizing the plume dispersion from vent releases and for predicting near-field plume concentration are detailed. A comparison is included of the field and wind tunnel experiments.

EPRI Project Manager: H. Till

Cross-References:
1. EPRI NP-1891 2. RP1073-2 3. Chemistry, Radiation, and Monitoring Program
4. Plume Diffusion

ELECTRIC POWER RESEARCH INSTITUTE
Post Office Box 10412, Palo Alto, CA 94303 415-855-2000

EPRI NP-1891

EPRI

EPRI NP-1891
RP1073-2
Final Report
June 1981

Nuclear Power Plant Building Wake Effects on Atmospheric Diffusion: Simulation in Wind Tunnel

Contractor: Colorado State University

This report describes wind tunnel simulations conducted to determine the aerodynamic effects of large structures on the dispersion of atmospheric plumes. Results are reported of a wind tunnel mock-up test designed to simulate a previous field study (EPRI Final Report NP-1380) and to demonstrate the applicability of the mock-up to meteorological simulations. Methods for maximizing the plume dispersion from vent releases and for predicting near-field plume concentration are detailed. A comparison is included of the field and wind tunnel experiments.

EPRI Project Manager: H. Till

Cross-References:
1. EPRI NP-1891 2. RP1073-2 3. Chemistry, Radiation, and Monitoring Program
4. Plume Diffusion

ELECTRIC POWER RESEARCH INSTITUTE
Post Office Box 10412, Palo Alto, CA 94303 415-855-2000

RP1073-2

EPRI

EPRI NP-1891
RP1073-2
Final Report
June 1981

Nuclear Power Plant Building Wake Effects on Atmospheric Diffusion: Simulation in Wind Tunnel

Contractor: Colorado State University

This report describes wind tunnel simulations conducted to determine the aerodynamic effects of large structures on the dispersion of atmospheric plumes. Results are reported of a wind tunnel mock-up test designed to simulate a previous field study (EPRI Final Report NP-1380) and to demonstrate the applicability of the mock-up to meteorological simulations. Methods for maximizing the plume dispersion from vent releases and for predicting near-field plume concentration are detailed. A comparison is included of the field and wind tunnel experiments.

EPRI Project Manager: H. Till

Cross-References:
1. EPRI NP-1891 2. RP1073-2 3. Chemistry, Radiation, and Monitoring Program
4. Plume Diffusion

ELECTRIC POWER RESEARCH INSTITUTE
Post Office Box 10412, Palo Alto, CA 94303 415-855-2000

CHEMISTRY, RADIATION, AND MONITORING PROGRAM

EPRI

EPRI NP-1891
RP1073-2
Final Report
June 1981

Nuclear Power Plant Building Wake Effects on Atmospheric Diffusion: Simulation in Wind Tunnel

Contractor: Colorado State University

This report describes wind tunnel simulations conducted to determine the aerodynamic effects of large structures on the dispersion of atmospheric plumes. Results are reported of a wind tunnel mock-up test designed to simulate a previous field study (EPRI Final Report NP-1380) and to demonstrate the applicability of the mock-up to meteorological simulations. Methods for maximizing the plume dispersion from vent releases and for predicting near-field plume concentration are detailed. A comparison is included of the field and wind tunnel experiments.

EPRI Project Manager: H. Till

Cross-References:
1. EPRI NP-1891 2. RP1073-2 3. Chemistry, Radiation, and Monitoring Program
4. Plume Diffusion

ELECTRIC POWER RESEARCH INSTITUTE
Post Office Box 10412, Palo Alto, CA 94303 415-855-2000

PLUME DIFFUSION

EPRI

EPRI NP-1891
RP1073-2
Final Report
June 1981

Nuclear Power Plant Building Wake Effects on Atmospheric Diffusion: Simulation in Wind Tunnel

Contractor: Colorado State University

This report describes wind tunnel simulations conducted to determine the aerodynamic effects of large structures on the dispersion of atmospheric plumes. Results are reported of a wind tunnel mock-up test designed to simulate a previous field study (EPRI Final Report NP-1380) and to demonstrate the applicability of the mock-up to meteorological simulations. Methods for maximizing the plume dispersion from vent releases and for predicting near-field plume concentration are detailed. A comparison is included of the field and wind tunnel experiments.

EPRI Project Manager: H. Till

Cross-References:
1. EPRI NP-1891 2. RP1073-2 3. Chemistry, Radiation, and Monitoring Program
4. Plume Diffusion

ELECTRIC POWER RESEARCH INSTITUTE
Post Office Box 10412, Palo Alto, CA 94303 415-855-2000